

Chapter 4 Seismic Hazard Assessment

4.1 Modeling of Ground Conditions

4.1.1 Outline of Shallow Ground Condition

The outline of shallow geological structure of Yerevan city is as follows:

- The Tertiary sedimentary rocks widely distribute in Yerevan. They outcrop in the south area of Yerevan city.
- The volcanic rocks cover the Tertiary sedimentary rocks in the north area of Yerevan city.
- The Terrace deposits cover the Tertiary sedimentary rocks in the west area of Yerevan city.
- Along the river, basaltic lava from recent activity or river deposits cover the above mentioned rocks partly.

The shallow ground of Yerevan city is composed by volcanic rocks, sedimentary rocks and terrace deposits. The surface layer is composed by cracked volcanic rock (basalt) in north area, by weathered sedimentary rock in south east area and by terrace deposits in south and west area. The properties of rocks are deeply influenced by the weathered condition. The schematic geological cross sections in Yerevan city are shown in Figure 4.1-1.

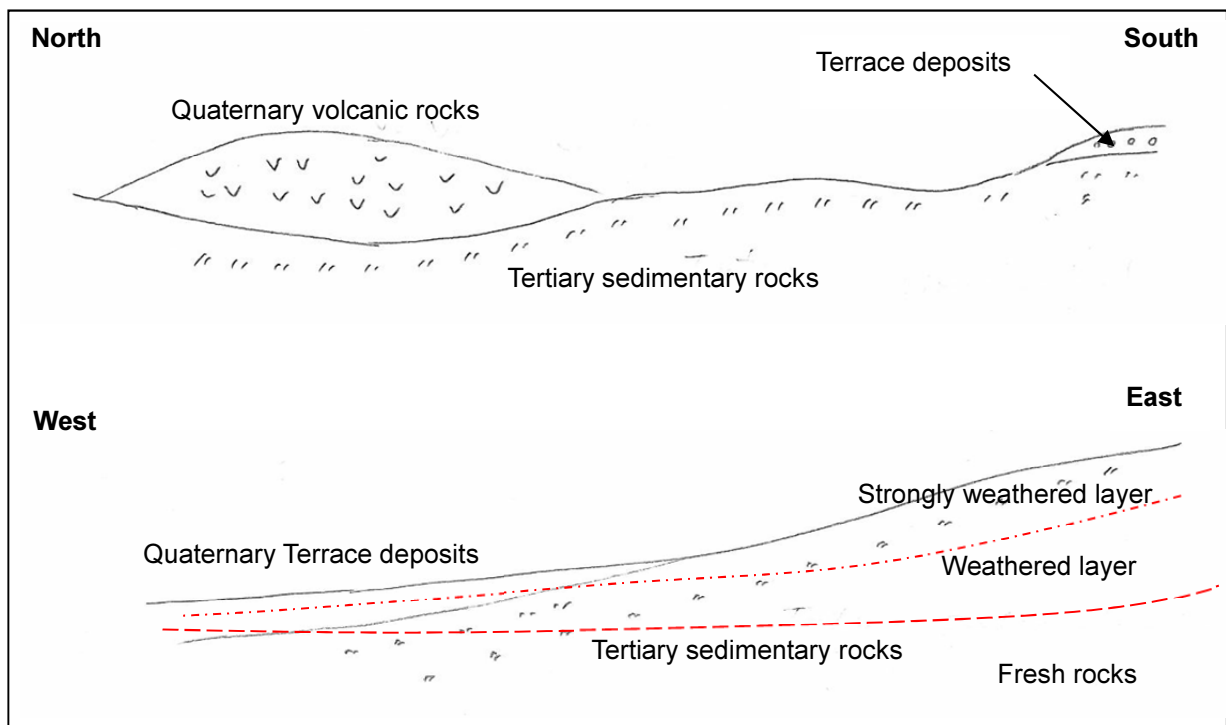


Figure 4.1-1 Schematic geological cross section in Yerevan city

4.1.2 Analysis of the S wave velocity structure of rocks

The S wave velocity (V_s) structure is studied based on the results of surface wave exploration, PS logging and microtremor survey. The altitude/depth of the upper end of layers, where S wave velocity is shown below, is determined at each geophysical survey points. The classification of S wave velocity is determined from the results of geophysical survey. In this study, $V_s \sim 760$ m/sec layer is selected as the engineering seismic baserock.

- 1) $V_s \sim 760$ m/sec (Engineering Seismic Baserock)
- 2) $V_s \sim 500$ m/sec
- 3) $V_s \sim 360$ m/sec

The altitude of $V_s \sim 500$ m/sec layer detected by surface wave exploration is shown in Figure 4.1-2 as an example.

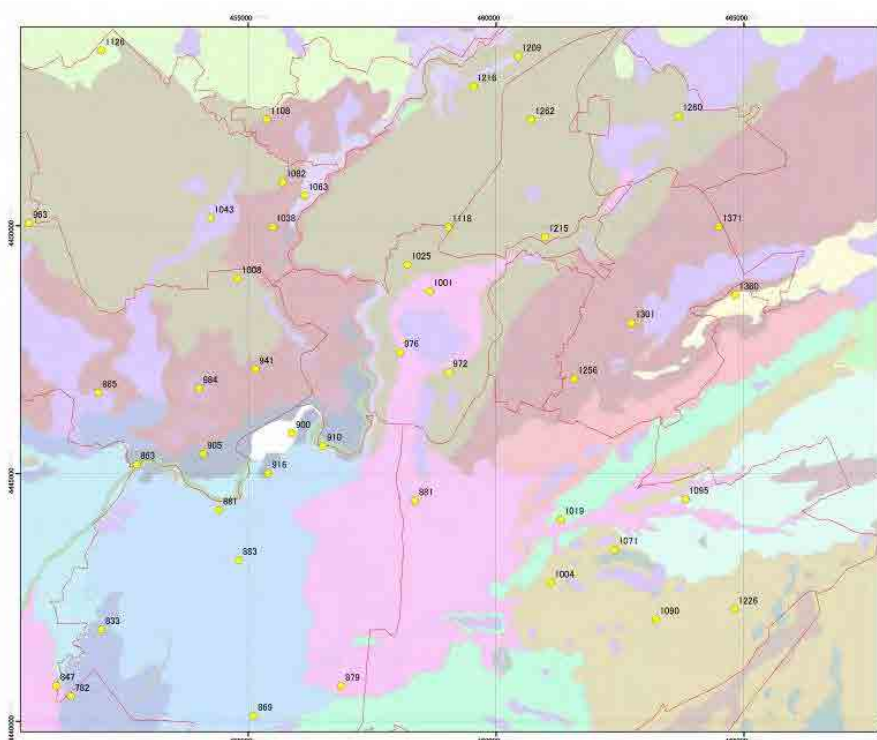


Figure 4.1-2 Altitude of the upper end of $V_s \sim 500$ m/sec layer by surface wave exploration

To make the ground model of all Yerevan city area, the shape of above mentioned three velocity layers should be estimated from point data by geophysical survey. For this purpose, the contour lines of three layers are drawn considering topography, geological condition and shape of fresh rocks, which is analysed by existing borehole logs. The altitudes of three velocity layers are shown in Figure 4.1-3 to Figure 4.1-5 by contour lines. The velocity structure model of rocks where V_s is larger than 360m/sec is created.

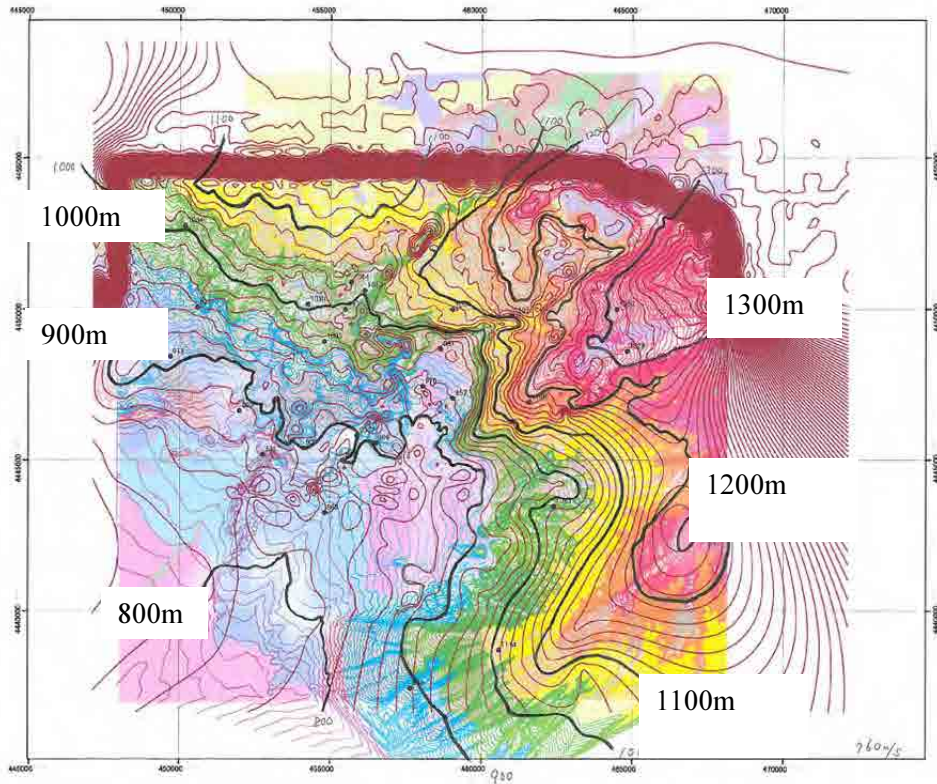


Figure 4.1-3 Altitude of the upper end of Vs~760m/sec layer

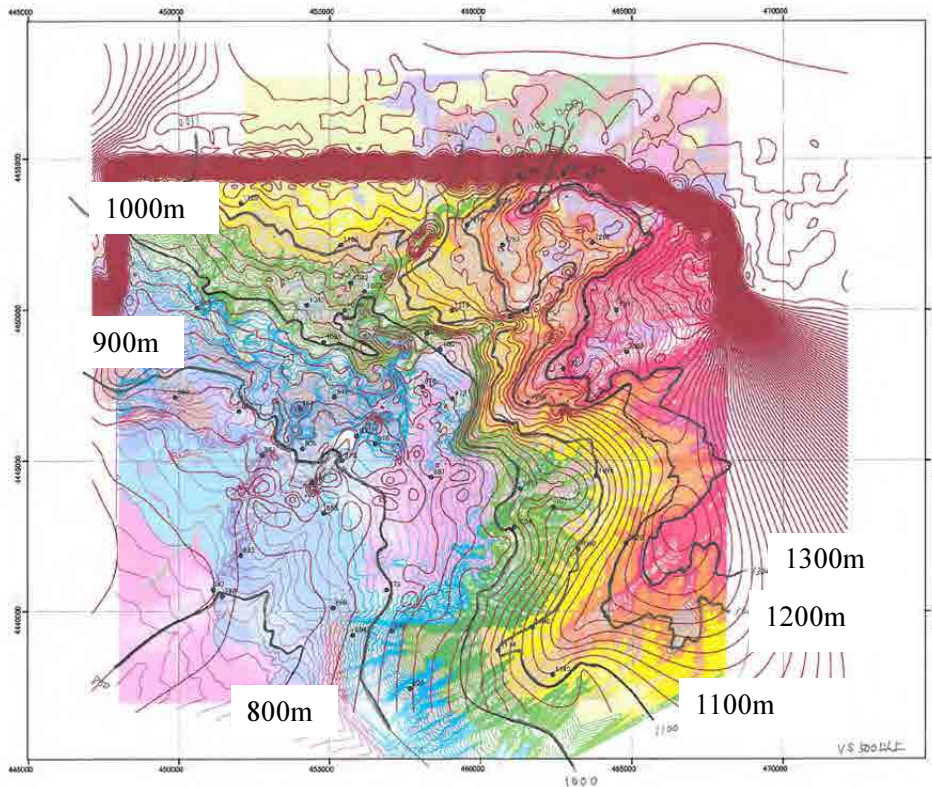


Figure 4.1-4 Altitude of the upper end of Vs~500m/sec layer

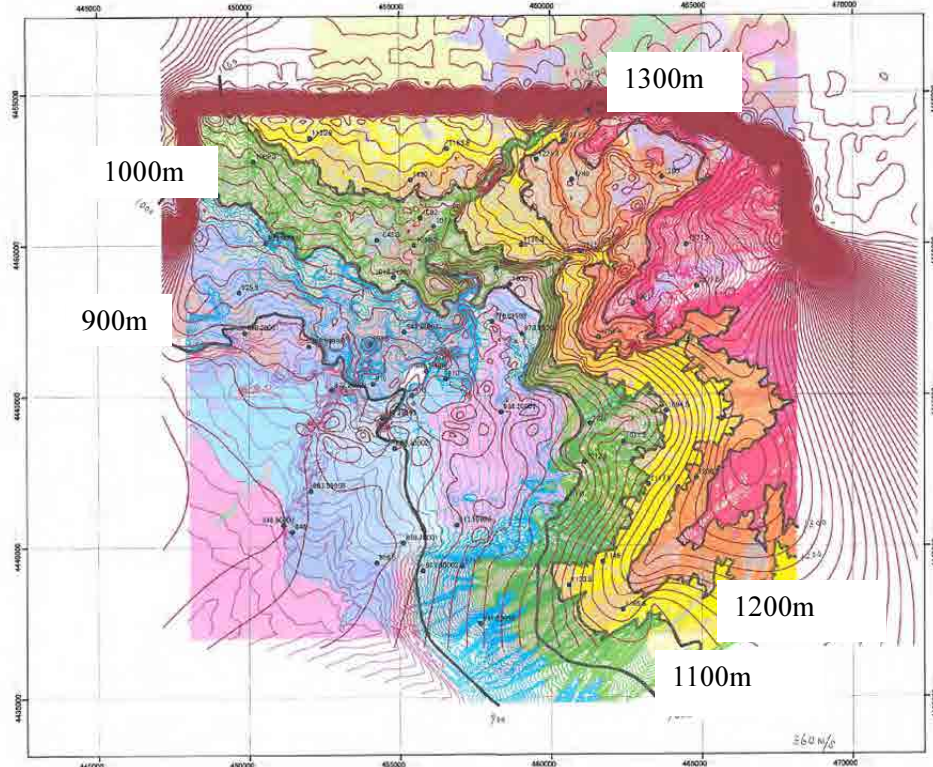


Figure 4.1-5 Altitude of the upper end of Vs=360m/sec layer

4.1.3 Analysis of the S wave velocity structure of shallow soils

The shallow soil layers from ground surface to Vs=360m/sec layer are studied based on the existing drilling logs, newly conducted drilling logs, PS logging results and surface wave exploration. The findings of the analysis are summarized below:

- 1) The S wave velocity layer from ground surface to Vs=360m/sec layer is composed by two.
- 2) The S wave velocity of these two layers can be estimated from surface geology. The surface geology is as follows:
 - Type 1: Quaternary volcanic rocks including welded Tuff
 - Type 2: Quaternary terrace deposits
 - Type 3: Tertiary sedimentary rocks

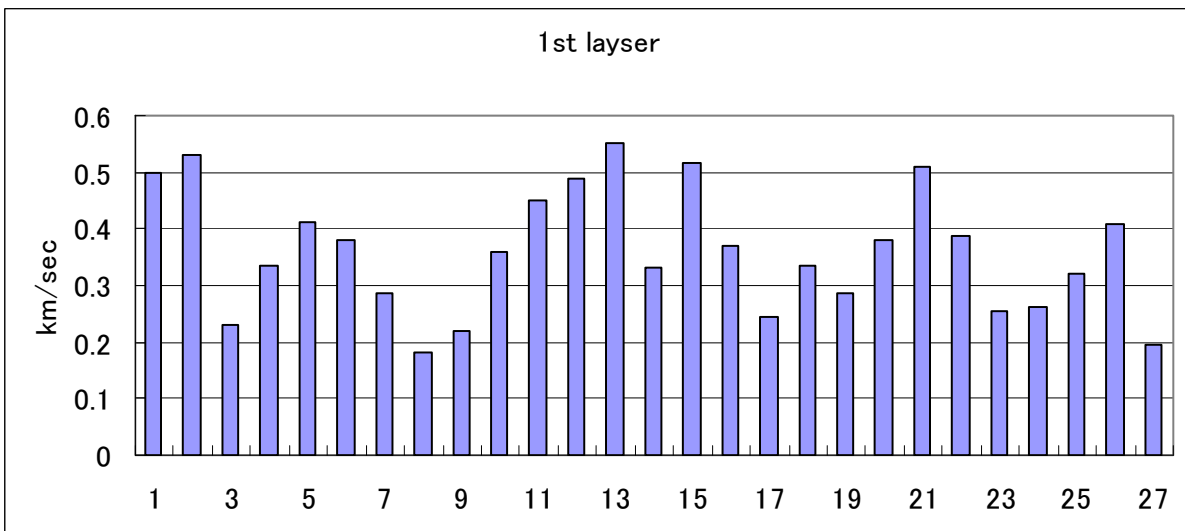
The S wave velocities of two shallow layers and the ratio of thickness of two layers are determined using the results of surface wave exploration and PS logging. At first, the unsuitable data is eliminated. The data with slower second layer than first layer is removed and extremely low velocity ($V_s < 100\text{m/sec}$) is also removed. Next, the average velocities of first and second layer are calculated for each geology type. The findings and results are shown below:

(1) Type 1

This type distributes in the north hill area of Yerevan city. The surface geology is shown in Table 4.1-1. V_s of first and second layers show equal or larger than 360m/sec. One data shows $V_s=1,020\text{m/sec}$ at second layer. This may be resulted from lack of $V_s=500\text{m/sec}$ layer. Figure 4.1-6 is the data of V_s of first layer. From this figure, the average V_s of shallow layer is decided as 360m/sec.

Table 4.1-1 Surface geology of Type 1

Symbol	Age
abQ3	Upper Quaternary Section (the upper part)
abQ2-3	Middle-to-Upper Quaternary Sections (the upper part)
tQ2	Middle Quaternary Section (the upper part)
bN22	Upper Pliocene
babN22Q1	Upper Pliocene-Lower Quaternary Section

Figure 4.1-6 V_s of first layer of Type 1**(2) Type 2**

This type distributes in the west area of Yerevan city. The surface geology is shown in Table 4.1-2. V_s of first layer is less than 360m/sec. Second layer sometimes show larger than $V_s=360\text{m/sec}$. This is interpreted that several velocity layers could not be separated by geophysical survey because they are thin and removed from analysis. Figure 4.1-7 is the data of V_s of first, second and third layers. The average V_s of third layer is 380m/sec and judged as rock which is modeled in section 4.1.2. The average V_s of first and second layers are 220m/sec and 290m/sec respectively. The average ratio of thickness of first layer and second layer is 0.42 : 0.58 (see Figure 4.1-8).

Table 4.1-2 Surface geology of Type 2

Symbol	Age
apQ42	Modern Section (the upper part)
apQ41	Modern Section (the lower part)
apQ2-3chr	Middle-to-Upper Quaternary Sections (the lower part)
apQ3ar	Upper Quaternary Section (the lower part)
laQ1-2	Lower-to-Middle Quaternary Sections
Q1nb2	Lower Quaternary Section (the upper part)
Q1nb1	Lower Quaternary Section (the lower part).

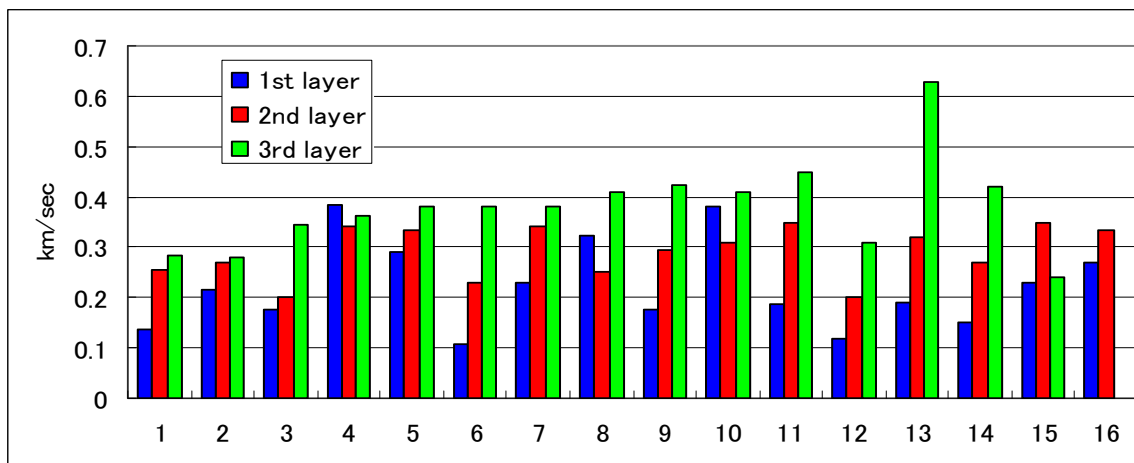


Figure 4.1-7 Vs of first, second and third layers of Type 2

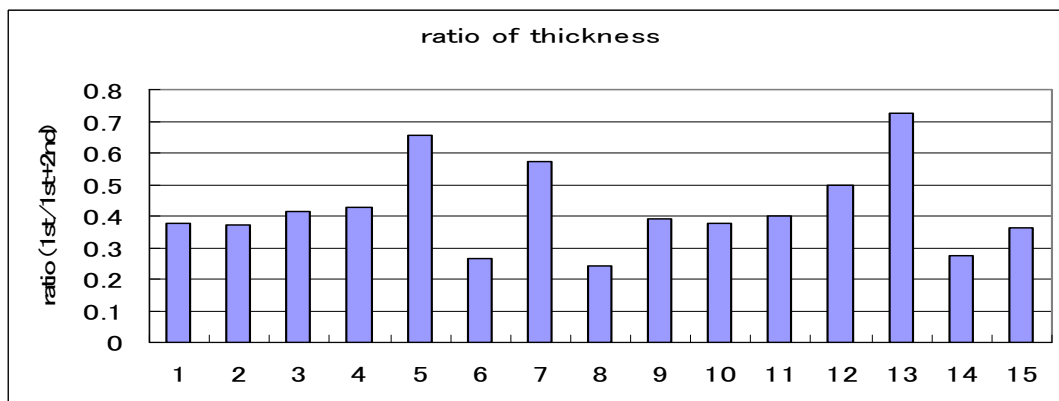


Figure 4.1-8 Ratio of the thickness of first layer to first + second layer (Type 2),
No16 is not used because third layer is not detected

(3) Type 3

This type distributes in the south and south-east part of Yerevan city. The surface geology is shown in Table 4.1-3. Vs of first and second layer show less than 360m/sec. Second layer sometimes show larger than Vs=360m/sec. This is interpreted that several velocity layers could not separate by geophysical survey because they are thin and removed from analysis. Figure 4.1-9 is the data of Vs of first, second and third layers. The average Vs of third layer is 380m/sec and judged as rock which is modeled in section 4.1.2. The average Vs of first and second layers are 220m/sec and 290m/sec

respectively. The average ratio of thickness of first layer and second layer is 0.44 : 0.56 (see Figure 4.1-10).

Table 4.1-3 Surface geology of Type 3

Symbol	Age
N13hr	Upper Miocene, Sarmatian (the upper part)
N13er	Upper Miocene, Sarmatian (the lower part)
N12dj (b)	Middle Miocene
N1hc1	Upper Oligocene - Lower Miocene
Pg3sh3	Lower-Middle Oligocene
Pg3sh2	Lower-Middle Oligocene
Pg3sh1	Lower-Middle Oligocene

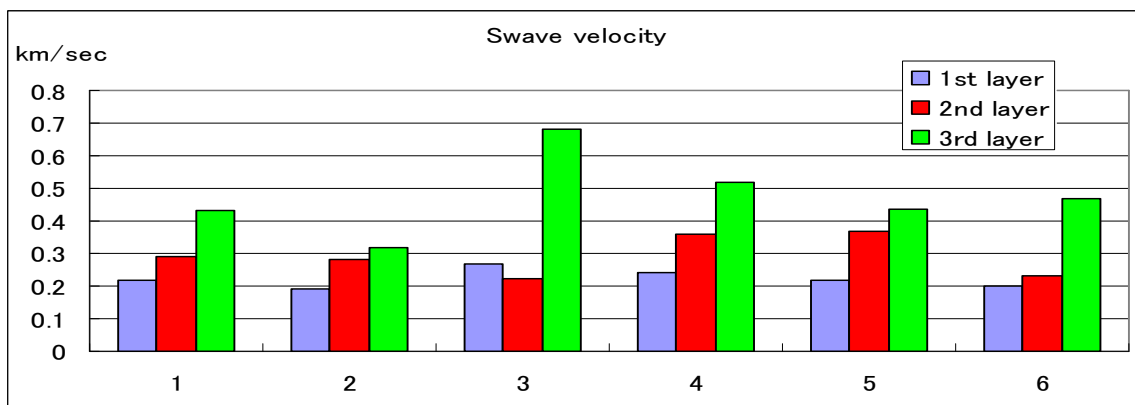


Figure 4.1-9 Vs of first, second and third layers of Type 3

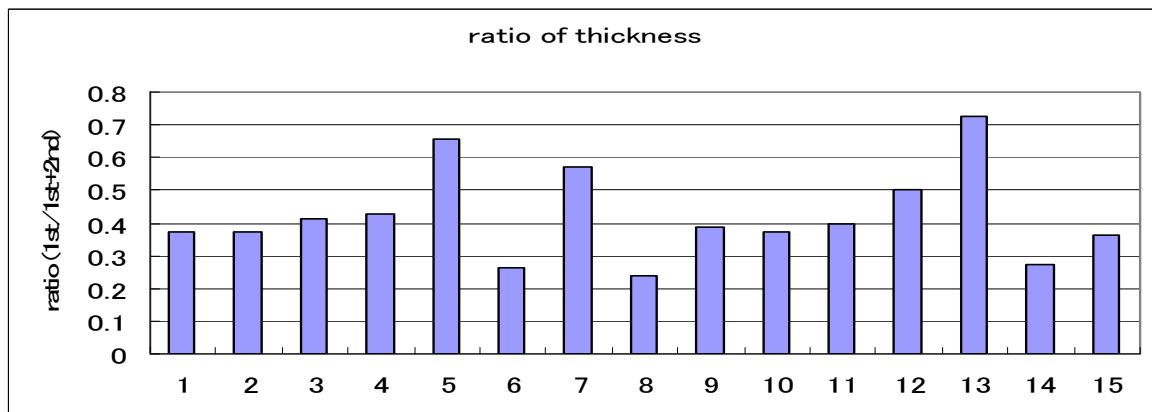


Figure 4.1-10 Ratio of the thickness of first layer to first + second layer (Type 3)

(4) Summary

Table 4.1-4 is the summary of analysis.

Table 4.1-4 Summary of S wave velocity structure in Yerevan

Type	Type 1	Type 2	Type 3	Deep /Shallow
Age, properties and conditions	Quaternary Volcanic rocks including welded Tuff	Quaternary Terrace sediments	The Tertiary sedimentary rocks including the rocks before Tertiary	
Area	North hill area	Western area	South and south-east area	
Age	Quaternary	Quaternary	Before Tertiary	
1 st layer	360 m/sec	220 m/sec	220 m/sec	Shallow layer
2 nd layer		290 m/sec	290 m/sec	
3 rd layer	360 m/sec			Deep layer
4 th layer	500 m/sec			
5 th layer	760m/sec			
Thickness ration between 1 st layer and 2 nd layer: Type2 = 0.42 : 0.58, Type3 = 0.44 : 0.56				

4.1.4 Ground modeling for hazard assessment based on the geological structure

The ground model for hazard assessment is created for each 250m x 250m square grid based on Figure 4.1-3 to Figure 4.1-5 and Table 4.1-4. The type of the ground of each 250m grid is shown in Figure 4.1-11.

The created numerical model is confirmed by comparing with the geological cross sections, which is made based on the existing drilling database. Figure 4.1-12 to Figure 4.1-14 are the example of S wave velocity section and geology cross section at same place. The geological cross sections are made based on the 555 selected drilling data from existing database. Followings are the criteria of borehole data selection;

- 1) The borehole should be in the study area.
- 2) Total depth should be more than 15m, because 15m is necessary to exam geological structure.
- 3) Total depth should be less than 100m, because the deep depth data sometimes includes typo.
- 4) When there are several data in the same grid, one typical data is selected.

The geological sections are shown in the lowest part in Figure 4.1-12 to Figure 4.1-14. In drawing the cross sections, following information are considered.

- Some of the gravels or the pebbles in the drilling log may be crackly basalt. If basalt is crashed during drilling, it looks like gravel or pebble.
- The clay layers between the tertiary sediment rocks are sometimes found in the drilling logs. The layer may be actually sediment rocks because it looks like clay when it is crashed during drilling.

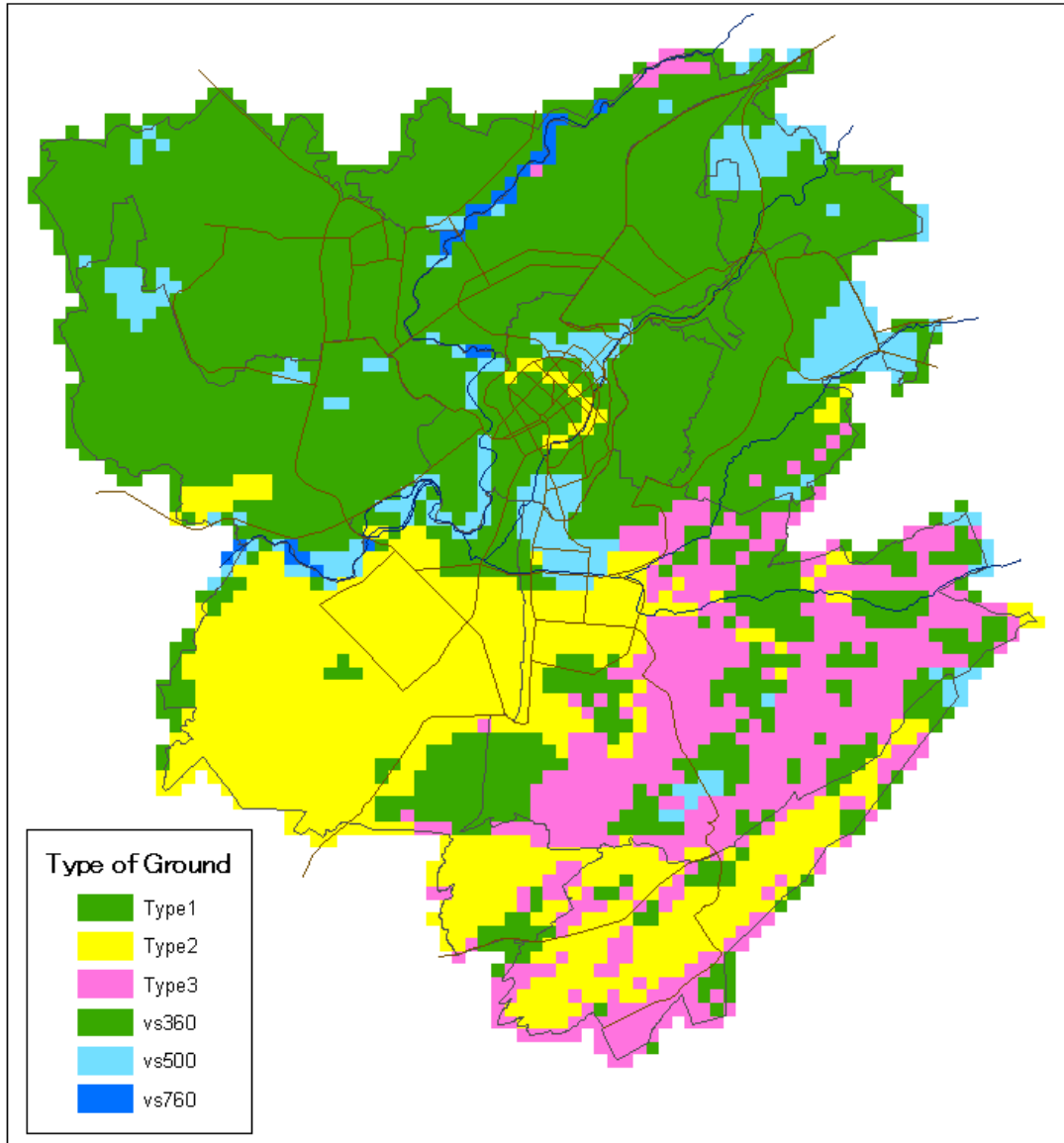


Figure 4.1-11 Type of ground; Vs360, Vs500, Vs760 means outcrop of corresponding rock layer

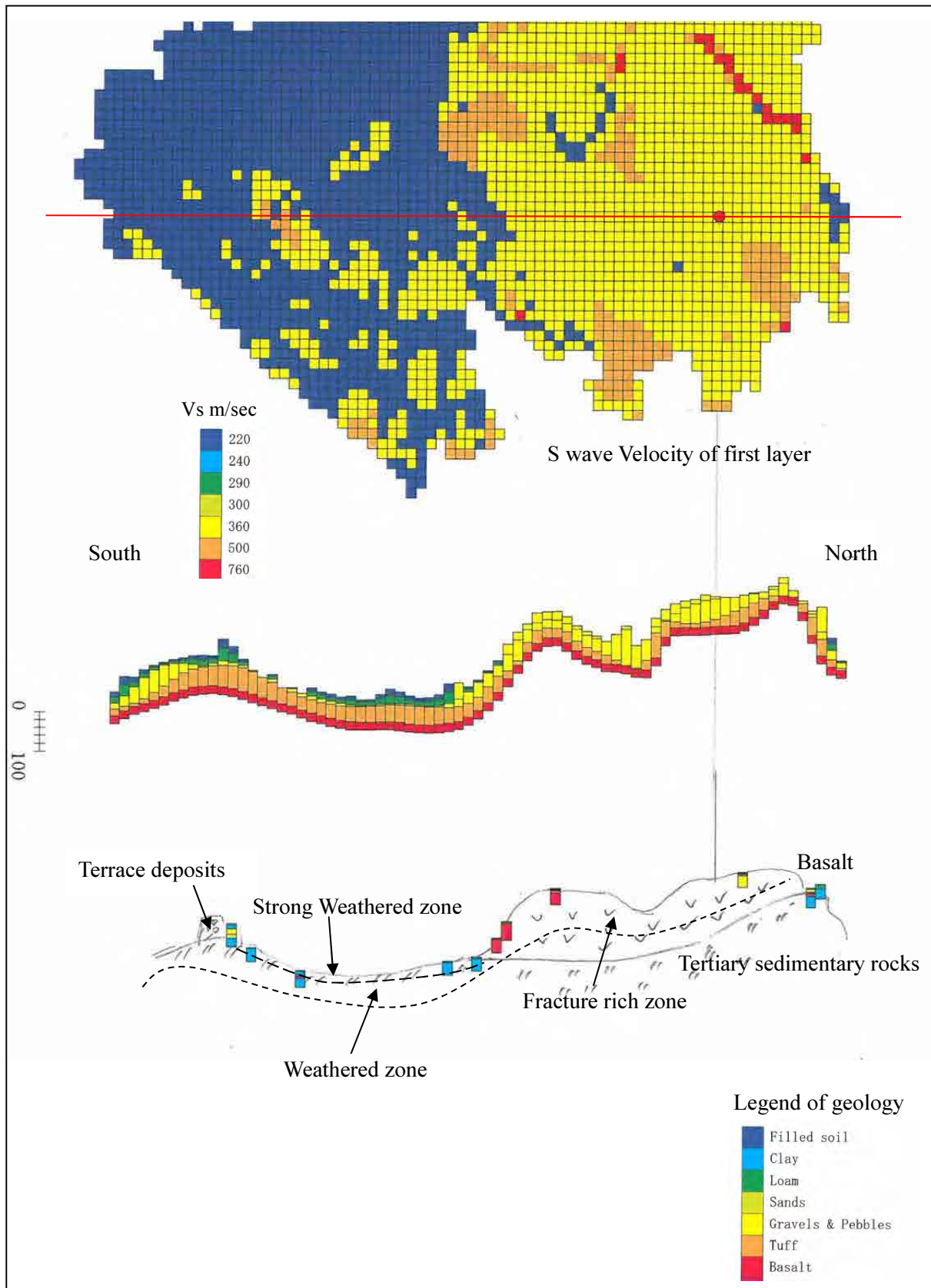


Figure 4.1-12 Comparison of S wave velocity section with the geology section
- N-S direction -

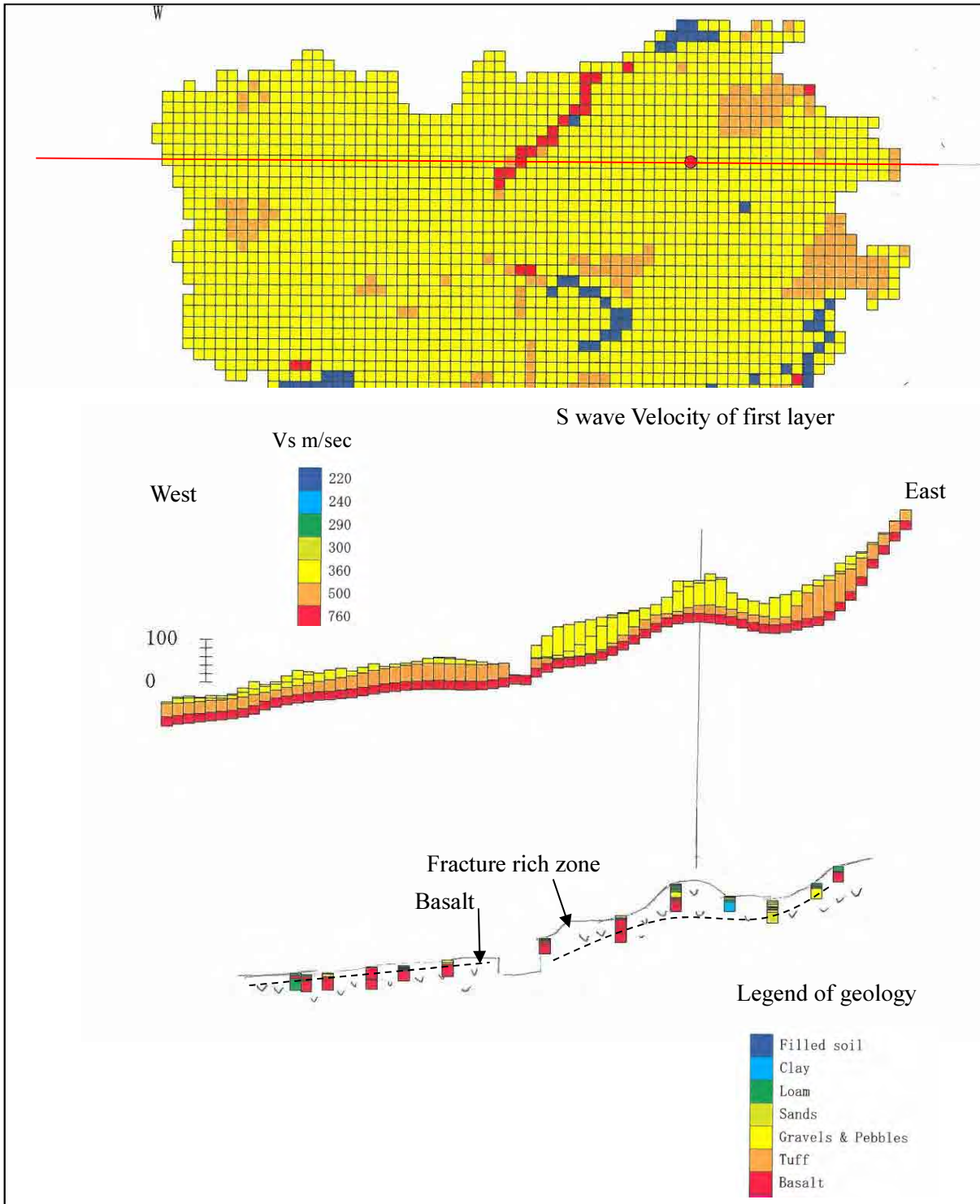


Figure 4.1-13 Comparison of S wave velocity section with the geology section
 - E-W direction in the north of Yerevan -

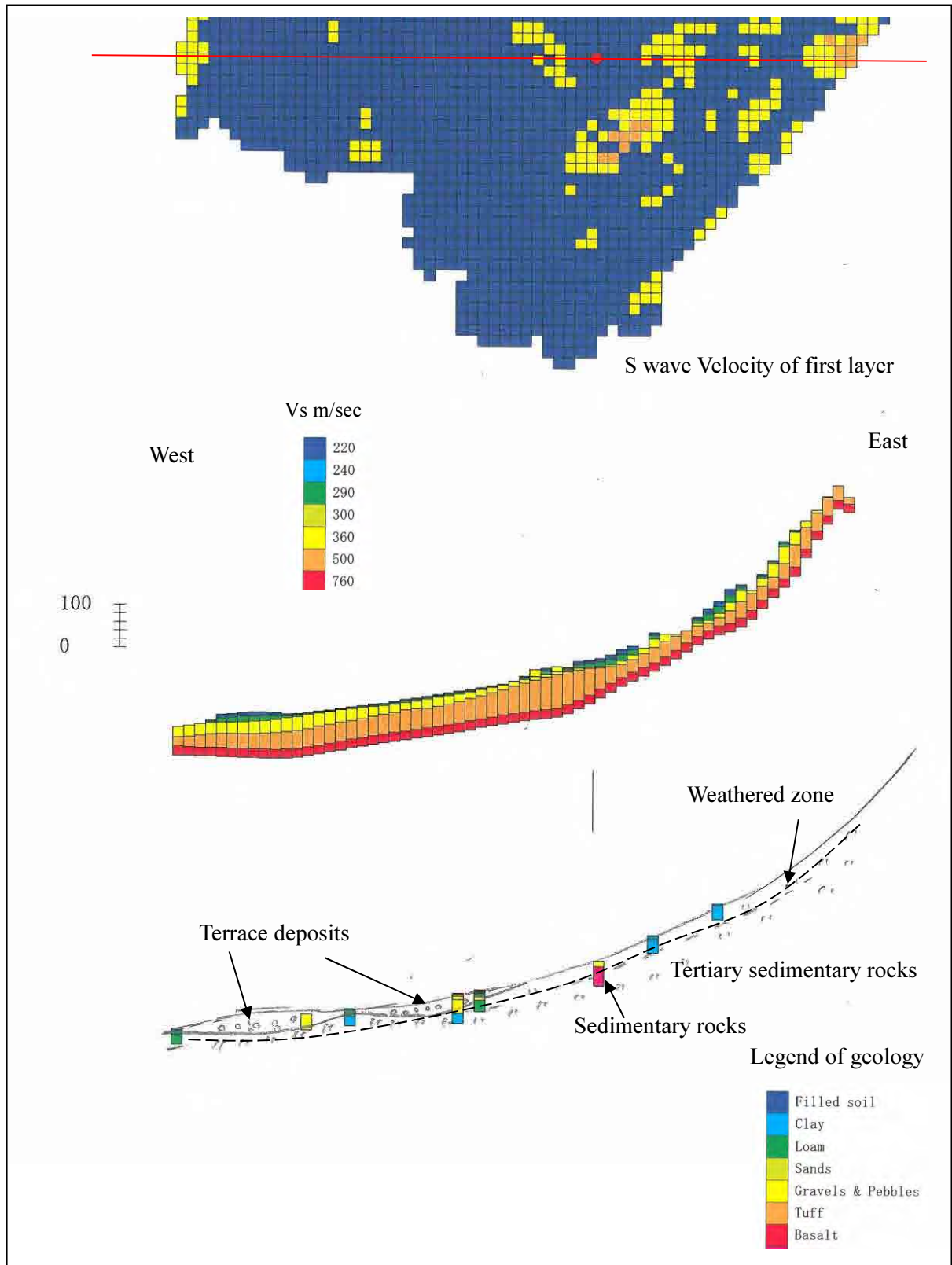


Figure 4.1-14 Comparison of S wave velocity section with the geology section
- E-W direction in the south of Yerevan -

4.2 Scenario Earthquakes

Following two scenarios are established for scenario earthquakes of Yerevan city.

- Segment 2 of Garni Fault (GF2 in Figure 4.2-1)
- Segment 3 of Garni Fault (GF3 in Figure 4.2-1)

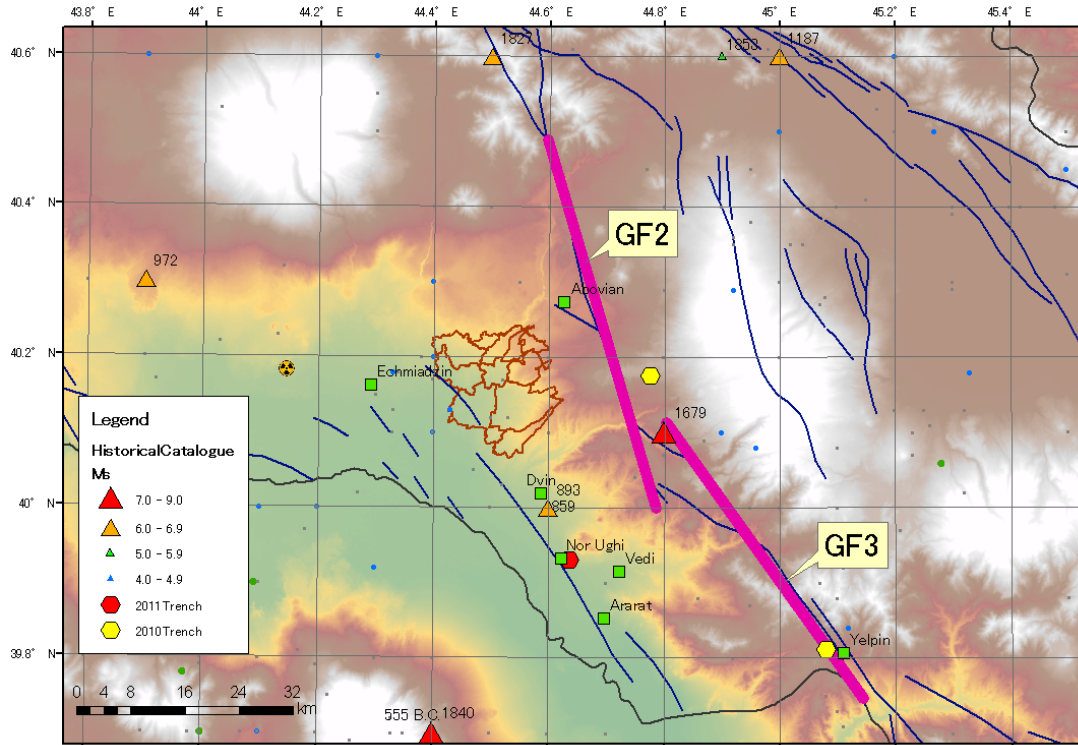


Figure 4.2-1 Fault Models of Scenario Earthquakes

It is estimated that Garni Fault is an active fault with about 200 km length and it is composed with five segments. Among them, GF2 and GF3 segments are situated near Yerevan. These segments are supposed to have occurred earthquakes within past several hundred years based on the historical records. The possibility of the earthquake occurrence due to the movement of these segments in near future is small reviewing that the standard recurrence interval of the earthquakes by the movement of inland active fault is longer than 1000 years. However, the possibility of the earthquake by these segments in near future cannot be fully denied considering the uncertainty of the earthquake generated source segment of the 1679 Garni Earthquake. Yerevan City has suffered severe damage during the 1679 event and it is easily presumed same situation if resemble earthquake to 1679 earthquake may occur again, therefore, GF2 and GF3 segments of Garni Fault are selected as the scenario earthquakes.

The fault parameters of the scenario earthquakes are tabulated in Table 4.2-1. The precise considering in setting the parameters are written in the following.

Table 4.2-1 Fault Parameters of Scenario Earthquakes

	Garni Fault (GF2)	Garni Fault (GF3)
Moment Magnitude (Mw)	7.0	7.0
Fault Type	Normal Fault with Right Lateral component	Normal Fault with Right Lateral component
Length (km)	57	50
Dip (degree)	90	90
Depth(Upper - Lower) (km)	3 - 12	3 - 12
Width (km)	9	9

4.2.1 Fault Type

Based on the trench survey in this project, the fault type of GF2 and GF3 segments of Garni Fault are supposed to be normal fault with right lateral component.

4.2.2 Length of Fault

The lines in Figure 4.2-1 are supposed rupture area of the scenario earthquakes. The segment 2 in the existing reports about Garni Fault by GEORISK extends to north over the northern end of GF2 in this study; however an earthquake with magnitude 7 occurred in 1827 at the northern end in segment 2 and this area is supposed to have ruptured already and released energy by this earthquake. Therefore, the northern end of GF2 is set to the point of divergence of Garni Fault just south of 1827 earthquake epicenter. The location of GF3 is set following existing information.

4.2.3 Dip of Fault

The dip of the GF2 and GF3 segment of Garni Fault is supposed steep because their mechanism is normal fault. Actually, the fault found at the trench site of Garni north and Yelpin showed large dip angle. The dip angle of the scenario fault model of Garni Fault is set to 90 degree because the dip direction shows east or west dipping site by site.

4.2.4 Depth of Fault

The seismogenic zone may not extend to deep ground because there are many volcanos in Armenia and it is geothermal area. The seismic activity is not high in the hypocentral region of the scenario earthquakes and accumulated data concerning the depth of the earthquake is not enough, however, the depth of the small earthquakes are shallower than 10 to 15km depth. Based on these information, the depth of the lower boundary of the fault is set to 12km. The depth of upper boundary of the Garni Fault is set to 3km because the ground surface is covered by Quaternary volcanic rock and shallow ground will not contribute to the generation of seismic motion.

4.2.5 Magnitude of Earthquake

The magnitude of the earthquakes can be estimated from the magnitude of the historical earthquakes which have occurred at the same fault or the length of the fault. As for the historical earthquakes occurred at the Garni Fault, the magnitude of 1679 Garni Earthquake and 1827 earthquake are around 7.0, and 1988 Spitak Earthquake is Ms 6.9. The earthquake with magnitude 7 class is dominant at Garni Fault.

Wells and Coppersmith (1994) proposed the empirical relation between the magnitude of the earthquake at the fault and the subsurface rupture length (RLD), rupture area (RA) or average displacement (AD) based on the statistical analysis using many past earthquake data. The estimated magnitude of the scenario earthquakes using the empirical relation from the length or the area of the scenario earthquake model and the displacement observed at the trench are Mw 6.9 to 7.0 for GF2, Mw 6.8 to 7.0 for GF3. These values are consistent with inferred magnitudes from the historical earthquakes

References:

Wells, D. L. and K. J. Coppersmith (1994) New Empirical Relationships among Magnitude, Rupture Length, Rupture Width, Rupture Area, and Surface Displacement. *Bull. Seismol. Soc. Am.*, 84, 974-1002.

Georisk report:

Report on the Garni Fault, 20p.

4.3 Earthquake Motion, Liquefaction Potential and Slope Stability

4.3.1 Analysis of Baserock Motion

Analysis of earthquake motion is composed by two steps, namely the calculation of baserock motion at first and the evaluation of subsurface amplification for the second. This methodology is adopted because the amplification of the earthquake motion is strongly affected by the ground condition near ground surface; on the other hand the baserock motion is comparatively stable. Therefore the separate calculation is a good idea. The earthquake motion at the engineering seismic baserock was calculated by the empirical attenuation equations. The layer with $V_s=760\text{m/sec}$ or larger is adopted for the engineering seismic baserock based on the geophysical exploration results.

(1) Selection of empirical attenuation equation

The attenuation equations are the empirical relations between the magnitude of the earthquakes, distance from the fault etc. with acceleration or spectrum which are made based on the statistical analysis of the past strong motion records. The empirical attenuation equations reflect the characteristics of the used database; therefore it is most preferable to use the formula which is made

based on the records observed in or around the study area. However, no equations are proposed based on the records observed in Yerevan or in Armenia. In this study, the suitable equations are selected among the equations made for Caucasia and newest ones reflecting the state-of-the-art technology.

The subjective attenuation equations are following 6 relations.

- 1) Smit et al. (2000)
- 2) AB10: Akker and Bommer (2010)
- 3) AS08: Abrahamson and Silva (2008)
- 4) BA08: Boore and Atkinson (2008)
- 5) CB08: Campbell and Bozorgnia (2008)
- 6) CY08: Chiou and Youngs (2008)

The target area of formula 1) is Caucasia and Europe, Mediterranean and Middle East are the target regions of formula 2). The formula 3) to 6) are produced through the NGA (Next Generation of Ground-Motion Attenuation Models) Project. These are studied for California but the used database is made from the world wide strong motion records. They are the state-of-the-art result in this field; therefore, they are included in the subjective equations.

The suitable attenuation equations are selected from above 6 equations by comparing the calculated value by the formula with the observed strong motion records in Armenia and Georgia. The equations which meet the observed records are selected finally. The used earthquakes for the analysis are following 3 earthquakes whose magnitudes are comparative with those of scenario earthquakes.

- 1988.12.7 Spitak Eq. (Mw=6.9), in Armenia
- 1991.4.29 Dzhava-Racha Eq. (Mw=7.1), in Georgia
- 1992.10.23 Barysakho Eq. (Mw=7.2), Georgia

The comparisons are shown in Figure 4.3-1. The results for the formula 1) are separately shown because the definition of the PGA of formula 1) is different from the others. Formula 2) AB10, 4) BA08 and 6) CY08 are selected based Figure 4.3-1. The calculated PGA by the formula 1), Smit et al. (2000), meets the observed records but couldn't adopted because it can't consider the fault as a surface and also it overestimates in case of short distance to the fault.

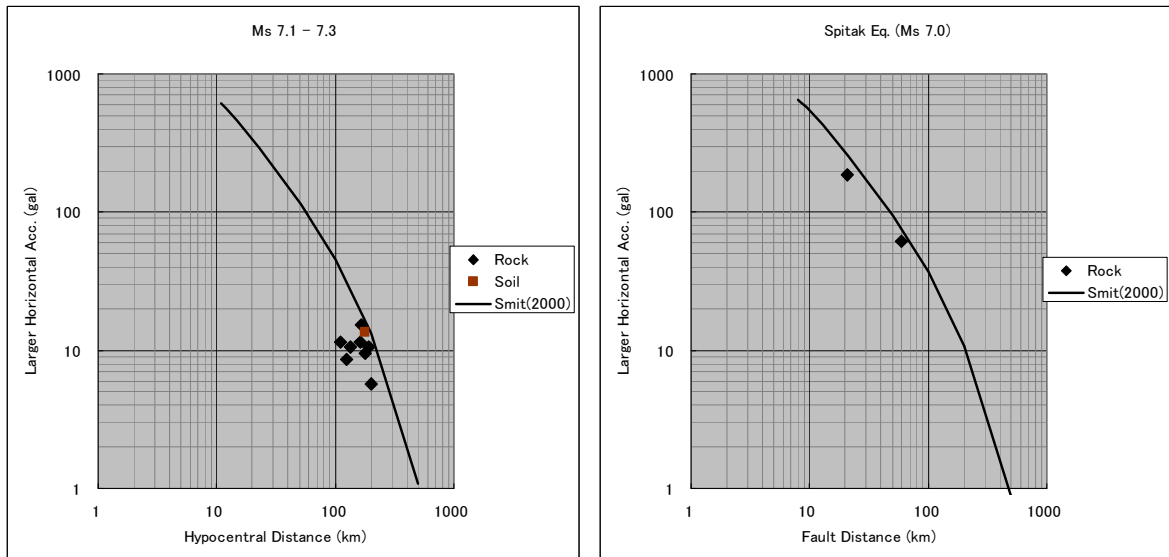


Figure 4.3-1(1) Comparison of observed records with attenuation formula(1)

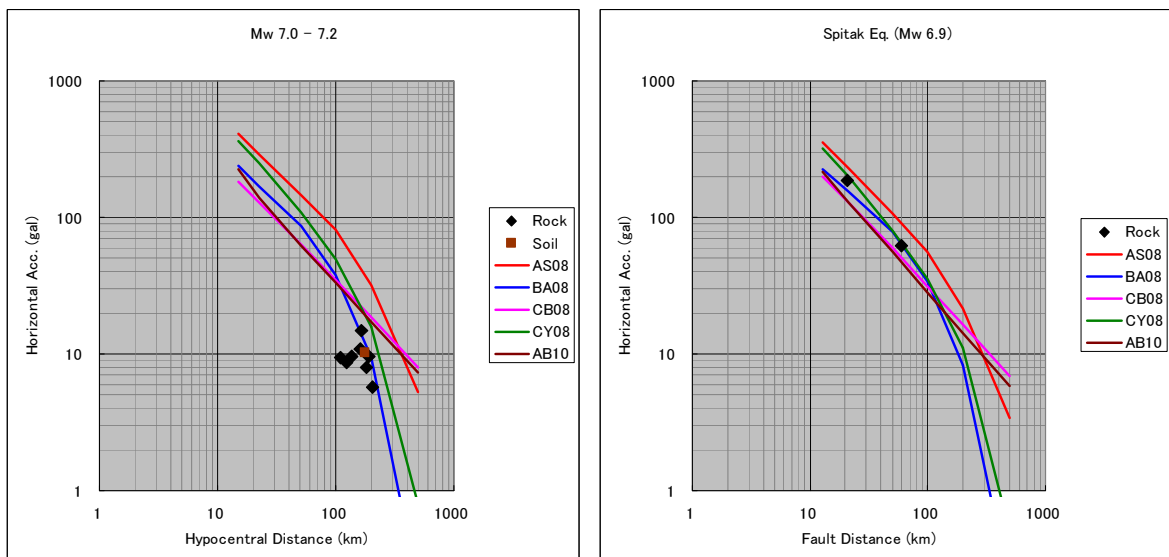


Figure 4.3-1(2) Comparison of observed records with attenuation formula(2)

(2) Baserock Motion

The calculated acceleration by the selected attenuation equations are averaged following the weights in the logic tree which is shown in Figure 4.3-2 and computed the acceleration at engineering seismic baserock. The calculated results are shown in Figure 4.3-3.

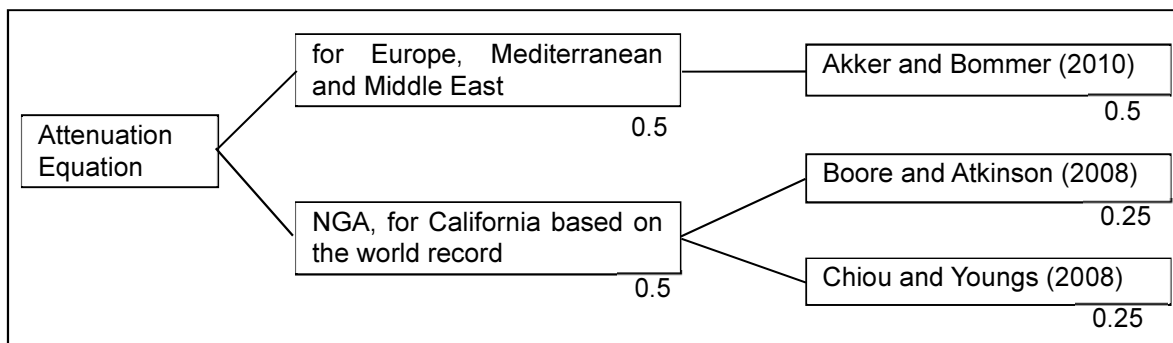


Figure 4.3-2 Logic tree for attenuation formula

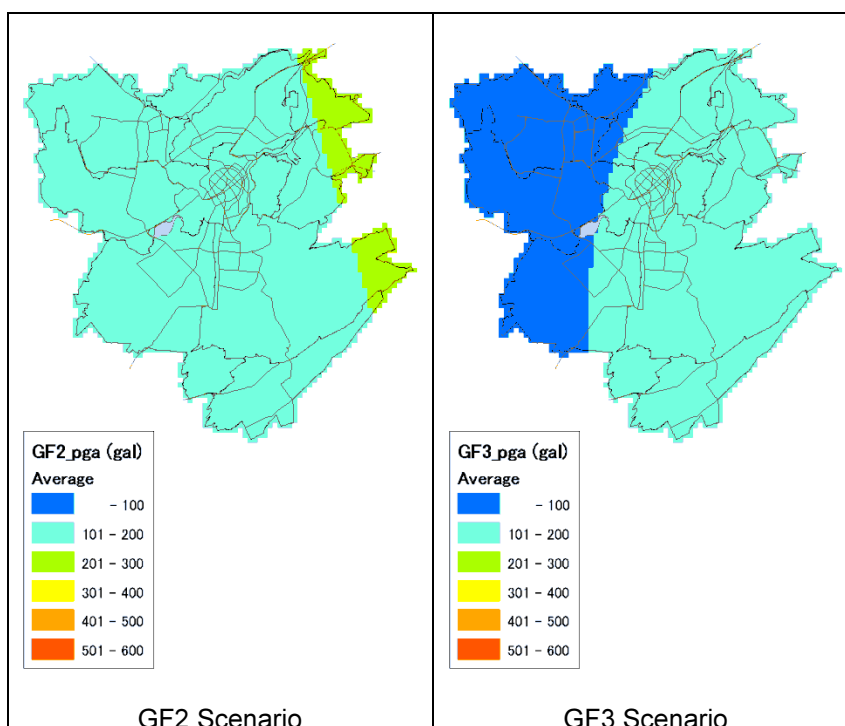


Figure 4.3-3 Acceleration distribution at engineering seismic baserock

4.3.2 Analysis of Surface Ground Motion

(1) Methodology to Evaluate Subsurface Ground Amplification

The subsurface amplification characteristic is evaluated by the 1D equivalent linear response analyses using SHAKE91 at every grid. The used ground models for the analysis are shown in Section 4.1. The conditions of the calculation are shown below.

1) Non Linear Properties

The non-linearity is generally considered for the soil layer whose V_s are smaller than 300 m/sec. The ground conditions in Yerevan are mostly stiff and in some part of south area, there distributes the soil of $V_s < 300$ m/sec. In the land slide area of south east Yerevan (Type 3 in Section 4.1), there

distributes clayey soil near ground surface. Also, in south west Yerevan (Type 2), there distributes gravel layer near ground surface as well.

The non-linearity of the soil is studied by laboratory tests but there are no testing equipments and data regarding non-linearity in Armenia. The typically used non-linearity characteristic curves in Japan (Figure 4.3-4) are used in this study.

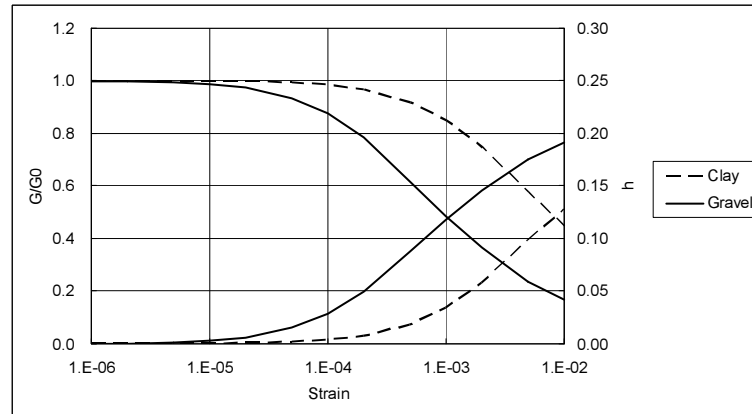


Figure 4.3-4 Non-linearity Characteristic Curves (Central Disaster Management Council (2003))

2) Input Waves

The result of response analysis is affected by the used input seismic wave to the baserock. It is preferable to use the wave form of the earthquake occurred in the source region of scenario earthquakes, which is observed in the study area. The wave form of the earthquake with comparative magnitude to the scenario earthquake, which occurred outside of the source region of scenario earthquakes and was observed in the study area, is the next candidate. However, it is not available such wave forms to meet the above conditions in Yerevan. So, input waves for the response analysis are selected from existing records following the criteria below. In any case, the waves should be observed on the stiff ground of $V_s=760$ m/sec or larger because V_s of basement of the ground model is 760 m/sec.

- a) The wave form of the magnitude 7 class earthquake occurred in Armenia, which was observed at comparative distance for the scenario earthquake model
- b) The wave form of the magnitude 7 class earthquake with same fault type, which was observed at comparative distance for the scenario earthquake model

The 1988 Spitak Earthquake ($M_w=6.9$) wave observed at Gukasyan, whose shortest distance from surface fault by Bommer and Ambraseys (1989) is 20 km, is available to meet the criteria a). Two records observed near fault are selected from 1999 Duzce Earthquake in Turkey ($M_w=7.2$) to meet the criteria b). The wave forms are shown in Figure 4.3-5.

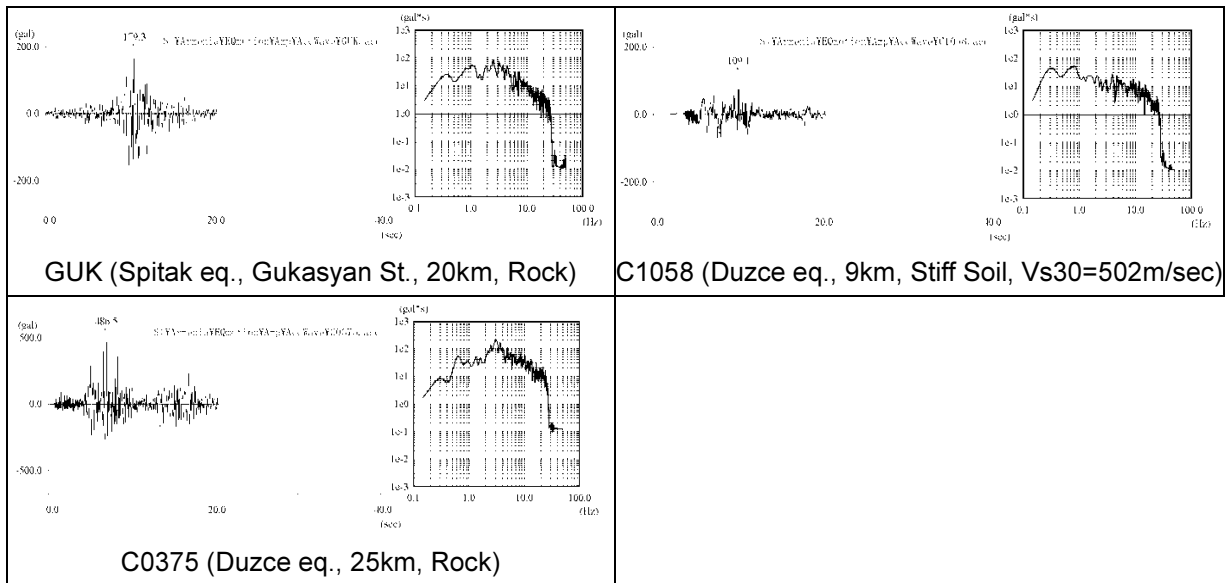


Figure 4.3-5 Input Wave Forms for Response Analysis

(2) Surface Ground Motion

The response analysis was conducted using 3 waves. The calculated accelerations at surface are averaged following the weights in the logic tree which is shown in Figure 4.3-6. The calculated results are shown in Figure 4.3-7.

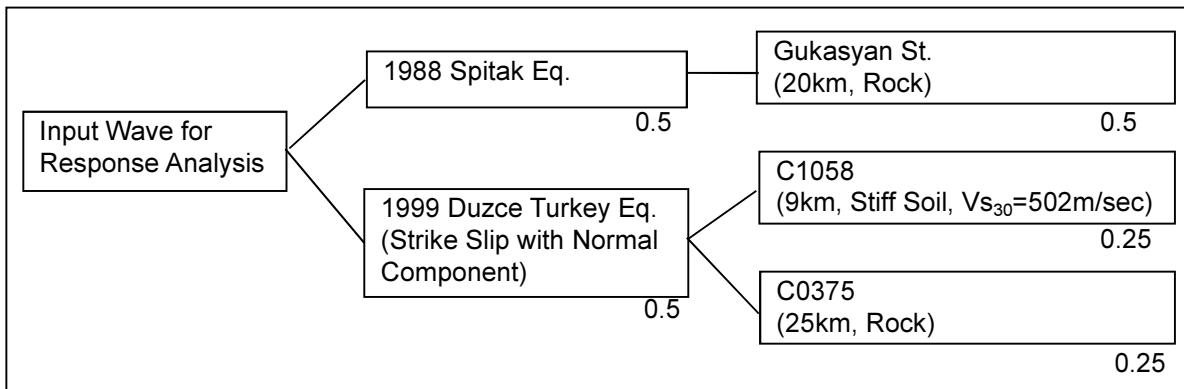


Figure 4.3-6 Logic tree for input wave form

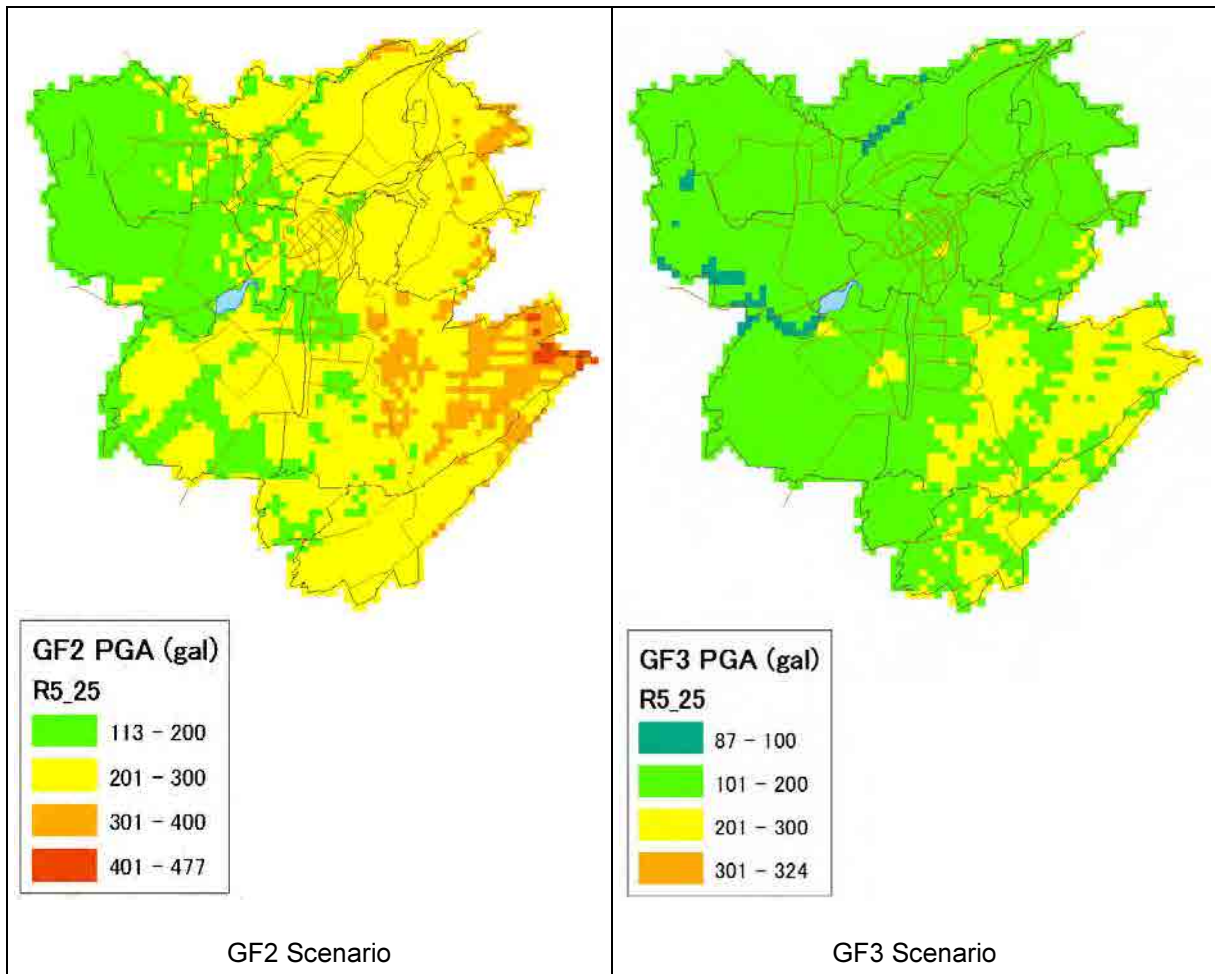


Figure 4.3-7 Acceleration distribution at ground surface

4.3.3 Analysis of Liquefaction Potential

Considering the available data, the F_L method (Japan Road Association, 2002) and P_L method (Iwasaki et al. (1982)) were adopted to estimate the liquefaction potential. These methods are popularly used in Japan and suitable for the seismic hazard assessment because they can evaluate the wide area based on the unified criteria.

(1) Methodology

The procedures and the criteria of the F_L method to assess the liquefaction potential are shown below. The liquefaction potential is given for each calculation depth as the resistivity to the liquefaction.

- 1) Estimate the liquefaction resistance of soils in a deposit (R).
- 2) Estimate the shear stress likely to be induced in the soil deposit during an earthquake (L).
- 3) Estimate the liquefaction potential ($F_L=R/L$) of the deposit, based on 1) and 2).
- 4) Judge the liquefaction potential is high if $F_L \leq 1.0$ and low if $F_L > 1.0$.

In this study, the earthquake type to decide the parameter c_w was supposed as “Type 2” according to the seismotectonic context of the scenario earthquakes.

$$F_L = R/L$$

F_L : liquefaction resistance factor

$F_L \leq 1.0$:	Judged as liquefied
$F_L > 1.0$:	Judged as not liquefied

R: cyclic shear resistance at effective overburden pressure

$$R = c_w \times R_L$$

c_w : correlation coefficient for earthquake type

Type 1 earthquake (plate boundary type, large scale)

$$c_w = 1.0$$

Type 2 earthquake (inland type)

$$\begin{aligned} c_w &= 1.0 && (R_L \leq 0.1) \\ &= 3.3 R_L + 0.67 && (0.1 < R_L \leq 0.4) \\ &= 2.0 && (0.4 < R_L) \end{aligned}$$

R_L : cyclic resistance ratio obtained by laboratory test

$$\begin{aligned} R_L &= 0.0882 (N_a/1.7)^{0.5} && (N_a < 14) \\ &= 0.0882 (N_a/1.7)^{0.5} + 1.6 \times 10^{-6} (N_a - 14)^{4.5} && (14 \leq N_a) \end{aligned}$$

Sandy Soil

$$N_a = c_1 N + c_2$$

$$\begin{aligned} c_1 &= 1 && (0\% \leq F_c < 10\%), \\ &= (F_c + 40) / 50 && (10\% \leq F_c < 60\%) \\ &= F_c / 20 - 1 && (60\% \leq F_c) \end{aligned}$$

$$\begin{aligned} c_2 &= 0 && (0\% \leq F_c < 10\%) \\ &= (F_c - 10) / 18 && (10\% \leq F_c) \end{aligned}$$

F_c : fine contents (%)

Gravelly Soil

$$N_a = \{1 - 0.36 \log_{10}(D_{50}/2.0)\} N_1$$

N: SPT blow count

N_a : N value correlated for grain size

N_1 : $170N/(\sigma_v' + 70)$

D_{50} : grain diameter of 50% passing (mm)

L: shear stress to the effective overburden pressure

$$L = \alpha / g \times \sigma_v / \sigma_v' \times r_d$$

r_d : stress reduction factor

$$r_d = 1.0 - 0.015x$$

x : depth below the ground surface (m)

α : peak ground acceleration (gal)

g : acceleration of gravity (= 980 gal)

σ_v : total overburden pressure (kN/m²)

σ_v' : effective overburden pressure (kN/m²)

The liquefaction of potential at each depth can be judged by F_L method but the effect to the structure at the ground surface is necessary for the hazard assessment. The P_L method by Iwasaki et al. (1988) was adopted for this purpose. P_L is calculated from F_L by following equation.

$$P_L = \int_0^{20} F \cdot w(z) dz$$

$15 < P_L$ Very high potential

$5 < P_L \leq 15$ Relatively high potential

$0 < P_L \leq 5$ Relatively low potential

$P_L = 0$ Very low potential

$$F = 1.0 - F_L \quad (F_L < 1.0)$$

$$= 0.0 \quad (F_L \geq 1.0)$$

$$w(z) = 10.0 - 0.5z$$

P_L : liquefaction potential index

F_L : liquefaction resistance factor

$w(z)$: weight function for depth

z : depth below the ground surface (m)

(2) Parameter Settings

1) Ground Water Level

The ground water level in Yerevan city is estimated from the information of water depth included in the existing borehole database. If several water depth data are included in one borehole, the shallowest data is adopted. As the ground water depth has strong relation with topography in general, the relation between ground water depth and the altitude is studied and shown in Figure 4.3-8. From this figure, the highest ground water level in rainy season is set by red colored line for the liquefaction analysis. Because the observed data include the deviation by observation error, difference of season, change of the situation of pumping for industrial use etc., the shallowest data is used to estimate the most severe condition. Figure 4.3-9 shows the ground water depth distribution for liquefaction analysis.

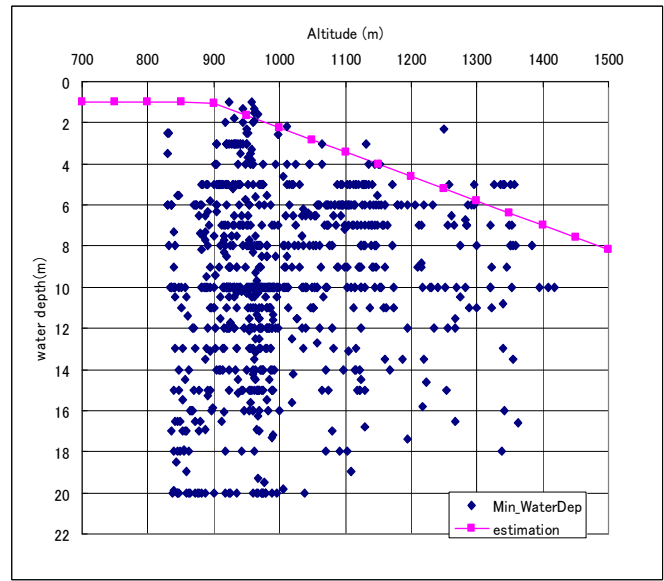


Figure 4.3-8 Relationship between ground water depth and altitude

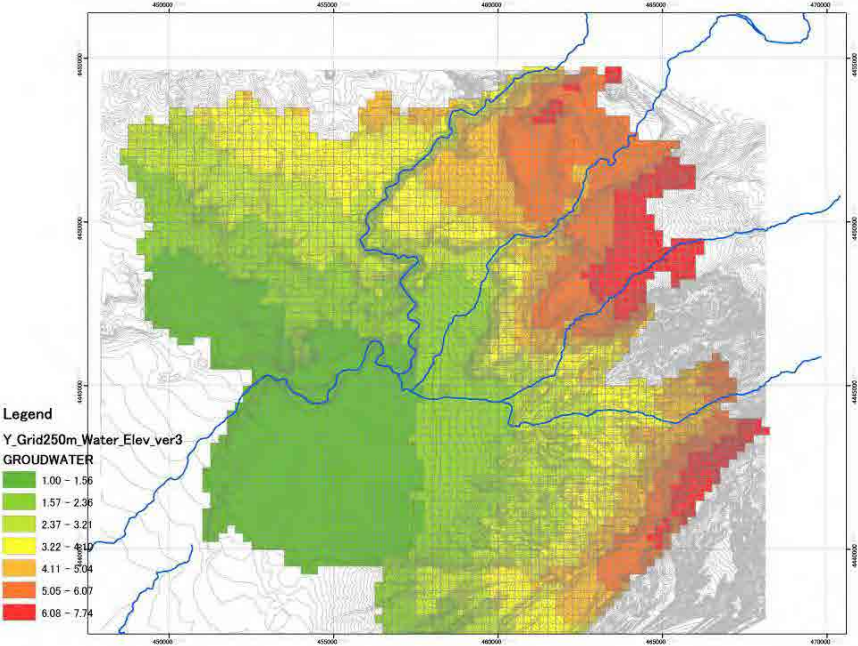


Figure 4.3-9 Estimated ground water depth

2) Thickness of the sandy layer

The sandy layer, which should be studied in Yerevan city, only included in the Ararat lowland deposits (IaQ₁₋₂). The distribution of sandy layer is estimated from the relation between the upper and lower depth of the sandy layer and the altitude as shown in Figure 4.3-10.

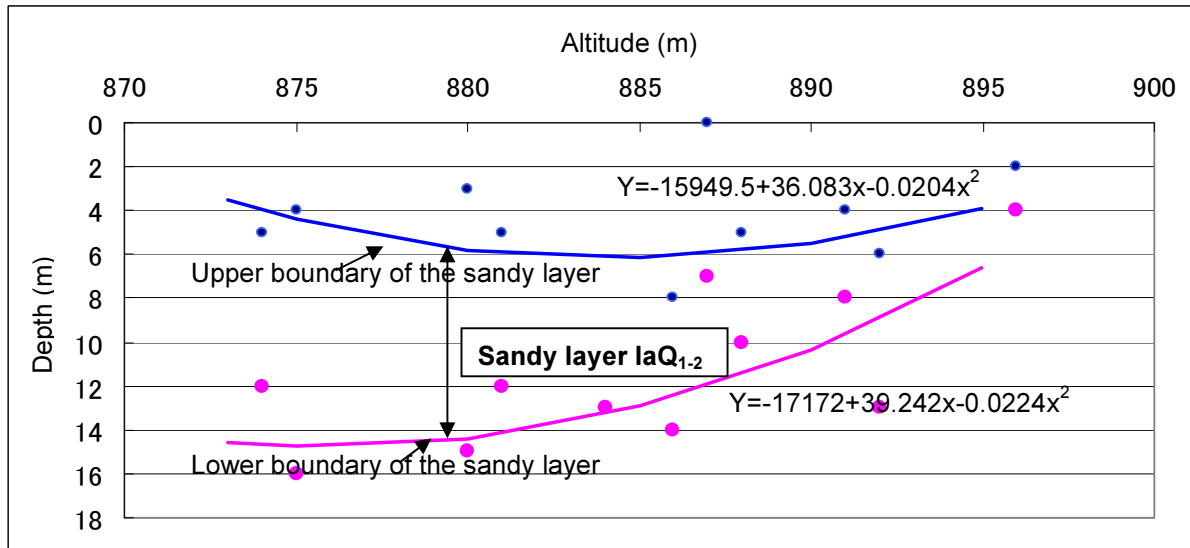


Figure 4.3-10 Relationship between the altitude and the upper/lower boundaries of sandy layers (IaQ₁₋₂, Ararat lowland)

3) N value

The standard penetration test is conducted during the new boring in this project. The N-values of the sandy layer are, however, show unreasonably high value comparing the soil condition: most data are larger than 50. This may be the effect of the inclusion of pebbles or gravels. Therefore, the N value is estimated from S wave velocity following Imai (1982) because S wave velocity and N value has strong relation. The estimated N value for $V_s=220\text{m/sec}$ layer is 14 and 33 for $V_s=290\text{m/sec}$ layer.

4) Other parameters

As the data regarding particle size, density and physical data, which are necessary for liquefaction analysis, are not found in existing boring database, laboratory tests are conducted using the soil sample by newly conducted 10 borings. The sand was found between 8 to 12 m and 15 to 16 m of BH-10. The average properties of them are as followings;

- | | |
|---|----------------------|
| a) D ₅₀ (Mean particle diameter) | 0.072mm |
| b) F _c (Fine fraction content) | 53.0% |
| c) Density Sand | 1.8g/cm ³ |
| Gravel / Pebbles | 2.0g/cm ³ |

(3) Liquefaction Potential

Figure 4.3-11 shows the liquefaction potential of each scenario earthquakes. According to these maps, fortunately, there are very little areas with sandy soil layers and the liquefaction potential in Yerevan is low.

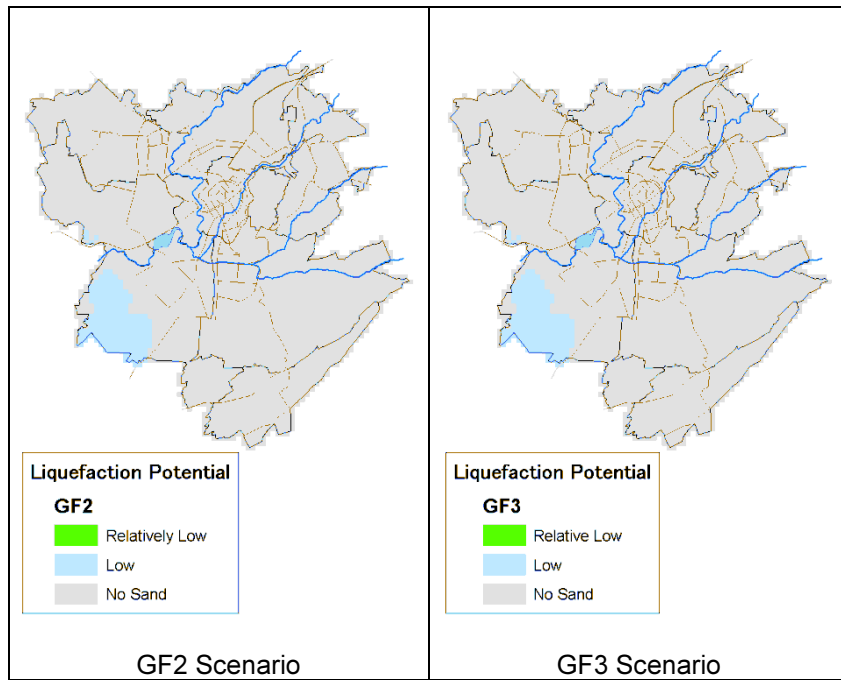


Figure 4.3-11 Liquefaction potential

4.3.4 Slope Stability

(1) Landslide hazard

Landslide hazard is assessed by the factors of geomorphologic and geological observation, land deformation, hydrological features, and the state of damage. The method of the assessment is based on the scores of each category in Japan and inductive element of the landslides in the territory of Yerevan city.

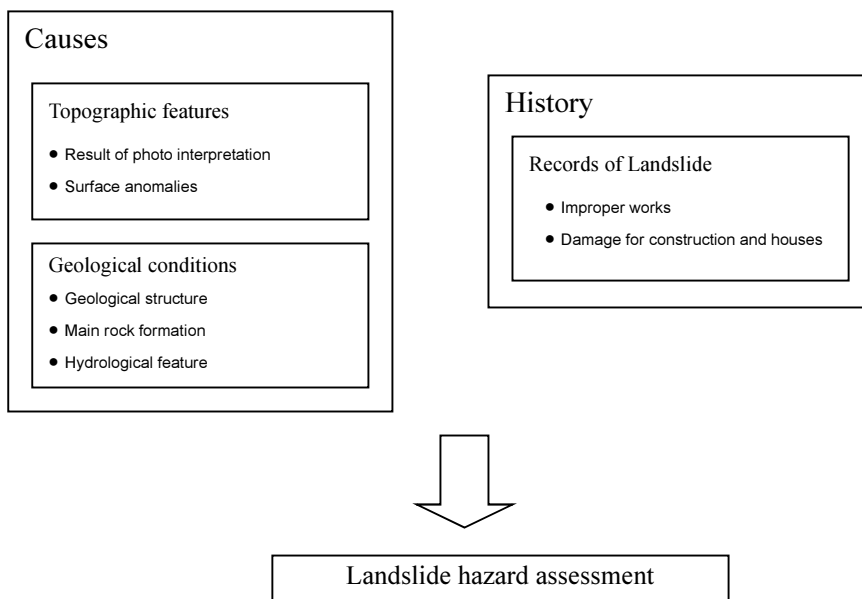


Figure 4.3-12 Flowchart of landslide hazard assessment

Landslide risk was evaluated by landslide hazard and influence to the risk objects, for example, houses and buildings, infrastructures and their locations. Location and distance indicate effectiveness of landslide to risk objects. Closer the distance from the landslide and risk object is, more serious and influential to the risk objects.

Table 4.3-1 Landslide hazard assessment categories and their scores

Category / Score		4	2	1	0	
A: Causes	Topographical features	Result of photo interpretation	exist clearly	exist but partial and not clear	exist but not clear	
		Surface anomalies	large and new cracks, steps and subsidence	small and old cracks, steps and subsidence	slight deformation	no anomalies
	Geological conditions	Geological structure		fault, fracture / dip slope	undip slope and others	
		Main rock formation	Hatsavan suite and Shorakhpiur suite	Hrazdan suite and Jrvezh suite	Other Tertiary rocks and sediments	Other Quaternary rocks and sediments
		Hydrological feature	much springs / seepage	little springs / little seepage	surface water / trace of water	no water observed
B: History	Records of Landslide	Improper works	obvious	slight	not exist	
		Damage for construction and houses	obvious	slight		no indication/ no constructions

Table 4.3-2 Landslide Risk for the houses and infrastructures

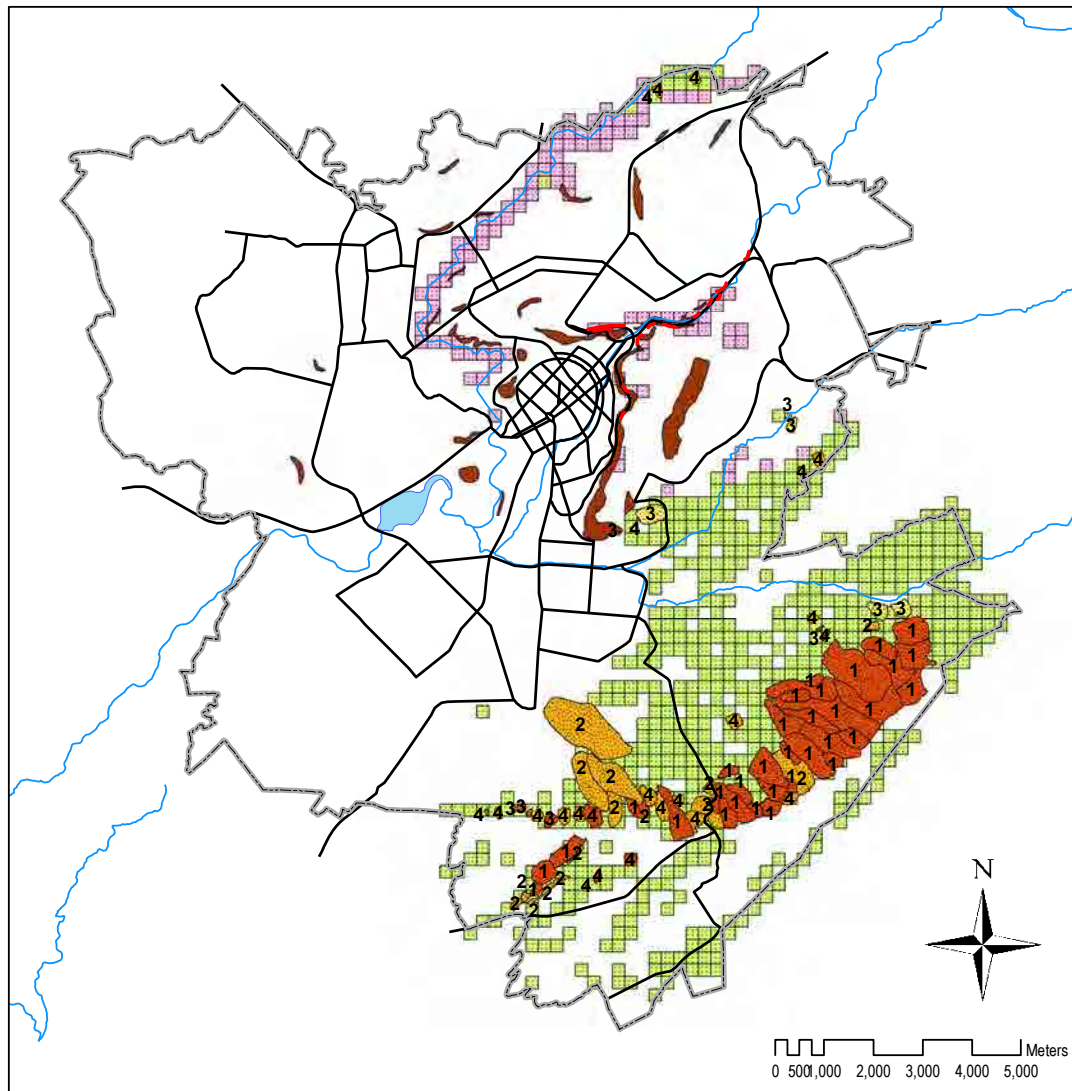
		Influence to the houses and infrastructures			
		A	B	C	D
Landslide hazard	A	1	2	3	4
	B	2	3	4	4
	C	3	4	4	4

1: Extremely High Risk, 2: High Risk, 3: Middle Risk, 4: Relatively Low Risk

Figure 4.3-13 shows existing landslide hazard and risk, potential hazard areas of landslide and slope hazards in the territory of Yerevan city. Most of the high hazard landslides belong to Shorakhpiur-Nubarashen (Sovetashen) Landslide Group. The landslides on east slope of Erebuni district (north-western slope of Nubarashen terrace) and slopes in Nor Kharberd are high hazardous landslides. Because most of those landslides are near or in the village or infrastructures existing areas (roads, water pipes, gas pipe, power lines, etc.), those landslides are also high risk.

Potential of the landslide can be evaluated from the relation between geology and slope angle. Most of the landslides are in the area of Hatsavan suite (conglomerates, sandstones, red-colored clays, aleurolites), Shorakhpiur suite (aleurolites, tuff sandstone, sandstone, and conglomerates), Hrazdan suite (marly clay, limy sandstone with inter-layers of oolitic limestone coquina and combustible

shale) and Jrvezh suite (gypsum-saliferous clay, sandstone, and basalt). Landslides occurred on the slopes of 5 to 30 degrees.



Legend

Landslide Hazard

Rank

- A High Hazard
- B Middle Hazard
- C Low Hazard

Risk Zones of Slope Hazards

- Slope Failure and Rock Fall for Buildings and Houses
- Slope Failure and Rock Fall for Main Roads

Potential Hazard Areas of Slope Hazards

- Type**
- Landslide
 - Slope Failure and Rock Fall

- River
- Lake
- Major Road
- City border

Numbers on the landslides indicate the landslide risk for buildings, houses and infrastructures.
 1: Extremely High Risk
 2: High Risk
 3: Middle Risk
 4: Relatively Low Risk

Figure 4.3-13 Landslide hazard and risk map

(2) Rock fall, slope failure, filled land failure and collapse of stone wall

In case of earthquake, rock fall, slope failure, filled land failure and collapse of stone wall occur as well as landslides.

Rock falls of fractured basalt and basaltic andesite lavas that developed large-debris breccia-like and columnar structures mostly is prone to occur on banks of the rivers (Hrazdan river, Getar river and Irvezh river) where steep and vertical hanging walls of different heights created.

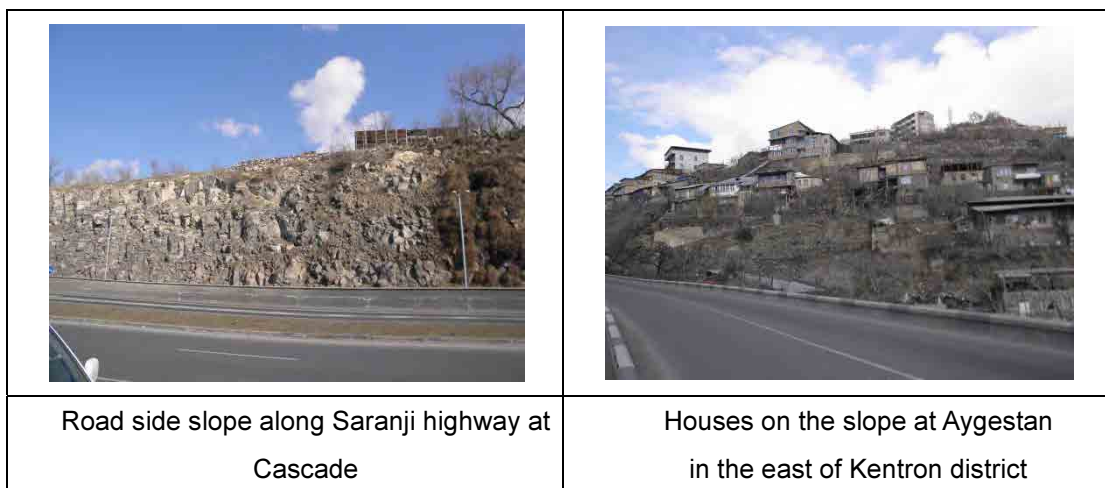
These slopes of volcanic rocks change their appearance, their stable situation is disrupted and fragments fall down into the valleys, forming huge accumulations of large-debris, called talus at the base of the slopes. As rock falls and slope failures occurred on those steep slopes, the potential of rock falls and slope failures is considered to be high at volcanic rock slope with the angle more than 15 degrees.

In the territory of Yerevan city, road side slope along Saranji highway at Cascade, Alexander Myasnikyan avenue, Nork-Sari-Tagh road and others are high hazard for rock fall. Those sections are consist of basalt and basaltic andesite with many cracks and at unstable conditions.

Some houses are constructed on the around 20 degrees slope with steel frame. Those houses and basement are prone to collapse by the shaking and deformation of the ground.

In Figure 4.3-13, “Slope Failure and Rock Fall for Buildings and Houses”, “Slope Failure and Rock Fall for Main Roads” are shown.

Stone walls are also dangerous in case of earthquake. Many of the stone walls are 2m or more high and supported by pillar with steel bar. But the intervals between pillars are 2 or 3m, that is not enough to support the wall in case of earthquake. Stone walls do not exist so many in commercial areas and business areas, but exist many in the suburb and rural areas.



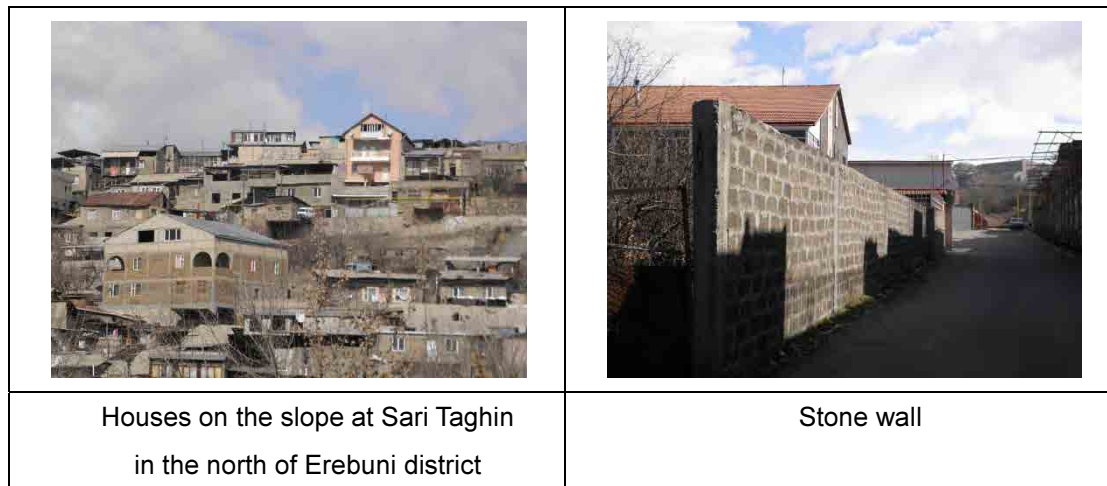


Figure 4.3-14 Road side slope , houses on the slope and stone wall

References:

Abrahamson N. and W. Silva, 2008, Summary of the Abrahamson & Silva NGA Ground-Motion Relations, *Earthquake Spectra*, Vol. 24, Issue 1, pp. 67-97.

Akker, S. and J. Bommer, 2010, Empirical Equations for the Prediction of PGA , PG V, and Spectral Accelerations in Europe, the Mediterranean Region, and the Middle East, *Seismological Research Letters*, Vol. 81, No.2, pp. 195-206.

Bommer, J. J. and N. N. Ambraseys, 1989, The Spitak (Armenia, USSR) Earthquake of 7 December 1988: A Summary Engineering Seismology Report, *Earthquake Engineering and Structural Dynamics*, Vol. 18, pp. 921-925.

Boore D. M. and G. M. Atkinson, 2008, Ground-Motion Prediction Equations for the Average Horizontal Component of PGA, PGV, and 5%-Damped PSA at Spectral Periods between 0.01 s and 10.0 s, *Earthquake Spectra*, Vol. 24, Issue 1, pp. 99-138.

Campbell K. W. and Y. Bozorgnia, 2008, NGA Ground Motion Model for the Geometric Mean Horizontal Component of PGA, PGV, PGD and 5% Damped Linear Elastic Response Spectra for Periods Ranging from 0.01 to 10 s, *Earthquake Spectra*, Vol. 24, Issue 1, pp. 139-171.

Central Disaster Management Council, 2003, 16 th Meeting of Working Group for Tonankai and Nankai Earthquake, Reference Material No. 2-3 (in Japanese).

Chiou B. S.-J. and R. R. Youngs, 2008, An NGA Model for the Average Horizontal Component of Peak Ground Motion and Response Spectra, *Earthquake Spectra*, Vol. 24, Issue 1, pp. 173-215.

Imai T. and Tonouchi K., 1982, Correlation of N value with S-wave velocity and shear modulus, ESPOT II.

- Iwasaki, T., Tokida, K., Tatsuoka, F., Watanabe, S., Yasuda, S. and Sato, H., 1982, Microzonation for Soil Liquefaction Potential Using Simplified Methods, Proc., 3rd Int. Conf. on Microzonation, Seattle, Vol.3, pp1319-1330.
- Japan Road Association, 2002. Specifications for Highway Bridges, Part V Earthquake Resistant Design.
- Smit, P., V. Arzoumanian, Z. Javakhishvili, S. Arefiev, D. Mayer-Rosa, S. Balassanian and T. Chelidze, 2000, The Digital Accelerograph Network in the Caucasus, in Balassanian, S. (ed.), earthquake Hazard and Seismic Risk reduction - Advances in Natural and Technological Hazards research. Kluwer Academic Publishers.

4.4 Earthquake Motion by Yerevan Fault

The Yerevan Fault locates south-west of Yerevan city. The seismic activity of Yerevan Fault is not well known, however if it ruptures, Yerevan city might be affected seriously. The nature of the Yerevan Fault is discussed from 1950s (e.g. Aslanyan, 1954, 1958; Gabriyelyan, 1959, 1981), but the seismic activity, length, depth, dip, segmentation etc. are clarified only a few even now. As most of the part of Yerevan Fault may be a blind fault; it is difficult to study especially near the Yerevan city by trench survey.

Since the nature of Yerevan Fault as the earthquake source model is not well understood scientifically, the Yerevan Fault is not adopted as the source of scenario earthquake in this project. It can be one of the earthquakes to be referenced. Therefore, it is valuable to know the investigated results especially estimated earthquake motion by Yerevan Fault activity for the risk management of Yerevan city.

In this section, the earthquake motion by Yerevan Fault is estimated. As the length of Yerevan Fault is not clarified, and also considering the case of movement of only small part of the fault, four magnitudes are adopted and the corresponding fault models are made as shown in Table 4.4-1 and Figure 4.4-1. The precise considering in setting the parameters are written in the following.

(1) Fault Type

The type of Yerevan Fault is supposed to be reverse fault from trench survey.

(2) Length of Fault

There are many ideas concerning the south east end of Yerevan Fault. One idea supposes the 30km length of the fault based on the gravity anomaly data and the shape of the sediment basin (see Report on the Yerevan Fault by Georisk). In this study, the Yerevan Fault is supposed to extend as far as the south east of Nor Ughi about 40km length in maximum because active fault is found at Nor Ughi by the pilot trench survey.

(3) Dip of Fault

As for the Yerevan Fault, north dipping reverse fault with 26 degree was found at Nor Ughi pilot trench site, however, the dip angle of the fault at deep ground is unknown. Tovmasyan (2008) studied the mechanism of 15 small to moderate earthquakes occurred within 30km from Yerevan

between 1973 to 2002 and found 11 events have reverse mechanism. The dip angle of the earthquakes of north dipping and east to west or north-west to south east striking earthquakes showed 55 to 72 degree after Tovmasyan (2008). The dip angle of Yerevan Fault model is set to 55 degree after Tovmasyan (2008) because Yerevan fault may not be the reverse fault with steep angle based on the pilot trench result.

(4) Depth of Fault

The depth of upper boundary of Yerevan Fault is set to 5km reflecting that Yerevan Fault is blind near Yerevan.

(5) Magnitude and Location

The length of the Yerevan Fault is supposed as 30 to 40 km in maximum. Based on the empirical relation by Wells and Coppersmith (1994), the maximum moment magnitude of the earthquake which may occur by the activity of Yerevan Fault may be Mw=6.8. However it may be possible to move only small part of Yerevan Fault and earthquake with smaller magnitude may occur. The largest earthquake which occurred near in south west of the Yerevan city in recent years is 1937.1.7 earthquake with magnitude 4.6 near Parakar. The damage in Yerevan city was slight. Based on these, the magnitude of 6.8 (maximum), 6.2, 5.6 and 5.0 are set to show the difference of the earthquake motion by the difference of magnitude. The fault lengths of these smaller earthquakes are estimated by empirical relation by Wells & Coppersmith (1994). The location of the fault is set as the part of fault model of maximum magnitude earthquake near Parakar.

The method of baserock motion analysis is same to the scenario earthquakes which are shown in Section 4.3. The method of amplification analysis is same but the used input wave is only Gukasyan wave by Spitak earthquake. The calculated surface ground acceleration is shown in Figure 4.4-2.

Table 4.4-1 Fault Parameters of Yerevan Fault

	Yerevan Fault			
Moment Magnitude (Mw)	6.8	6.2	5.6	5.0
Fault Type	Reverse Fault			
Length (km)	40	15	6.7	3.0
Dip (degree)	55 (to north-east)			
Depth(Upper - Lower) (km)	5 - 12	5 - 11	5 - 8	5 - 6
Width (km)	8.6	7.5	3.3	1.5

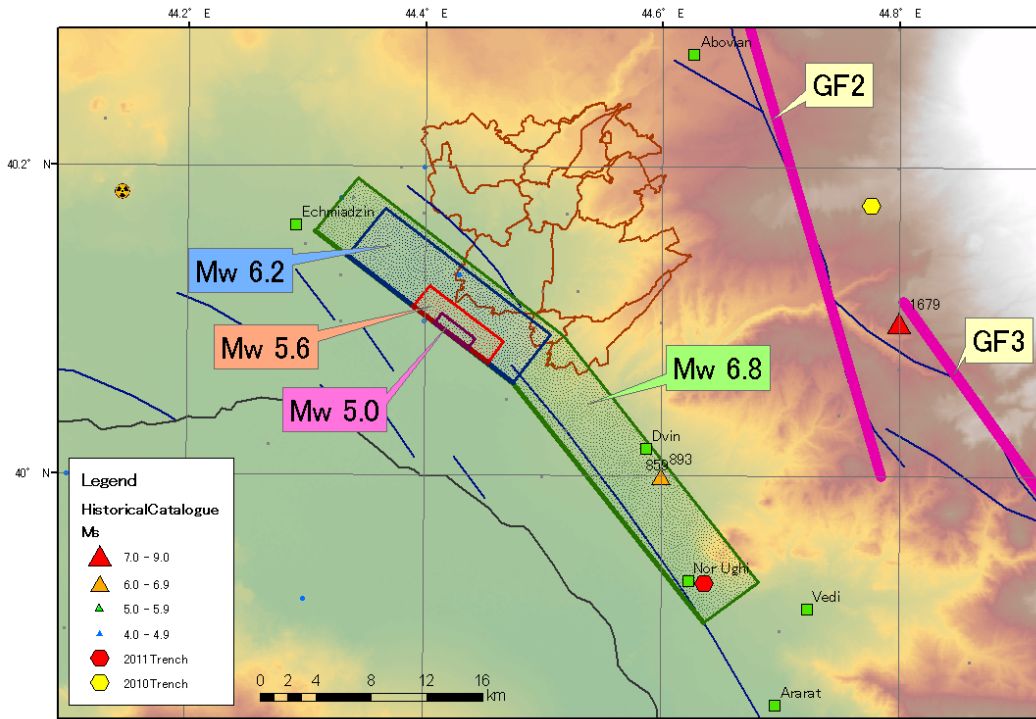


Figure 4.4-1 Source Fault Models of Yerevan Fault

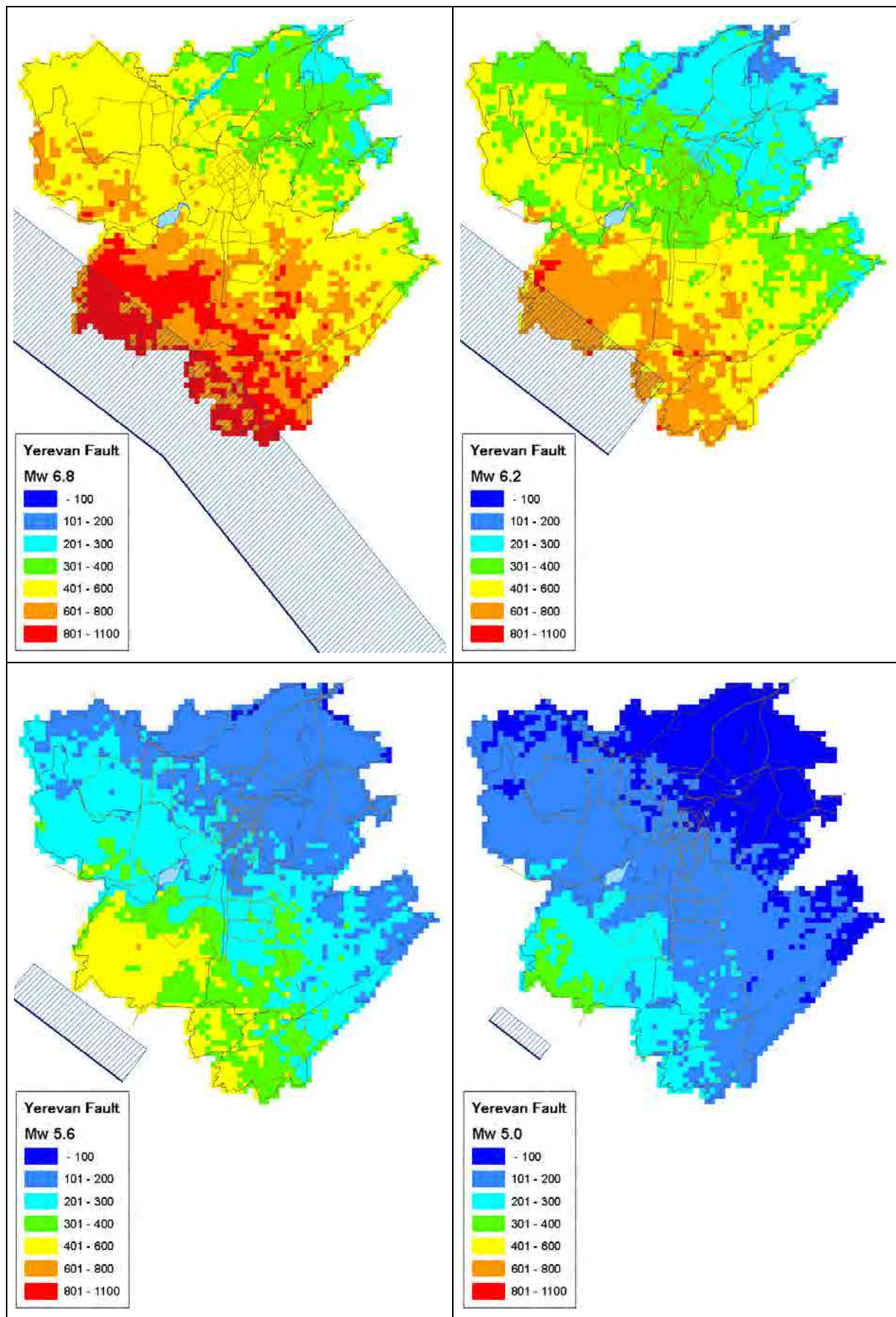


Figure 4.4-2 Acceleration distribution at ground surface by Yerevan Fault

References:

- Aslanyan, A. T., 1954, Deep fault near Yerevan City. Volume of contribution summaries of the 6th Science and Technology Conference of the Transcaucasian High Technological University Professors and Lecturers (in Russian)
- Aslanyan, A. T., 1958. Regional geology of Armenia, HaiPetHrat, Yerevan (in Russian)
- Gabrielyan, A. A., 1959, Main issues of the geotectonics in Armenia. Publishing House of the AS of the Armenian SSR, Yerevan (in Russian)
- Gabrielyan, A. A., O. A. Sargsyan, and G. P. Simonyan, 1981, Seismotectonics of the Armenian SSR. Publishing House of the Yerevan State University, Yerevan (in Russian)
- Tovmasyan, A. K., 2008, Focal Mechanisms of Yerevan Earthquakes, The modern main issues of Geology and Geography, 297-305.
- Wells, D. L. and K. J. Coppersmith (1994) New Empirical Relationships among Magnitude, Rupture Length, Rupture Width, Rupture Area, and Surface Displacement. Bull. Seismol. Soc. Am., 84, 974-1002.

Georisk report:

Report on the Yerevan Fault, 43p.

Chapter 5 Inventory Survey of Structure

5.1 Building Sampling Survey

5.1.1 Outline

A building sampling survey was conducted to get necessary information for structural types and vulnerability assessment. Number of surveyed buildings is as follows and buildings are selected randomly. Structural sheet called 'Passport' was prepared for surveyed buildings. The survey was conducted by "SEISMANAKHAGITC" LLC under the JST.

- Multi-story residential buildings : 100 nos
- Individual houses : 30 nos
- Schools and hospitals : 20 nos Total 150 nos.

5.1.2 Structural types of multi-story residential buildings

Structural types and brief description of multi-story residential buildings based on the sampling survey are shown in Table 5.1-1. Categories are three types for stone buildings and five types for RC structures. Most of buildings had been constructed before the Spitak earthquake in 1988, and 'monolithic' has been constructed after the earthquake.

Table 5.1-1 Structural types and brief description of multi-story residential buildings

No.	Structural type/ Popular name	Number of stories	Constructed year	Brief description of structure/construction
1	Stone, individual design	Mainly 4, 3~6	Till 1958. 3-story by 1940.	Mydis type wall (cut stones are provided at both side and mortar/crushed stones are filled at center). Lime mortar is used. Wall thickness is 60cm. Wooden floor and concrete stairs.
2	Stone, series1-451	4~5	1958~ till the beginning of 1970s	Mydis type wall is used. Thickness is 50cm with cement mortar. Precast concrete void slab. Anti-seismic belts are provided around floor slabs.
3	Stone, series 1A-450	4~5	Beginning of 1970s ~1988	Mydis type wall. Thickness is 50cm with cement mortar. Precast concrete void slab. Anti-seismic belts are provided around floor slabs. Vertical reinforcement of RC members were provided for walls.
4	Frame panel, series 111, Precast RC frame	9	1975~1988	RC resisting frame for longitudinal direction. Column and structural panel (wall) for transverse direction. Column sizes are 40cmx40cm. Precast void slab.
5	Lift slab	12 and 16	1970~1988	Cat-in-situ core wall and precast columns with cast-in-situ flat slabs. Flat slabs are lifted to the right position utilizing columns.
6	Frame and frame ,Badalyan type and Maroukyan type	12 (10) and 14 (18) for Badalyan. 9~12 for Maroukyan.	1960s ~1988.	Precast RC frames for both directions. Column size is 50cmx50cm. It is evaluated that the ductility is better than that of 'frame panel', considering the position of re-bar joints. Column size of Maroukyan is 40cmx40cm. No construction in Spitak area.
7	Large panel (series 1-451LP, others)	9 and 5. Includes 4, 8	1970~ until now.	Wall type precast RC structure.
8	Monolithic Cast-in -situ RC resisting frame.	Midium to high-rise.	After Spitak and after 1994 .	Cast-in-situ RC resisting frame including frame with RC wall. Design based on new seismic code of 1994. Non-structural wall is light weight concrete blocks.

5.1.3 Constructed year and number of stories of multi-story residential buildings

Constructed year and number of story is summarized and is shown in Figure 5.1-1. Design and construction based on ‘series’ has started in 1960s. Fabrication of precast members has started at factories in mid. of 1960s, and was developed in 1970s. Monolithic is commonly designed and constructed after the Spitak earthquake in 1988, and based on new code RABC in 1994.

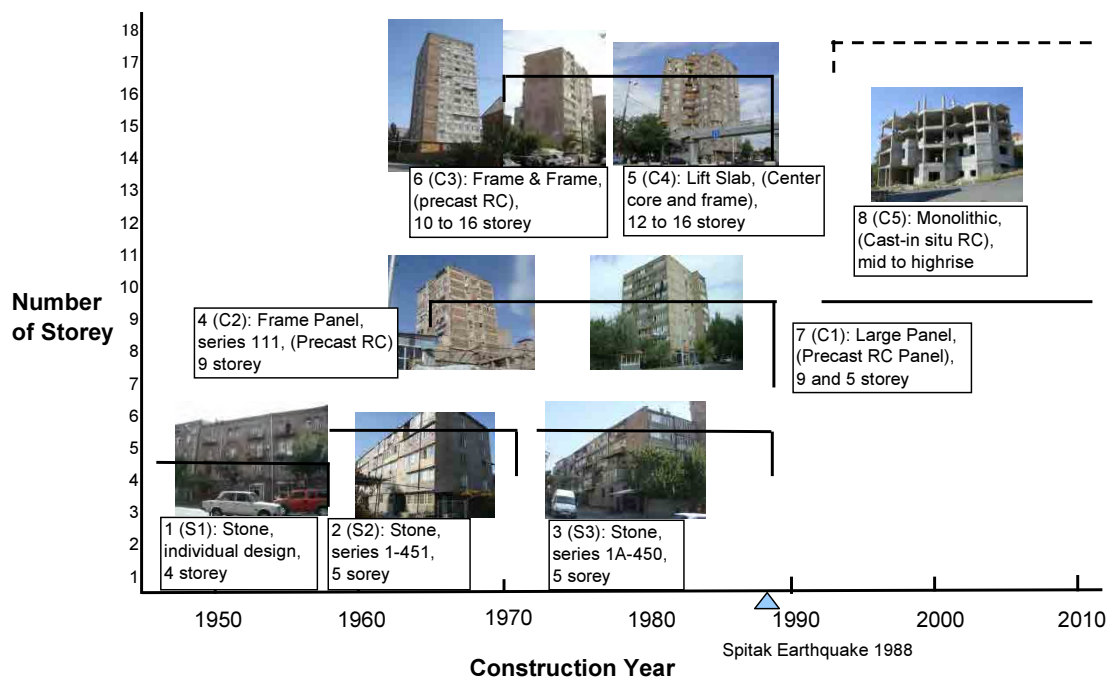


Figure 5.1-1 Constructed year and number of story

5.1.4 General description and external view of multi-story residential buildings

(1) Stone building, individual design

Stone buildings, by individual design are shown in Figure 5.1-2. Mydis type wall with lime mortar and crushed stone is used.



(left) 4-story at the city

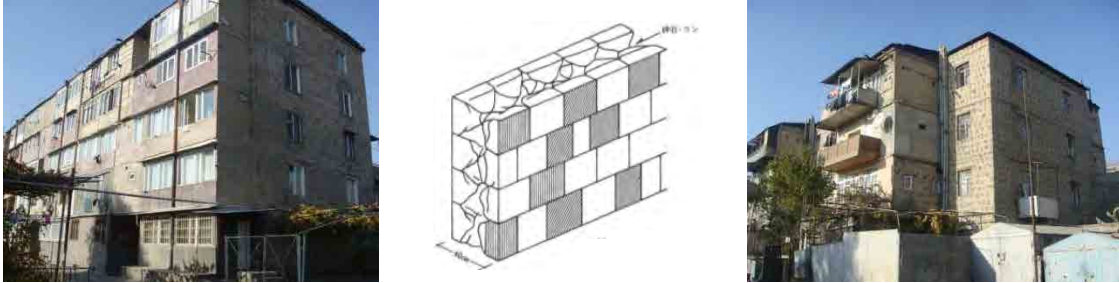
(center) 4-story at Kentron

(right) An example of floor plan

Figure 5.1-2 Stone buildings, by individual design

(2) Stone building, series 1-451

Stone buildings, series 1-451 is shown in Figure 5.1-3. Mydis type wall with cement mortar and crushed stone is standard. Stone masonry type with clear joint (right of Figure 5.1-3) is rarely used where located at inner court that cannot be seen from main roads.



(left) Series 1-451 with extension (center) Mydis type wall (ref 2.) (right) Stone masonry type at Shengavit
Figure 5.1-3 External view of series 1-451, and Mydis type wall

(3) Stone building, series 1A-450

Stone buildings, series 1A-450 is shown in Figure 5.1-4, and typical section is in Figure 5.1-5.



Figure 5.1-4 Stone buildings, 1A-450 at Malatia-Sebastia

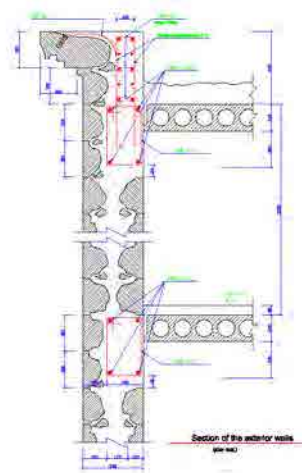


Figure 5.1-5 Typical section of series 1A-450

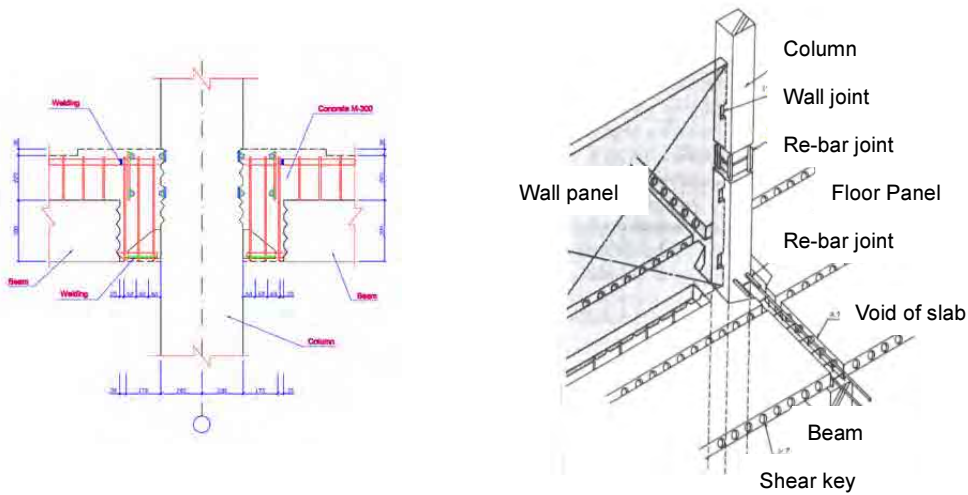
(4) Frame panel, series 111

‘Frame panel, series 111’ is shown in Figure 5.1-6. Frame resisting structure of precast members for longitudinal direction, and precast structural panel for transverse direction. Non-structural precast panels are provided for external wall. Main joints for members are shown in Figure 5.1-7.



(left) and (center) ‘Frame panel’ at Malatia-Sebastia (right) ‘Under construction’ (by NSSP EEC)

Figure 5.1-6 ‘Frame panel, series 111’ buildings



(a) Joint of beam and column (b) Joints of members (ref.2)

Figure 5.1-7 Main joints of ‘Frame panel’

(5) Lift slab

‘Lift slab’ is representing construction method. Cast-in-situ wall is provided at core. Flat slabs cast at lower floor are lifted to the right position utilizing precast columns. Thickness of core wall is 40 to 50cm. Column size is 40 to 50cm. External view and plan are shown in Figure 5.1-8 and Figure 5.1-9.



(left) 12-story single core type at Shengavit (right) 12-story double core type at Nor Nork
(center) Construction abandoned building at Ajapnyak

Figure 5.1-8 External view of ‘lift slab’ buildings

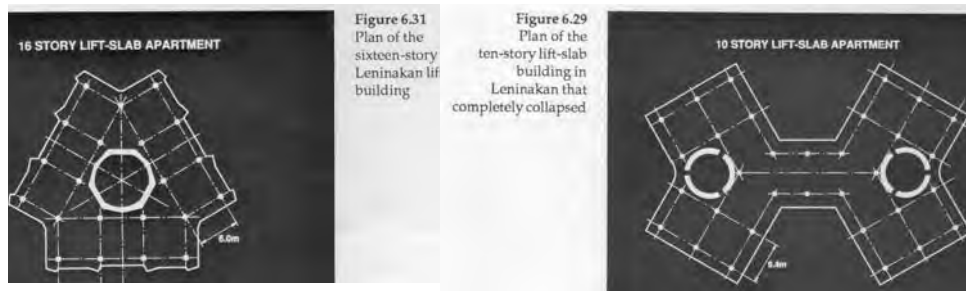


Figure 5.1-9 Typical plan of 'Lift slab' (ref.1)

(6) Frame and frame

There are two types for 'Frame and frame', Badalyan type and Maroukyan type, and are shown in Figure 5.1-10. No construction at Spitak area. Precast frames of Badalyan type is shown in Figure 5.1-11 and Figure 5.1-12. After the installation of precast members, concrete is cast at site to unify the structure.



(a) 14-story Badalyan at Malatia-Sebastia (b) Maroukyan at Kentron

Figure 5.1-10 'Frame and frame' buildings



Figure 5.1-11 Badalyan type under construction

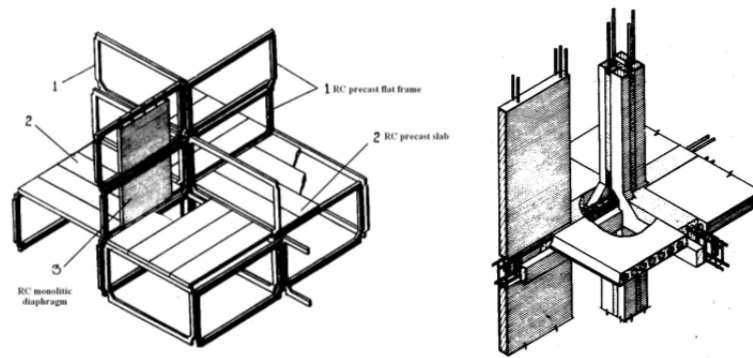


Figure 5.1-12 Precast members of Badalyan
(panel shown is non-structural wall)

Joint of beam and column by Maroukyan system is shown in Figure 5.1-13. Position of welding for main re-bar of beam is the center of column for lower re-bar, and the center of beam for upper re-bar.

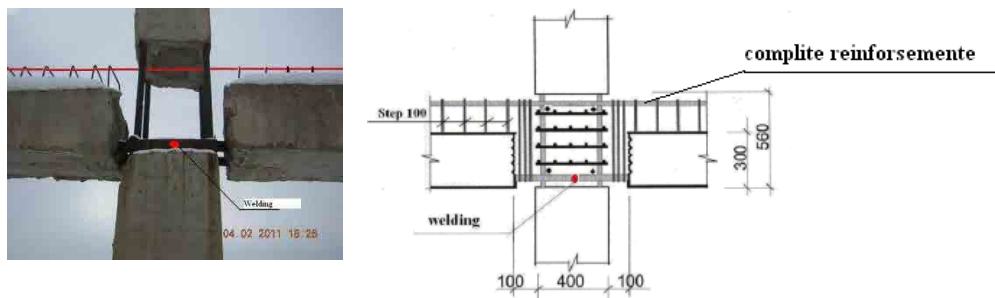


Figure 5.1-13 Joint of beam and column by Maroukyan type

(7) Large panel

‘Large panel’ is wall type precast RC structure. There are three types of 9-story, square plan and rectangular plans. There are also 5-story and 4-story. Connection detail of ‘Large panel’ is similar to that of Japanese wall type precast RC structure (ref. 2). It is said that some deviation is observed for the construction quality because the construction NORM (standard) has not been utilized well.



(a) 9-story at Erebuni (b) 9-story at Davtashen (c) 9-story at Shengavit (d) 5-story at Maratia-Sebastia

Figure 5.1-14 ‘Large panel’ buildings

(8) Monolithic

‘Monolithic’ which is cast-in-situ RC structure is shown in Figure 5.1-15. Typical finishing is light weight block wall with stone finish. Frames with RC wall structure are also used for high-rise buildings.



(left) Under construction at north of Kentron

(right) Under construction in Yerevan

(center) Under construction at north of Kentron

Figure 5.1-15 ‘Monolithic’ buildings

5.1.5 Structural category of individual houses

Almost all individual houses are stone houses. Structural category based on type of material for stone joints of wall is proposed. There is correlation between type of joint and constructed year. Proposed structural category and supposed constructed year is shown in Figure 5.1-16.



Figure 5.1-16 Proposed structural category and supposed constructed year

5.1.6 Structural category of schools and hospitals

Four types of structural category, stone structure, mixed structure of stone and RC, precast frame of IIS-04 and monolithic are proposed for schools and hospitals. Proposed structural category and supposed constructed year is shown in Figure 5.1-17.

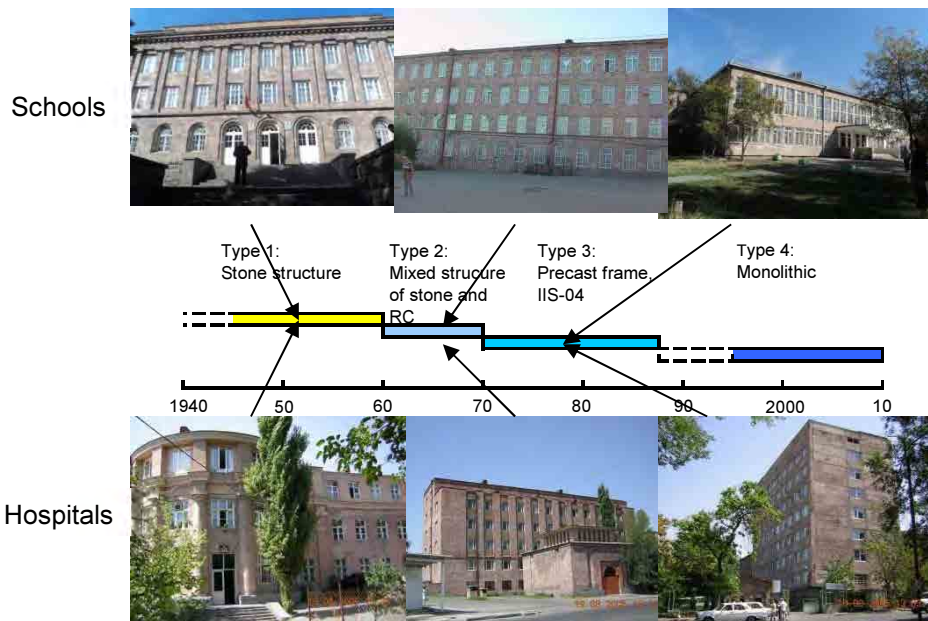


Figure 5.1-17 Proposed structural category and supposed constructed year

5.2 Building Inventory Survey

5.2.1 Multi-story residential buildings

As far as existing multi-story residential buildings, 3 types of stone structure and 5 types of reinforced concrete structure are categorized by the building sampling survey. Building inventory survey for multi-story residential buildings by visual inspection of external view was conducted. As a result, 4,371 buildings were counted based on a GIS map by ARS (2001) and a CAD map by Cadastro (2005). The ratio of each structural type is shown in Figure 5.2-1. An example of GIS map is shown in Figure 5.2-2. Number of building of each structural type in Yerevan and damages of similar structural type at the Spitak earthquake in 1988 is shown in Table 5.2-1.

Number of existing multi-story residential buildings for each structural type per grid of 250m x 250m is shown in Figure 5.2-3 and Figure 5.2-4. Many ‘frame panel’ buildings are located at Malatia-Sebastia and Avan district. Many ‘lift slab’ buildings are located at Ajapnyak and Nor Nork district.

Stone buildings by individual design are located at Kentron and Shengavit district mainly. Stone buildings, series 1-451 are located at Kentron, Shengavit and north side of the city. Stone buildings, series 1A-450 are distributed uniformly as shown. ‘Monolithic’ is located at Kentron and Arabkir district.

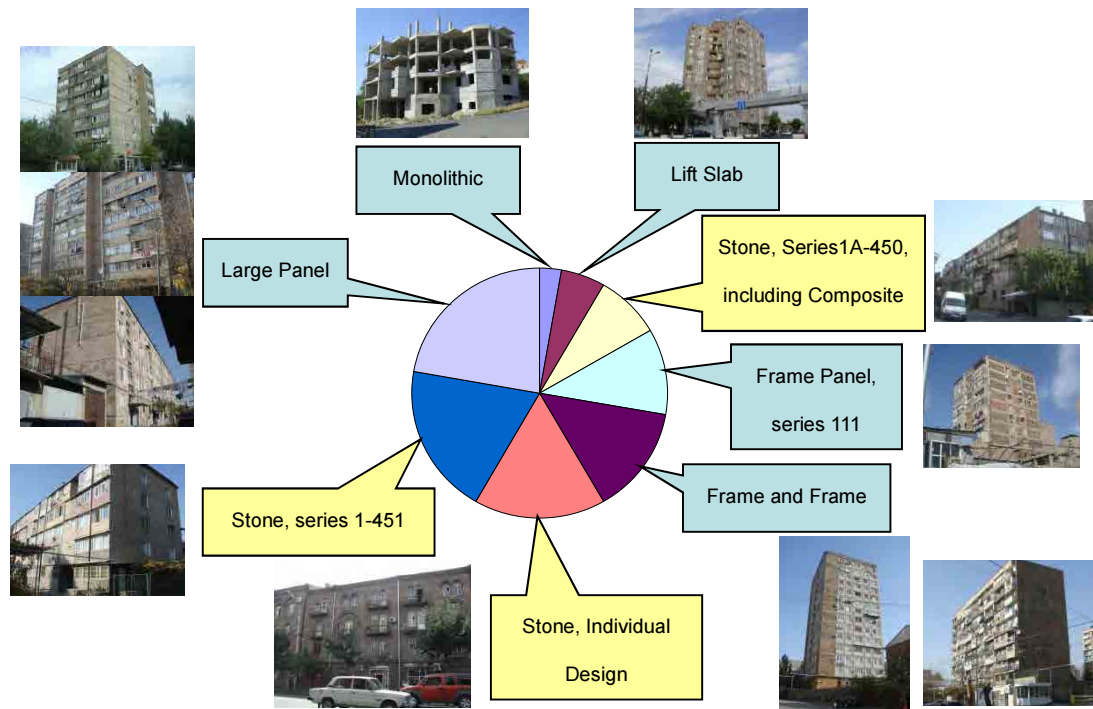


Figure 5.2-1 A ratio of each structural type

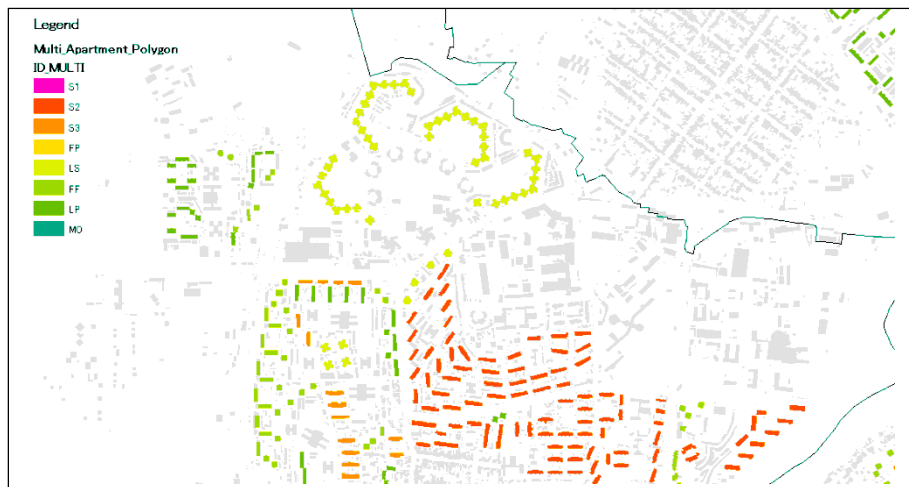


Figure 5.2-2 Example of GIS map for multi-story residential buildings

Table 5.2-1 Number of multi-story residential buildings and damages at the Spitak earthquake

Type (popular name)	Multi-story residential building in Yerevan (total 4371 nos)	Damage of similar type at Spitak in 1988	Ratio of heavily damaged (by EERI report, ref.1)
1. Stone, individual design	 (802)		Damage detail is shown for series 1-451 and 1A-450 in EERI report (ref.1). Spitak : 88% (22/25)
2. Stone, series 1-451	 (1001)		Gyumri : 38% (184/492) Stepanaban : 29% (10/35) Vanadzor : 41% (99/244) Ghouskasian : 45% (5/11)
3. Stone, series 1A-450	 (311)		Figure by NSSP EEC
4. Frame panel, series 111	 (412)		Gyumri : 95% (127/136) Vanadzor : 0% (0/108) , moderate damage: 88nos. Figure by NSSP EEC
5. Lift slab	 (95)		Gyumri : 100% (2/2) Figure by NSSP EEC
6. Frame & frame	 (526)	No construction at Spitak area.	
7. Large panel	 (1197)		Spitak : 0% (0/1) Gyumri : 0% (0/16) Vanadzor : 0% (0/4) Figure by EERI report (ref.1)
8. Monolithic	 (27)	No construction at Spitak area.	Construction has started in 1990s.

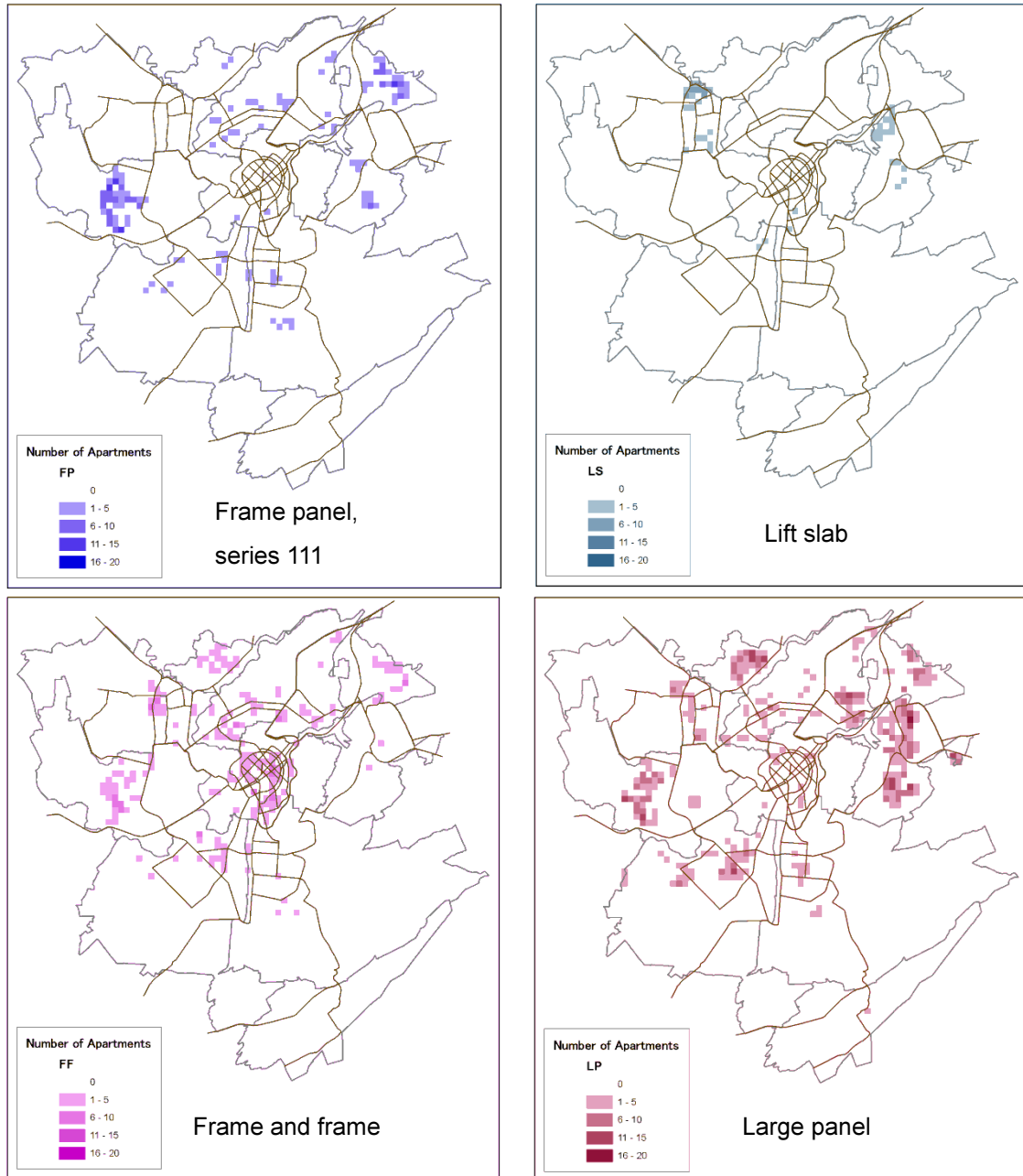


Figure 5.2-3 Number of existing multi-story residential buildings for each structural type per grid of 250m x 250m (1)

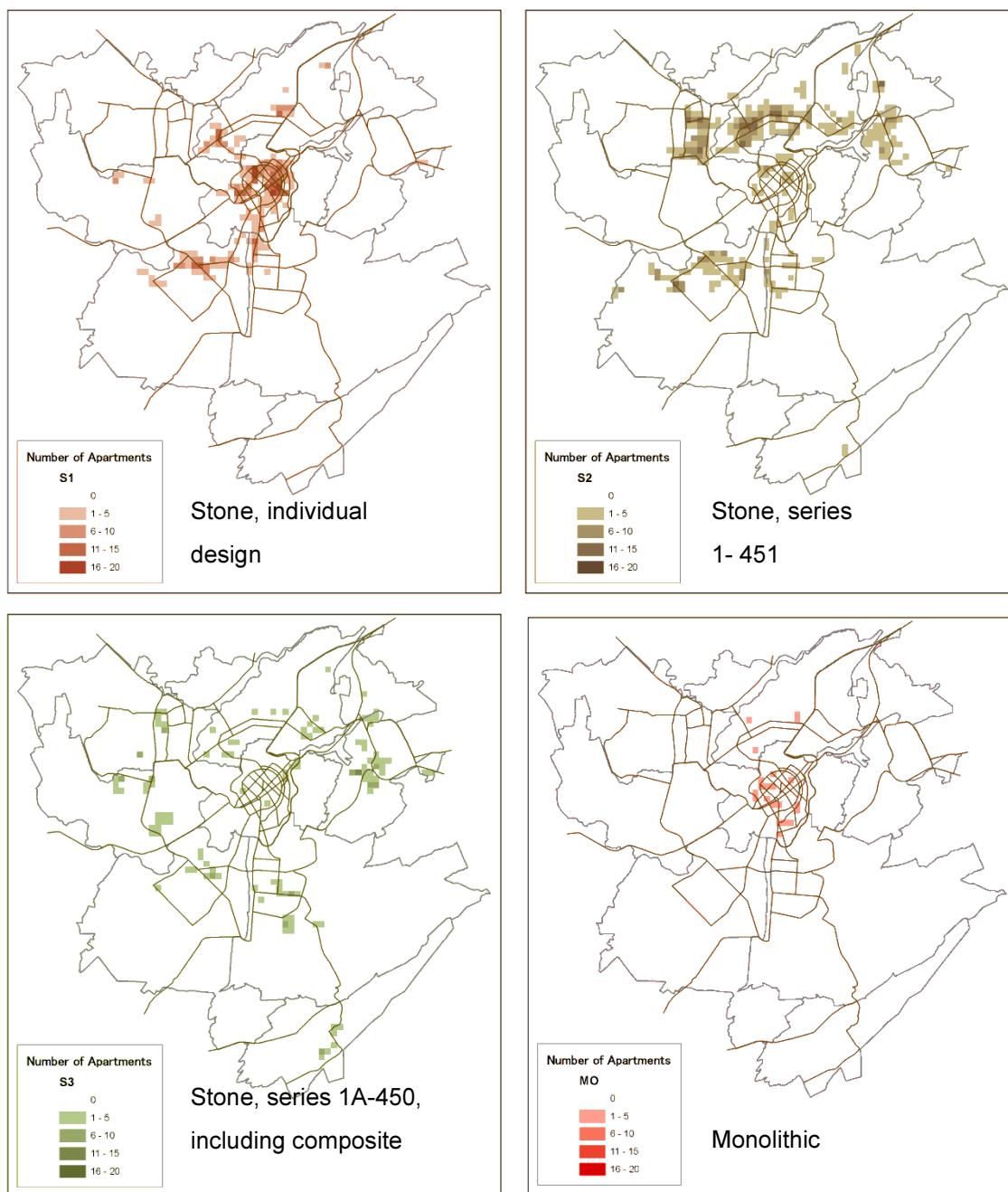


Figure 5.2-4 Number of existing multi-story residential buildings for each structural type per grid of 250m x 250m (2)

5.2.2 Individual houses

Structural type of individual houses was categorized by the material of joint mortar for stone walls. Structural type of individual houses was evaluated from the information of constructed year of houses by RS, which covers approximately 40% of existing houses. A ratio of structural type for a known area was applied to an area of unknown area that has similar historical formulation of the area through empirical evaluation. In addition, clay mortar joints were supposed for houses constructed in 50s at ‘Kond’ and ‘Saritagh’ areas. Supposed number of individual houses for each structural type per grid of 250m x 250m is shown in Figure 5.2-5.

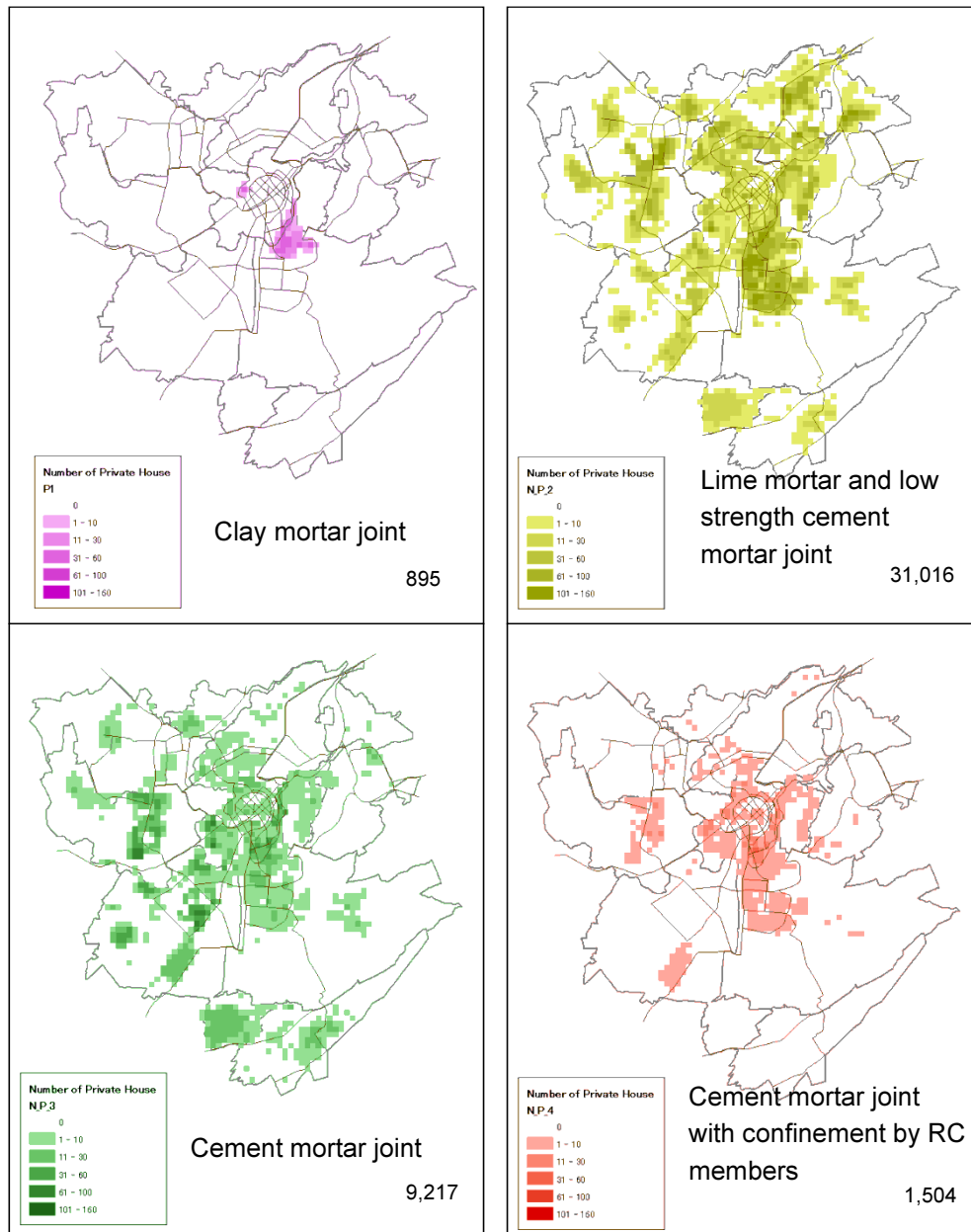


Figure 5.2-5 Supposed number of Individual houses for each structural type per grid of 250m x 250m

5.2.3 Schools and Hospitals

Location of schools and hospitals was surveyed from the atlas issued by Cadastro. Schools and hospitals (excluding clinics) categorized by three groups based on constructed year are shown in Figure 5.2-6, and Table 5.2-2. Each school and hospital has plural buildings generally.

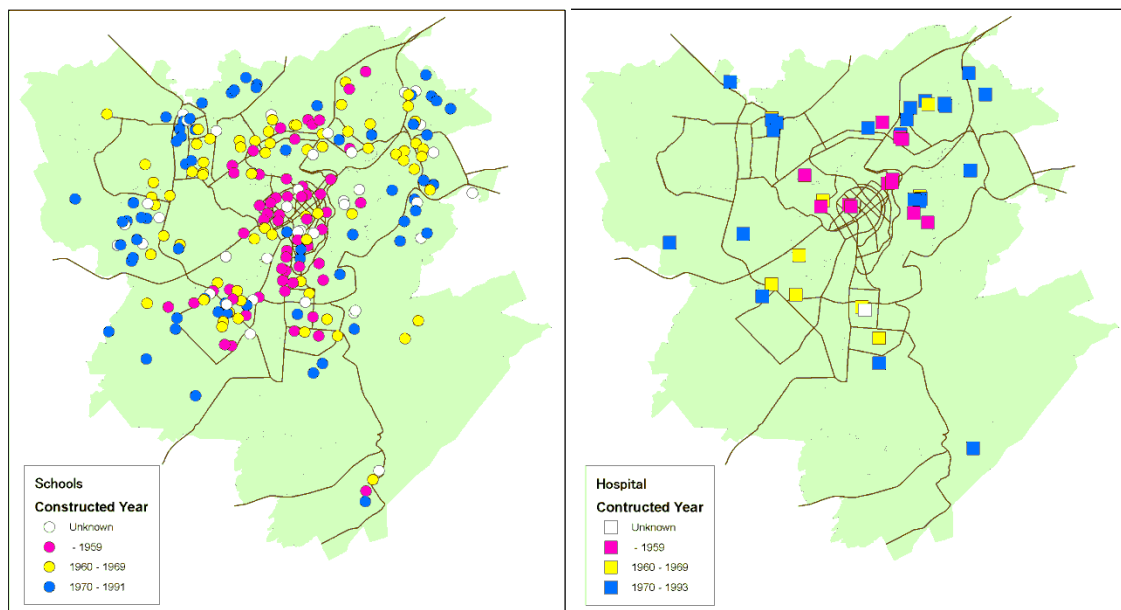


Figure 5.2-6 Building inventory for schools and hospitals

Table 5.2-2 Number of schools and hospitals based on the category of constructed year

Constructed year	School	Hospital (clinic is not included)
~ 1959	57	12
1960 ~ 1969	69	9
1970 ~ 1993	66	22
Unknown	37	1
Total	229	44

According to the Statistical data (www.edu.am) dated on 2009, there are 263 general education schools in Yerevan city. Approximately 120,600 students attend these schools. The management and funding of 202 schools are executed by the government and 43 schools are private.

According to the Statistical data (www.healthinfo.am), there are more than 130 medical facilities including clinic with 13 thousand doctors and midwives in Armenia. Approximately 80% of those facilities are located in Yerevan.

5.3 Vulnerability Function of Buildings

5.3.1 General

Vulnerable function (damage function) which shows the relation between damage ratio and seismic intensity of buildings was developed as follows. Vertical axis of proposed function is damage ratio of buildings, damage grade 4 plus 5 of EMS 98 (Figure 5.3-1), is used, which will be similar to category

4 plus 5 of RABC2006. Since there is no clear definition of relation between MSK seismic intensity and acceleration in Armenia, peak ground acceleration was used for horizontal axis.

Grade 4: Very heavy damage (heavy structural damage, very heavy non-structural damage)	Serious failure of walls; partial structural failure of roofs and floors 	Large cracks in structural elements with compression failure of concrete and fracture of rebars; bond failure of beam reinforced bars; tilting of columns. Collapse of a few columns or of a single upper floor. 
Grade 5: Destruction (very heavy structural damage)	Total or near total collapse 	Collapse of ground floor or parts (e. g. wings) of buildings. 

Figure 5.3-1 Damage grade 4 and 5 of EMS 98

5.3.2 Factors to be considered

Following three factors have been considered to develop vulnerability function (damage function) for buildings.

- 1) Damage data at the Spitak earthquake in 1988
- 2) Natural period of buildings and soil category
- 3) Strength and ductility of structures (Seismic design and construction quality control)

As far as seismic design of existing buildings in Yerevan, seismic intensity 8 was used generally. It had been allowed before the Spitak earthquake in 1988 to use seismic intensity 7 for the construction area of ground category I (hard rocks, etc.) only, but clear difference of designed members has not been confirmed compared with those designed by seismic intensity 8, according to the sampling survey. As a result, difference of design seismic intensity in Yerevan was not incorporated.

Further, it is a fact that various buildings do not correspond to their initial design such as constructive changes by residents for basements, additions, repairs, demolition of support columns and walls, etc. and sometime illegal constructions. Though it may be better to taking into account for damage estimation for buildings, quantitative evaluation is difficult to identify how many buildings. Therefore this effect is not taking into consideration this time, and there is a possibility that the practical damage is a little bit more than this project results.

(1) Damage data at the Spitak earthquake in 1988

Damage data owned by Armenian side is very limited, and data of reports by researchers of USA and Japan was used. Figure 5.3-2 shows the relation of observed damage ratio of multi-story residential buildings at the Spitak earthquake in 1988 by the EERI report (ref. 1) and estimated ground acceleration by the Japanese report (ref. 2). It is noted that the relation of soil type and building period affected the damage ratio of buildings. According the Armenian report (ref. 3), estimated acceleration at Gyumri is in the range of 0.3G to 0.4G which is lower than the estimation

of the Japanese report. Typical predominant period of soil at Gyumri is estimated as 0.5 to 0.9sec. (ref. 3). No heavily damage was reported at Aparan by the report (ref. 3).

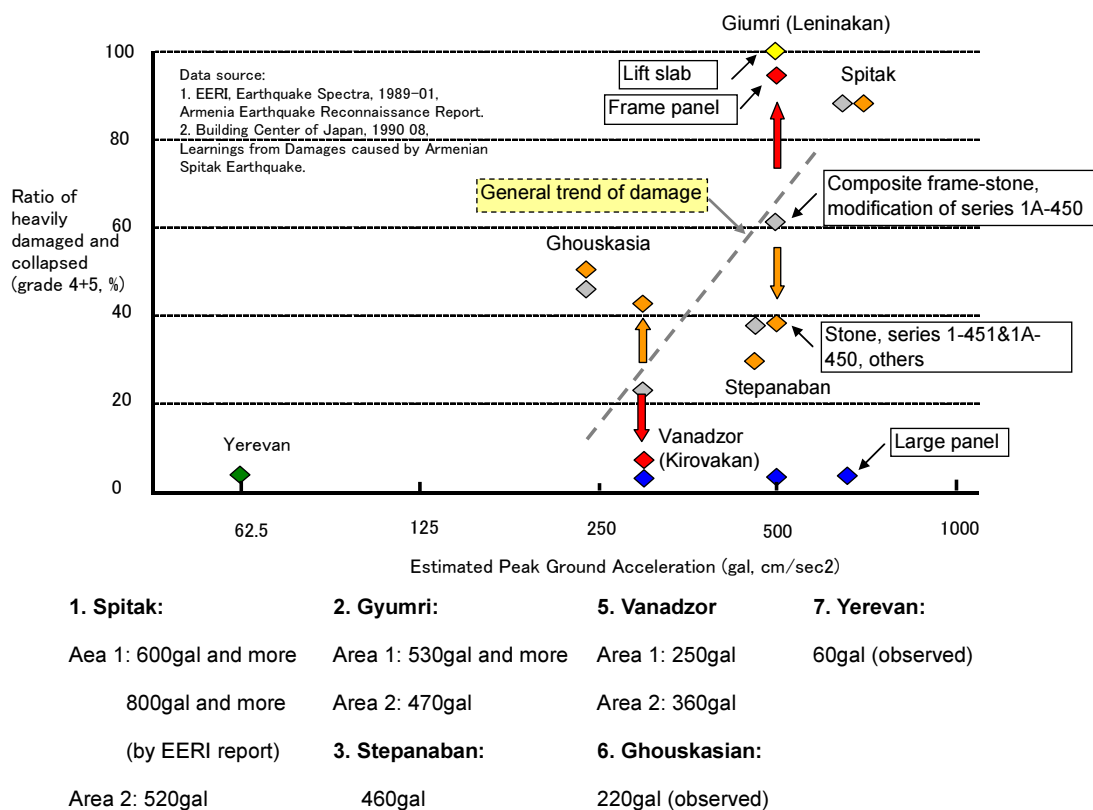


Figure 5.3-2 Observed damage ratio and estimated acceleration at Spitak earthquake in 1988

(2) Vibration period of buildings and soil category

Response spectrum is shown in Armenian Building Code, RABC II-6.02-2006. Figure 5.3-3 shows seismic response of buildings (Dynamic Coefficient β x Coefficient of Soil Conditions k_0) for each type of soil and natural vibration period of typical structural types by the Code. Difference of response by soil category is relatively big for the range of longer period.

Response amplification factor for short period range, supposing stone buildings of series 1-450, was studied applying three earthquake waves, with damping constant 5% for reference (Figure 5.3-4). As a result, response by Ghoukasian wave observed at the Spitak earthquake was higher than others by 10 to 30 %.

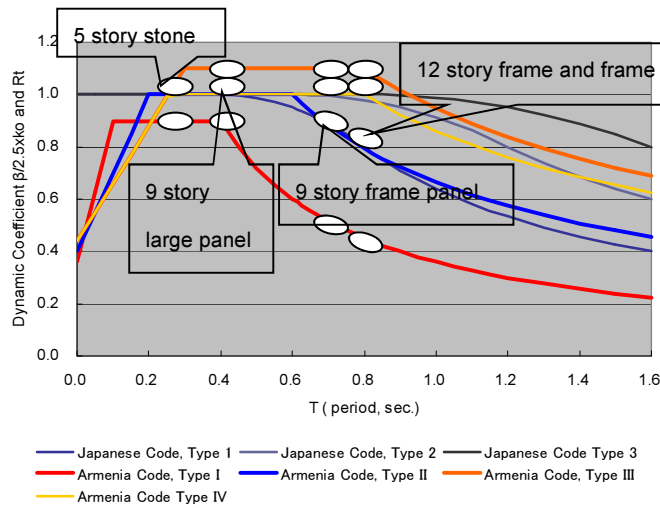


Figure 5.3-3 Response coefficient by soil type and vibration period of buildings

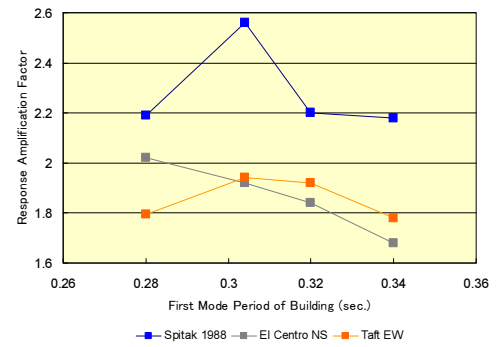


Figure 5.3-4 Response amplification factor of stone buildings

There is no official map for practical use showing soil category in Yerevan. Four categories of soil in RABC are indicated but it was evaluated that two category divided by ground predominant period of around 0.6sec is reasonable for developing vulnerability function taking into consideration both building response for each type and limitation of resolution of vulnerability function. Four soil categories in Yerevan have been revealed and two soil categories for vulnerability function has been proposed by JST based on predominant period, and is shown in Figure 5.3-5.

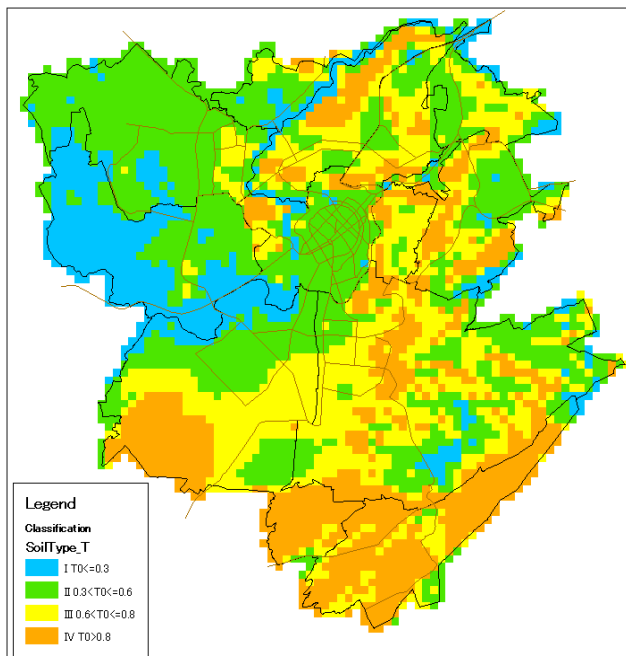


Figure 5.3-5 Proposed soil category in Yerevan by JST

T_0 (predominant period) ≤ 0.6 sec. (type I & II), $0.6 \text{ sec.} < T_0$ (type III & IV)

(3) Strength and ductility of structures (Seismic design and construction quality control)

Some researches concerning a study of natural vibration of buildings and vibration tests have been executed in Armenia, while researches for strength and ductility of existing buildings are not many (ref. 3). The seismic evaluation by the Japanese code (ref. 5) was applied for typical existing buildings in case drawings and documents are available. Engineering judgment was provided where construction quality at sites was problem.

Basic idea of the seismic evaluation is expressed by the multiplication of strength index (C) and ductility index (F), and seismic index of structure 'Is' is estimated. This ductility index is equivalent to the reverse value of the coefficient k1 of Armenian code RABC.

As far as stone buildings, in-plane strength of walls was estimated, and ductility index of 1.0 was used for conventional stone buildings. This is equivalent to 1st level screening, and seismic index of structure, Is, was estimated. As far as RC structure, strength and ductility of 'frame panel, series 111' and 'frame and frame' was estimated, this is equivalent to simplified 3rd level screening.

To develop damage function incorporating an idea of 'Is', the distribution of 'Is' for a structural type was assumed and damaged ratio was estimated related to the size of ground acceleration, as shown in Figure 5.3-6. Horizontal load bearing capacity was estimated through push over analysis, and then time history analysis was executed with assumptions for 'frame panel' and 'frame and frame'.

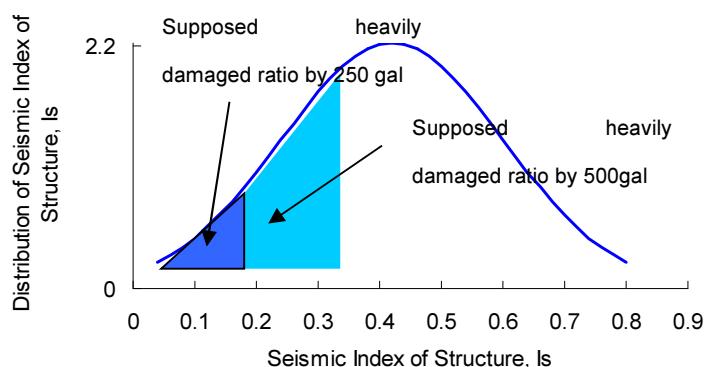


Figure 5.3-6 Supposed heavily damage ratio and distribution of 'Is'

5.3.3 Multi-story residential buildings

Structural evaluation for eight types of buildings is indicated as follows.

(1) Stone building by individual design

Mydis type walls and wooden floor is typical. Compressive strength of lime mortar was assumed as 10kg/cm^2 , wall thickness is 60cm, average unit weight is 1.5 ton/m^2 . It was assumed that half of wall thickness is effective and shear strength is 1/10 of compressive strength of mortar. Ductility index is assumed as 1.0. As a result, equivalent seismic index of structure, Is, of 0.07 to 0.09 was estimated. Influence of adjacent buildings was ignored for the evaluation of strength.

(2) Stone building, series 1-451

Mydis type walls and pre-cast concrete void slab is typical. Cement mortar of compressive strength 25kg/cm^2 was assumed, wall thickness is 50cm , and average unit weight is 1.5 ton/m^2 . It was assumed that half of wall thickness is effective and shear strength is $1/10$ of compressive strength of mortar. Ductility index is assumed as 1.0 . As a result, equivalent seismic index of structure, I_s , 0.13 was estimated.

Damages of stone buildings, series 1-451, at the Spitak earthquake is shown in Figure 5.3-7. It is evaluated that the lack of unification between anti-seismic belts and floor void slabs, and floor void slabs supported by longitudinal walls, caused bigger damages such as out-of-plane collapse of stone bearing walls located at side of buildings ((a) of Figure 5.3-7).



(a) Out-of-plane collapse of stone walls (ref. 1) (b) Partial collapse of building at Gyumri (by NSSP EEC)

Figure 5.3-7 Damages of stone buildings, series 1-451, at the Spitak earthquake

(3) Stone building, series 1A-450

Heavily damages were observed at the Spitak earthquake (Figure 5.3-8). It has been evaluated that possible causes of bigger damages for design and construction. As far as the construction quality, it was not enough, especially reinforced concrete portion for stone walls and the ductility was not provided as expected. As far as the layout of stone bearing walls related to the design (Figure 5.3-9), failure at side portion of a building might be caused by seismic load of transverse direction, and failure at center portion might be caused by seismic load of longitudinal direction. This means that unification between pre-cast floor slabs and stone walls were not enough to transfer seismic load of floors to bearing walls. As a result, vulnerability function of this 1A-450 was evaluated to similar to that of series 1-451.



(a) Collapse of side portion at Gyumri (by NSSP EEC) (b) Collapse of center portion at Gyumri (by NSSP EEC)

Figure 5.3-8 Damages of stone buildings, series 1A-450, at the Spitak earthquake

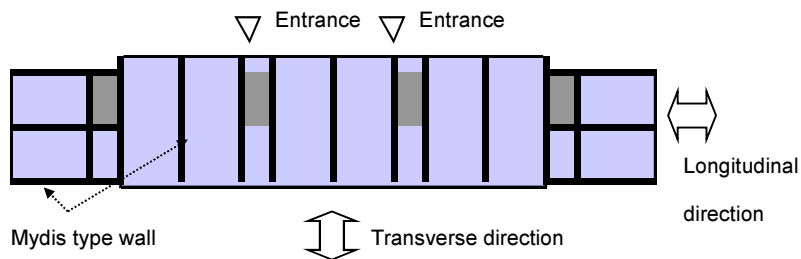


Figure 5.3-9 Layout of stone bearing walls for series 1A-450

(4) Frame panel, series 111

According to results of the seismic evaluation of frames for longitudinal direction, strength index C was 0.13 at ground floor. Ductility index F was supposed to be 1.0 to 1.2, and two category of soil is incorporated. Seismic performance of transverse direction was assumed to be same to longitudinal direction. To evaluate the factor of response spectrum, push over analysis for longitudinal direction (stiffness of non-structural walls was ignored) including evaluation of ductility of frames was done. The structure shows brittle behavior. Then time history analysis was executed using typical seismic waves including Ghousekasian wave observed at the Spitak earthquake, and damage ratio with supposed conditions was estimated as shown in Figure 5.3-10. In the analysis, damping constant of 3% was used for 9-story building. Vibration period (ignoring stiffness of non-structural walls) was 1.3 sec. The estimated acceleration at Gyumri is indicated as 0.4G per the report (ref. 3) in this figure.

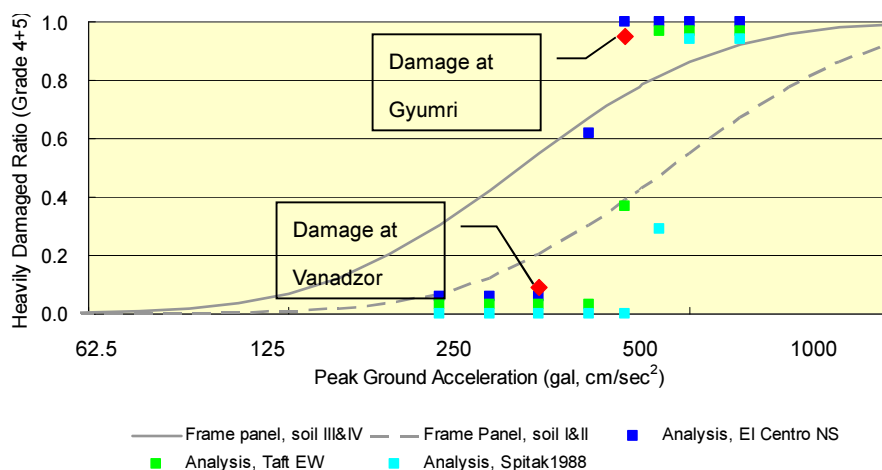
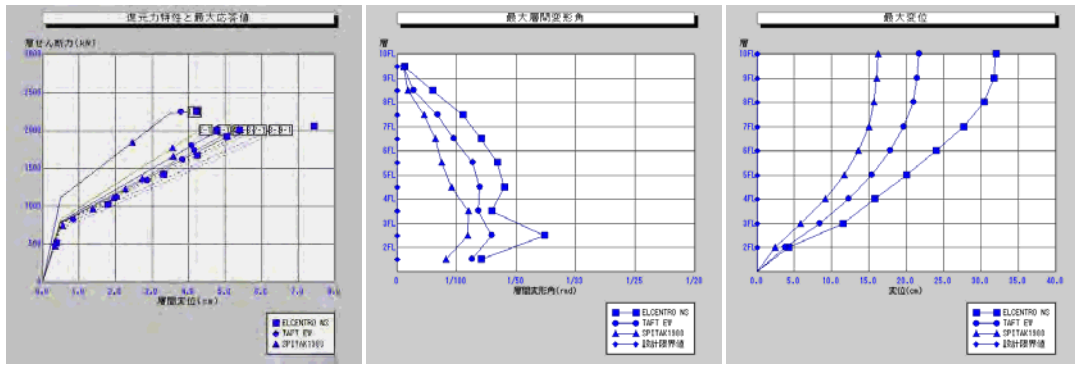


Figure 5.3-10 Proposed damage function and damage ratio by time history analysis

Results of time history analysis, applying three waves (El Centro NS, Taft EW and Ghousekasian, 400gal input) are shown in Figure 5.3-11.

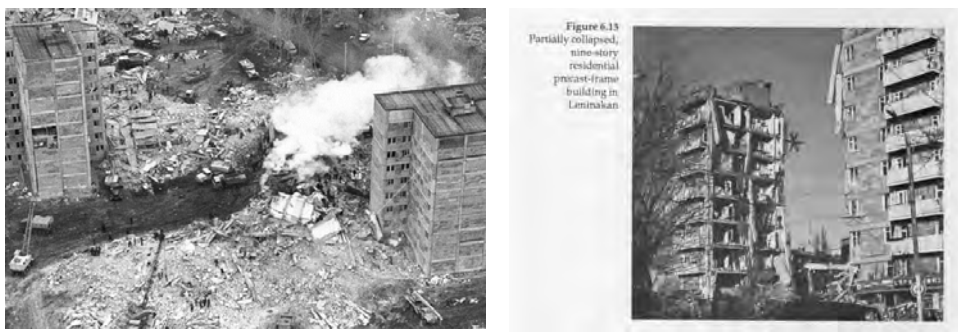


a) Story shear force – story deflection b) Story deflection angle c) Deflection at each story

Figure 5.3-11 Results of time history analysis

According to US report (ref. 1), predominant period of typical soil at Gyumri is 1.0 sec. and the Armenian report (ref. 3) shows 0.5 to 0.9sec. Japanese report (ref. 2) shows 0.6 sec.

Damages of ‘frame panel’ buildings at the Spitak earthquake in 1988 are shown in Figure 5.3-12.



(a) Collapsed ‘frame panel’ at Gyumri (by Nssp EEC) (b) Partially collapsed ‘frame panel’ at Gyumri (ref. 1)

Figure 5.3-12 Damages of ‘frame panel’ at the Spitak earthquake

(5) Lift slab

Structure of ‘lift slab’ is cast-in-situ core wall and precast RC columns with cast-in-situ flat slab. Design seismic load is supported by core wall with 40 to 50cm thickness. Lift slab structures were suffered heavy damage at the Spitak earthquake (Figure 5.3-13, ref. 1, 2). It is noted that quantity of horizontal reinforcing bars of core wall was not enough, which would be one of reasons of heavy damage, according to the report (ref. 1). Vulnerability function of ‘lift slab’ was evaluated to be similar to that of ‘frame panel, series 111’.



(left) Collapsed 10-story 'lift slab' at Gyumri (provided by NSSP EEC)
 (center) Heavily damaged 16-story 'lift slab' at Gyumri (ref.1)
 (right) Precast column and cast-in-situ flat slab of an abandoned building (in Yerevan by JST)
 Figure 5.3-13 Damages of 'Lift slab' at Spitak earthquake and joint of column and slab

(6) Frame and frame

'Frame and frame' is a frame resisting structure for both directions. According to the seismic evaluation, strength index C was 0.09, ductility index F was 1.5. This 'frame and frame' structure shows more ductility compared with that of 'frame panel'. Horizontal load bearing capacity divided by building weight was 0.06, and expected ductility was approximately 2 by the pushover analysis. Results of time history analysis using typical seismic waves including Ghousekasian wave, and damage ratio with supposed conditions are shown in Figure 5.3-14. In the analysis, damping constant of 3% was used for 14-story building. Vibration period (ignoring stiffness of non-structural walls) was 2.0 sec.

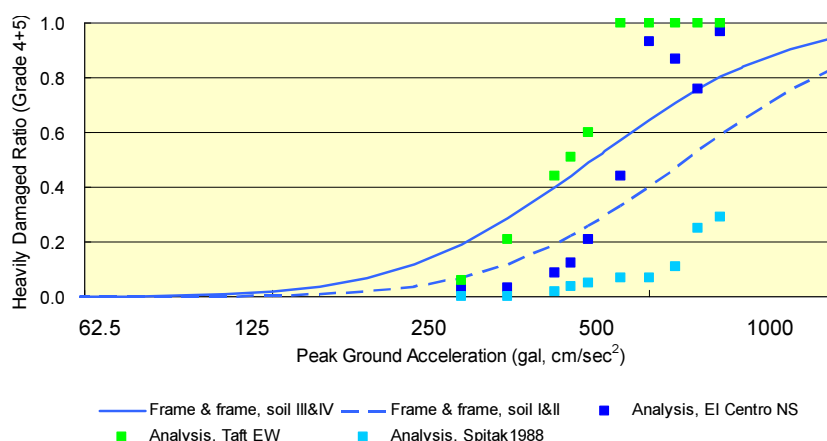
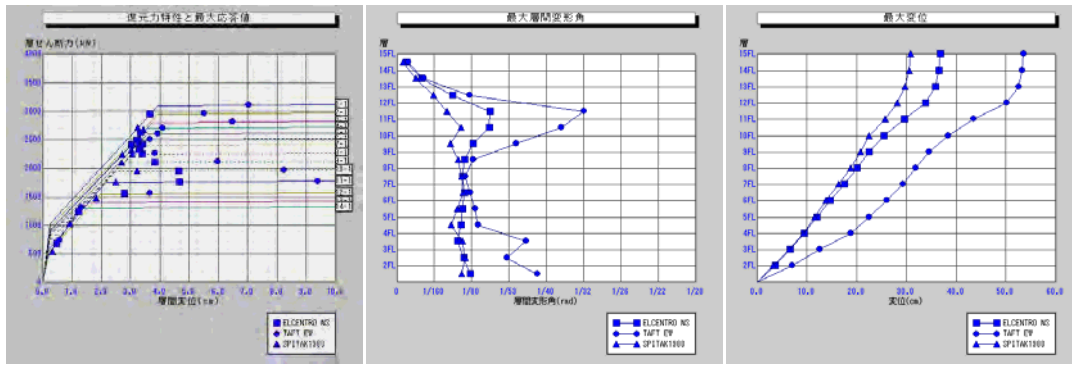


Figure 5.3-14 Proposed damage function and damage ratio by time history analysis

Results of time history analysis applying three waves (El Centro NS, Taft EW and Ghousekasian, 400gal input) are shown in Figure 5.3-15.



a) Story shear force – story deflection b) Story deflection angle c) Deflection at each story

Figure 5.3-15 Results of time history analysis

(7) Large panel

‘Large panel’ is a wall type precast reinforced concrete structure. 9-story and 5-story buildings are usual. Wall ratio (numerical value of total length of wall (cm) divided by floor area (m²)) was calculated for 9-story with square plan. Floor area is 382.1m² excluding balcony. Wall thickness is 25cm for internal, and 30cm for external (effective thickness is supposed as 20cm excluding insulation material). Wall ratio using equivalent thickness of 12cm is 29.2cm/m². Wall ratio of Japanese code for 5-story is 15cm/m² and was supposed as 27 cm/m², if it is possible to apply for 9-story. Large panel structures suffered slight damage only at the Spitak earthquake (Figure 5.3-16, ref. 1).



Figure 6-27 Completed large-panel building in Leninakan that sustained only minor cracking at some panel joints.



Figure 6-28 Five-story large panel building in Spitak that was undamaged. It appeared to be the only undamaged building in Spitak.

a) 9-story with minor damage at Gyumri

b) 5-story with minor damage at Spitak

Figure 5.3-16 ‘Large panel’ at the Spitak earthquake (ref.1)

(8) Monolithic

‘Monolithic’ are buildings based on the seismic design code RABC 1994 (latest version was issued in 2006), which was revised after the Spitak earthquake 1988. Yerevan is located at seismic zone 3 and the expected maximum ground acceleration which is 0.4G is used for design.

As a result, earthquake damages, soil type and analytical method together with empirical evaluation are incorporated for the development of vulnerability function (damage function). Proposed vulnerability function for multi-story residential buildings is shown in Figure 5.3-17.

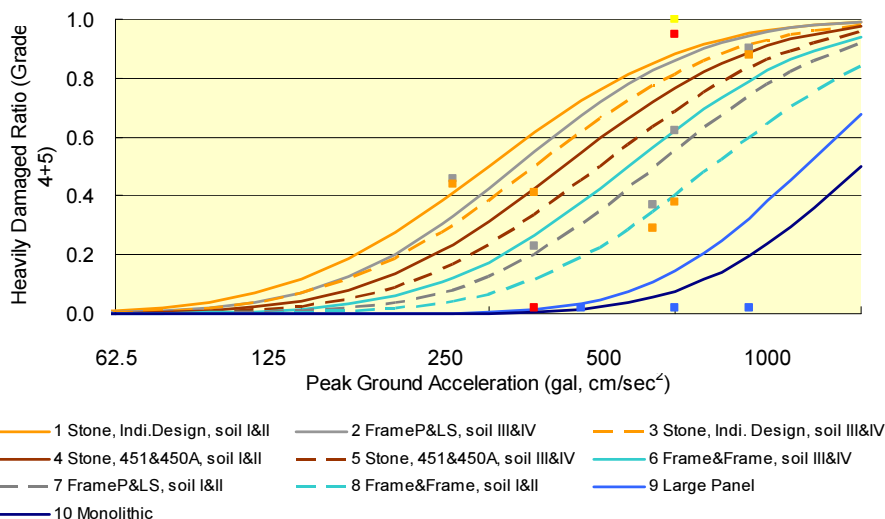


Figure 5.3-17 Proposed damage function for multi-story residential buildings

5.3.4 Individual houses

Type of joint mortar of stone walls, such as clay mortar, lime mortar including low strength cement mortar, cement mortar, and cement mortar with confined by reinforced concrete members are categorized, refer to Sec. 5.1.5 for material of mortar joints and assumed constructed year.

Following evaluation was done. Assumed compressive strength for lime mortar was M10 (10kg/cm²) and category of low strength mortar with M10-M25 was evaluated as a same category. Cement mortar was assumed as M25-M50. Cement mortar with confined by reinforced concrete members was assumed as M50 and ductility was assumed as 2.0, while the ductility of other types was supposed as 1.0. Assumed distribution of Seismic index of structure, ‘Is’ for each type of structure is shown in Figure 5.3-18. Proposed vulnerability function for low-rise individual houses is shown in Figure 5.3-19. Damage data of individual houses at Gyumri by the Spitak earthquake is shown for comparison (ref.4) and see Sec. 5.3.2 for estimated ground acceleration at Gyumri.

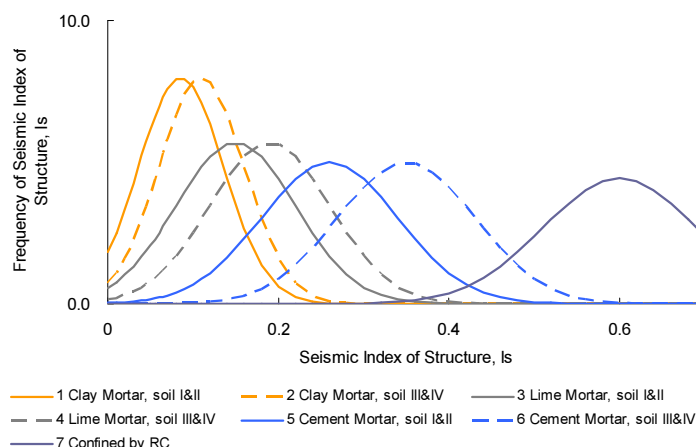


Figure 5.3-18 Assumed distribution of seismic index of structure, ‘Is’

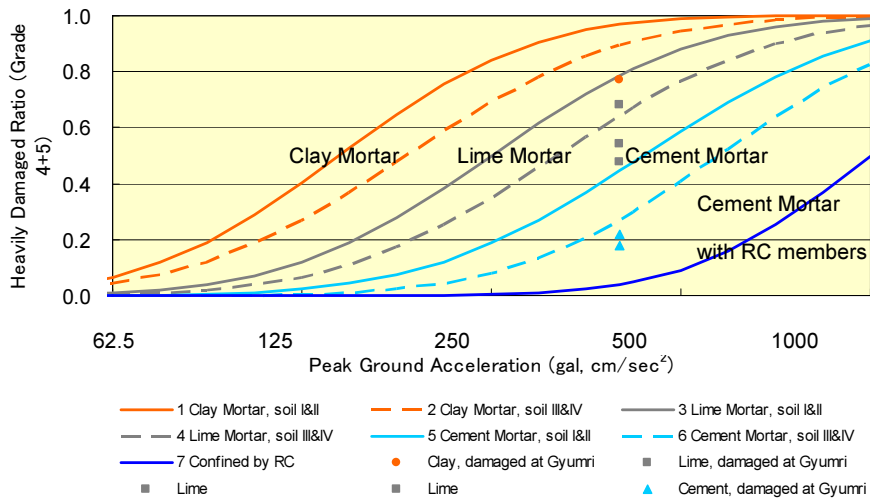


Figure 5.3-19 Proposed vulnerability function for individual houses

5.3.5 Schools and Hospitals

Schools and hospitals were classified by stone structure, mixed structure of stone and RC, precast frame of series IIS-04, and monolithic. Refer to Sec.5.1.6 for the proposed category and assumed constructed year for classification. Seismic performance of precast frame, series IIS-04, was assumed to be similar to ‘Frame panel, series 111’ of multi-story residential buildings, based on empirical evaluation. Performance of stone buildings was evaluated as higher compared with stone multi-story residential buildings because of better construction quality at sites. Most of buildings of mixed of stone and RC structure were suffered moderate damage at the Spitak earthquake. Proposed vulnerability function for school and hospital buildings is shown in Figure 5.3-20.

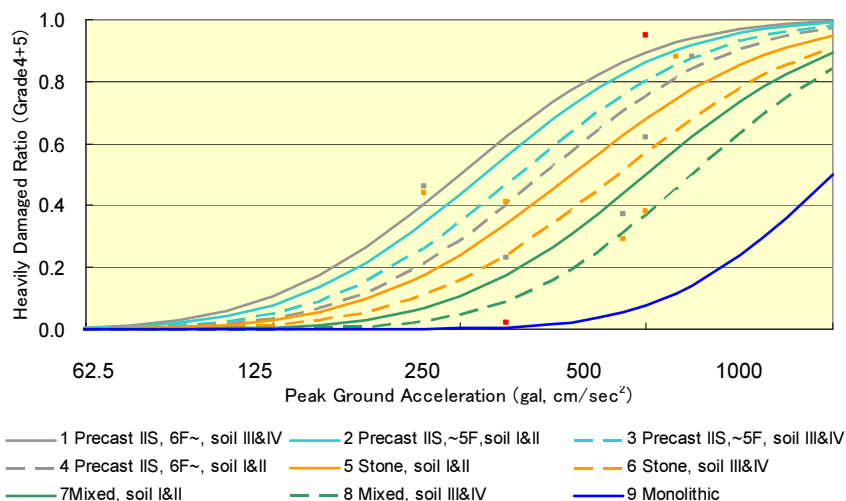


Figure 5.3-20 Proposed vulnerability function for schools and hospitals

References for Sec. 5.1 - 5.3:

1. EERI, Earthquake Spectra, 1989, “Armenia Earthquake Reconnaissance Report (in English)”, USA.

2. Building Center of Japan, 1990, “Learnings from Damages caused by Armenian Spitak Earthquake (in Japanese)”, Japan.
3. Khachyan H., Margaryan T. and others, 1998, “Spitak Tragedy Should Not Happen Again - On the assessment of the Spitak earthquake (in Russian)”, Ministry of Urban Development, Armenia.
4. Nazaretyan S.N. and others, 2010, “Assessment of Basic Data for Organization and Planning of Rescue Works in the case of a Seismic Disaster in Armenian (in Russian)”, Journal of Crisis Management Agency.
5. The Japan Building Disaster Prevention Association, (2001), “Standard for Seismic Evaluation of Existing Reinforced Concrete Buildings (English Version)”, Japan.

5.4 Inventory Survey of Infrastructure

5.4.1 Target Structure of Survey

The Yerevan city recognizes the structure 48 in the city. Among these, small structures such as a pedestrian were excluded from investigation. Therefore, estimation of damage was carried for 40 major structures and flyover in two cases of scenario earthquakes in Yerevan City. The list and locations of the 40 structures are shown in Table 5.4-1 and Figure 5.4-1.

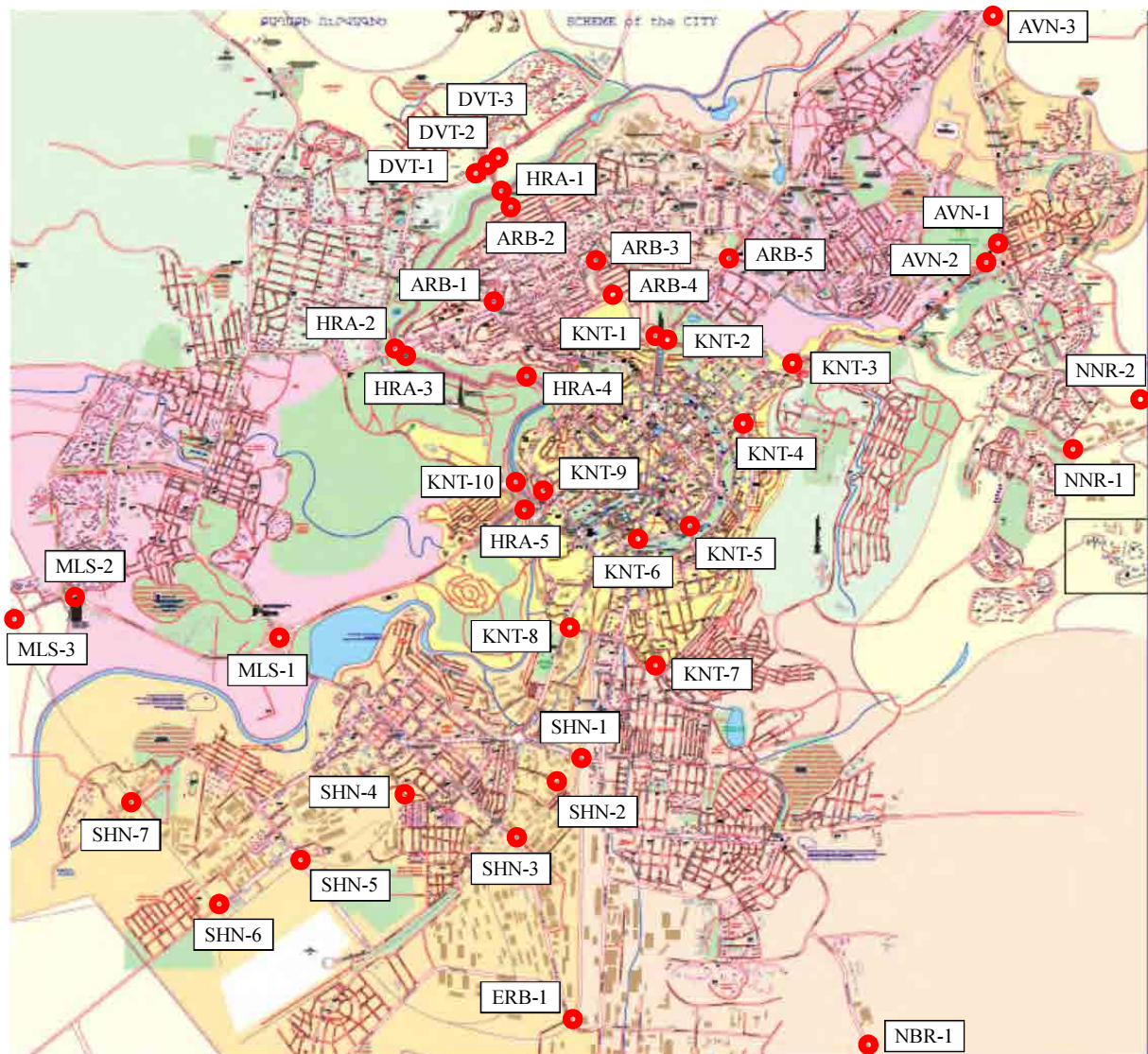


Figure 5.4-1 Location of Target Structures

Table 5.4-1 List of Target Structures

No.	Name	District	ID	Route	Crossing	Latitude	Longitude	Completion Year
1	Overpass bridge on the Friendship Square	Arabkir	ARB-1	Kasyan Str	Kievyan Str	44.4931	40.1978	
2	Bridge on Vatutin str.	Arabkir	ARB-2	Hovsep Emin Str	Vagharshyan Str	44.4962	40.2064	
3	Bridge on Riga str.	Arabkir	ARB-3	Riga Str	Railway	44.5074	40.2034	
4	Bridge on Saralanji HW near Riga str.	Arabkir	ARB-4	Saralanji HW	Riga Str	44.5102	40.1988	
5	Bridge on Komitas ave.	Arabkir	ARB-5	Komitas Ave	Azatutyan Ave	44.5259	40.2055	1985
6	Avan 1st bridge	Avan	AVN-1	GUI Ave - Atchryan Str	Atchryan Str	44.5607	40.2093	1973
7	Avan 2nd bridge	Avan	AVN-2	Rubinyants Str - GUI Ave	Atchryan Str	44.5589	40.2064	1973
8	Bridge on Yerevan - Sevan HW	Avan	AVN-3	Tbilisyan Road - Sevan HW	Atchryan Str	44.5618	40.2364	1973
9	Bridge of 2nd road	Davtashen	DVT-1	Sasna Tsrer Str	Yeghvard Road	44.4889	40.2118	
10	Central bridge of Davtashen transport	Davtashen	DVT-2	Sasna Tsrer Str	Yeghvard Road	44.4906	40.2128	
11	Bridge of 7th road	Davtashen	DVT-3	Sasna Tsrer Str	Yeghvard Road	44.4922	40.2136	
12	Bridge on Arin-Berd str.	Erebuni	ERB-1	Arin-berd Str	Railway	44.5066	40.1246	1957
13	Davtashen bridge	---	HRA-1	Sasna Tsrer Str	Hrazdan River	44.4941	40.2087	2000
14	Kiev bridge	---	HRA-2	Kievyan Str	Hrazdan River	44.4826	40.1915	1956
15	Bridge near the Kiev bridge	---	HRA-3	Left - Right Banks	Hrazdan River	44.4828	40.1911	1954
16	Bridge near the Yerevan HES	---	HRA-4	Left - Right Banks	Hrazdan River	44.4983	40.1892	1954
17	Haghtanak bridge	---	HRA-5	Argishti - Admiral Isakov Ave	Hrazdan River	44.4997	40.1747	1945
18	Overpass bridge of new highway	Kentron	KNT-1	Saralanji HW - Azatutyan Ave	Saralanji HW	44.5166	40.1943	
19	Overpass bridge of new highway	Kentron	KNT-2	Saralanji Str - Azatutyan Ave	Saralanji HW	44.5174	40.1943	
20	Bridge on Heratsi str.	Kentron	KNT-3	Saralanji HW	Heratsi Str	44.5324	40.1926	2008
21	Bridge on Charents str.	Kentron	KNT-4	Charents Str	Heratsi Str	44.5266	40.1851	
22	Bridge on Khanjyan str.	Kentron	KNT-5	Khanjyan Str	Vardanants Str	44.5205	40.1750	
23	Bridge on Tigran Mets ave.	Kentron	KNT-6	Tigran Mets Ave	Agatangeghos - Khanjyan Str	44.5137	40.1732	
24	Bridge on Khorenatsi str.	Kentron	KNT-7	Nork Saritagh Str	Khorenatsi Str	44.5174	40.1598	
25	Subway bridge over Kristapor str.	Kentron	KNT-8	Subway	Kristapor Str	44.5084	40.1632	2001
26	Bridge on G. Lusavorich str.	Kentron	KNT-9	Lusavorich Str	Mesrop Mashtots Ave	44.5028	40.1768	
27	Overpass bridge near the Hrazdan Stadium	Kentron	KNT-10	Athens Str	---	44.4977	40.1779	1971
28	Bridge on Isakov ave.	M. Sebastia	MLS-1	Admiral Isakov Ave	Sebastia Str	44.4678	40.1597	
29	Argavand bridge	M. Sebastia	MLS-2	Admiral Isakov Ave	Arno Babajanyan Str	44.4430	40.1597	
30	Bridge on Isakov ave. to Echmiadzin HW	M. Sebastia	MLS-3	Admiral Isakov Ave	Railway	44.4330	40.1580	1966
31	Bridge near Nubarashen	Nubarashen	NBR-1	M-15	Nubarashen Str	44.5526	40.1020	1980
32	Bridge on Galshoyan str.	Nor Nork	NNR-1	Galshoyan Str	Tevosyan Str	44.5719	40.1851	1979
33	Jrvezh river bridge	Nor Nork	NNR-2	Kochinyan Str	Jrvezh River	44.5891	40.1897	1981
34	Bridge on Garegin Nzhdeh str.	Shengavit	SHN-1	Garegin Nzhdeh Str	Subway & Railway	44.5075	40.1502	1963
35	Subway bridge over Shahamiyanner str.	Shengavit	SHN-2	Subway & Railway	Shahamiyanner Str	44.5050	40.1459	
36	Subway bridge over Tamantsineri str.	Shengavit	SHN-3	Subway & Railway	Tamantsineri Str	44.4977	40.1403	
37	Subway bridge over railway	Shengavit	SHN-4	Subway	Railway	44.4808	40.1451	
38	Shirak str. 1st bridge	Shengavit	SHN-5	Shirak Str	Railway	44.4687	40.1397	1963
39	Overpass bridge on Araratyan str.	Shengavit	SHN-6	Araratyan Str	Railway	44.4549	40.1308	1983
40	Shirak str. 2nd bridge	Shengavit	SHN-7	Shirak Str	Railway	44.4407	40.1416	1978

5.4.2 Inventory Survey

(1) Main Point of Survey

Some measures are required for structures evaluated to have high risk of damage, to ensure sufficient strength against earthquake. Especially support and seating length are able to be reinforced after completion easily. Inventory survey was carried out paying attention in Table 5.4-2.

About girder structure, connecting girders is one of the measures. However, the structure change from a simple beam to a continuous beam changes distribution of a moment remarkably. Therefore, it is necessary to examine the main girder strength of the present bridge closely to select the measure. The completion year of bridge is so old that collecting all the information such as drawings and specifications required for the examination is almost impossible

Regarding quality, from a viewpoint of the improvement in earthquake-proof, the measure should be repair or reinforcement of the entire bridge. Only partial repair cannot attain its purpose.

Therefore, in this investigation, support and seating length should be the main focus. Especially seating where superstructure and substructure are connected should be investigated in detail.

(2) Survey Content

The inventory survey, the focus points to keep in mind, based on the survey format in Table 5.4-3 shows.

(3) Present Condition of the Inventory Survey

Result of the inventory survey of target structures as survey format with photo sheet to be attached to the Data Book.

Table 5.4-2 Focus Point in Investigation

Item	Assumption Measure	Main Point
Girder Structure	Continuous connection between girders, Replacement of superstructure, Replacement of bridge	Bridge/Span Length, Bridge Width
Support	Unseating Prevention System	Seating and Girder End Scale
Seating Length	Seating Extension System	Seating Length, Span Length
Quality	Repair and Reinforcement of the Bridge, Replace the Bridge	Degradation degree

Table 5.4-3 Inventory Sheet for Survey

INVENTORY SHEET						Inspection Date: 2010/11/25
Name	Overpass bridge on the Friendship Square			Name Code:	ARB-1	
Location	44.49306875 N	40.19783191 E		Bridge Type:	Road	
Year Built	-----					
(1) GENERAL:						
Road Type	1	2	3	Lane	2	
	City Street Single lane	City Avenue 2 or 4 lanes	Major Motorways >4 lanes	3 numbers		
Subject of Crossing	1	2	3	4	3	
	River	Road	Fry over / Interchange	Railway		
Bridge Length	1	2	3	Length	3	
	Short <20m	Middle 21m to 75m	Long > 76m	238.20 m		
Bridge Alignment	1	2	3		3	
	Straight	Skewed	Curved			
(2) SUPERSTRUCTURE:						
Spans Distribution	1	2		Span	2	
	Single span	>2		7 spans		
Girder Type	1	2	3		3	
	Arch or Rigid Frame	Continuous	Single / Gerber girder			
Bearing Type	1	2	3		1	
	Falling Prevention	Normal	M-M			
Bridge Span (0.7+0.005*span)	A1 - P1	P1 - P2	P2 - P3, -, P5	P5 - P6	P6 - A2	16.00 m (0.780 m)
	16.00 m (0.780 m)	32.00 m (0.860 m)	40.00 m (0.900 m)	32.00 m (0.860 m)	16.00 m (0.780 m)	
Seating Length	0.70 / 0.70 m	0.70 / 0.70 m	0.70 / 0.70 m	0.70 / 0.70 m	0.70 / 0.70 m	
Bridge Seat	1	2			2	
	Wide	Narrow				
(3) SUBSTRUCTURE:						
Max. Height of Substructure	1	2	3	Max. Height	2	
	less than 5m	5 to 10m	more than 10m	6.80 m		
Foundation Type	1	2			1	
	Except Pile	Pile				
Material of Substructure	1	2			1	
	RC	Brick / Plane concrete				
Ground Classification	1	2	3	4	2	
	Rock	Medium Stiff	Soft	Very Soft		
(4) CONDITION OF STRUCTURE:						
Condition of Structure	1	2	3		1	
	Good	Fair	Not good			
(5) HAZARD:						
Seismic Intensity	1	2	3	4 / 5	-----	
	5.00	5.50	6.00	6.5 / 7.0		
Liquefaction Potential	1	2	3		1	
	None	Probably	Yes			

5.5 Vulnerability Function of infrastructure

"Katayama's method" which is a method with relatively simple evaluation used in several studies similar to this study, was applied in this study. Katayama's method takes the statistics of the earthquake damage of the past of Japan, and the item which affected this. The point that this can evaluate earthquake-proof performance by appearance investigation is the feature. The procedure of Katayama's method is as follows.

- ✓ Clarifying structures, materials and ground conditions by inventory survey
- ✓ Estimating seismic intensity through analysis on ground and seismicity
- ✓ Determining a grade in 10 categories shown in Table 5.5-1
- ✓ Calculating a final score through multiplying weighting factors corresponding to the grade of each category

- ✓ Estimating the modulus, based on the final score and criterion

Table 5.5-1 Grade for Damage Evaluation (Katayama's method)

Item		Grade	Weighting Factor	Code
Hazard	Seismic Intensity Japan Meteorological Agency	- 5.0	1.0	1
		5.0 - 5.5	1.7	2
		5.5 - 6.0	2.4	3
		6.0 - 6.5	3.0	4
		6.5 -	3.5	5
	Liquefaction potential	None	1.0	1
		Probably	1.5	2
Yes		2.0	3	
Superstructure	Span distribution	1	1.0	1
		2 or more	1.75	2
	Girder type	Arch or Rigid frame	1.0	1
		Continuous	2.0	2
		Single or Gerber girder	3.0	3
	Bearing type	Falling prevention devise	0.6	1
		Normal	1.0	2
		Two bearings moving in different direction	1.15	3
	Minimum width of bridge seat	Wide	0.8	1
		Narrow	1.2	2
Substructure	Maximum height of abutment /pier	≤ 5 m	1.0	1
		5 m ~10 m	1.35	2
		≥ 10 m	1.7	3
	Foundation type	Others	1.0	1
		Pile bent	1.4	2
	Material of abutment/pier	Reinforced concrete	1.0	1
		Plain concrete or others	1.4	2
	Ground class	Class 1 (Stiff)	0.5	1
		Class 2 (Moderate)	1.0	2
		Class 3 (Soft)	1.5	3
Class 4 (Very soft)		1.8	4	

One of the factors determining Katayama's method has been adopted the JMA seismic intensity scale (Japan Meteorological Agency). The Peak Ground Acceleration was calculated in the hazard analysis and converted to JMA Intensity by the empirical equation by Midorikawa et al. (1999).

$$\text{JMA Intensity} = 0.55 + 1.9 \times \log(\text{PGA in gal})$$

Definition of the modulus and criterion for the damage estimation are set up, based on actual records of earthquake damages in Japan, as shown in Table 5.5-2. The definition and values were used for damage estimation in this study.

Table 5.5-2 Criterion of Katayama's Method

Rank	Degree of damages	Criterion
A	- High possibility of bridge collapse - Occurrence of big displacement - Long-term impassable, requiring reconstruction	30 or more
B	- Moderate possibility of bridge collapse - Occurrence of displacement - Temporarily impassable, requiring repair or/rehabilitation	26 to less than 30
C	- Low possibility of bridge collapse - Occurrence of minor displacement - Basically passable after safety inspection	Less than 26

Deterioration of structures such as the segregation of calcium from concrete, corrosion of reinforcing bar/steel, structural cracks on concrete was found during the site inspection. These are remarkable compared to the structure in Japan. The deterioration seems to be due to shoddy workmanship, such as lack of cement in concrete and insufficient vibration at the time of concrete placing, and aging deterioration. The deterioration was considered to affect seriously to the stability of bridges at the time of an earthquake. Thus, the entry should include an evaluation of the quality of the decision (Table 5.5-3), because Katayama's method was developed based from the Japanese earthquake damages.

Table 5.5-3 Grade for Damage Evaluation (Quality)

Item	Grade	Weighting Factor	Code
Quality of condition	Normal	1.0	1
	Slightly deteriorated *	1.2	2
	Deteriorated *	1.5	3

*Deteriorated: Softening of concrete surface, segregation of calcium, structural cracks, corrosion of reinforcing bar/steel, etc.

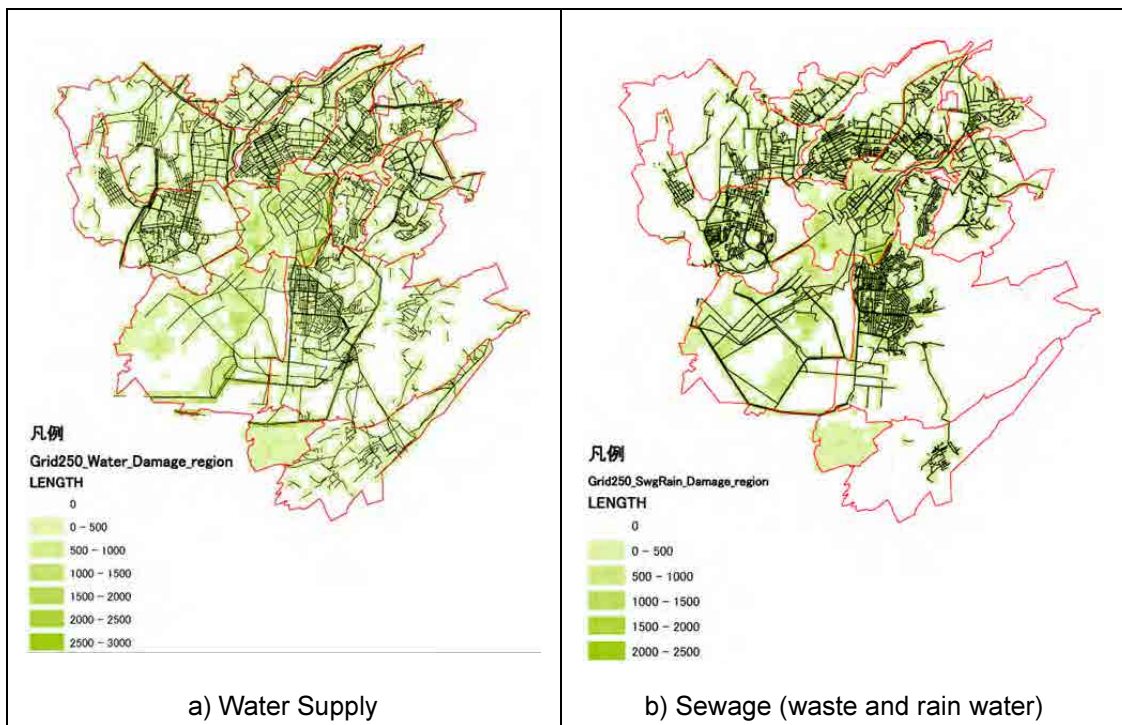
5.6 Inventory of Lifelines

The inventory data which was prepared based on the collected materials described in Sec. 2.7.6 is shown below. Since the network information of water supply, sewerage (waste water and rain water), electricity and gas in two districts (Kentron and Shengavit) are not included in the collected materials, the distribution of pipelines or cables in two districts are estimated based on the empirical relation between the length of pipelines or cables and the number of buildings. The relation between length of pipelines or cables and the number of buildings by materials and diameter of pipes are derived from the data in other ten districts and applied to Kentron and Shengavit to estimate the pipeline or cable length in each 250m grid. Finally, the length of pipelines or cables by material or diameter of pipes in each 250m grid is prepared as the inventory database. The final estimated length of lifelines is shown in Table 5.6-1. The distributions of pipelines or cables are show in Figure 5.6-1.

When such practical data become available, they can be input to the database and it is possible to estimate damage to lifeline facilities using such practical data.

Table 5.6-1 Summary of lifeline length

No.	District	Population	Area km ²	Water Supply km	Sewage		Electricity		Gas		Telephone km
					Waste Water km	Rain Water km	Aerial km	Under Ground km	On the Ground km	Under Ground km	
					km	km	km	km	km	km	
1	Ajapnyak	108,200	26.0	132.3	62.4	12.4	185.8	51.1	95.3	11.7	27.3
2	Avan	51,000	8.2	48.7	28.5	12.7	59.6	40.2	44.3	1.6	14.3
3	Arabkir	130,800	13.2	114.0	70.8	24.2	154.7	69.9	103.4	9.6	30.2
4	Davtashen	41,100	6.5	37.2	22.6	1.9	68.4	25.3	13.8	1.6	7.2
5	Erebuni	121,900	49.4	218.7	164.8	30.5	355.9	71.3	173.2	5.2	35.7
6	Kentron	130,600	13.4	153.3	104.6	31.4	237.2	67.7	130.5	2.6	62.9
7	Malatia-Sebastia	141,800	25.3	131.2	109.3	23.5	232.6	53.9	97.5	10.4	31.6
8	Nor Nork	147,000	14.5	63.5	42.0	15.4	133.1	70.1	50.8	0.6	25.7
9	Nork-Marash	11,300	4.7	33.5	24.6	1.4	48.7	9.5	37.1	0.9	7.8
10	Nubarashen	9,700	17.2	57.7	14.2	0.0	80.2	0.4	22.0	5.8	3.8
11	Shengavit	146,500	40.6	217.4	161.4	18.7	275.1	74.2	162.8	9.0	36.8
12	Kanaker-Zeytun	79,300	7.6	85.6	60.0	10.6	118.1	94.4	96.3	8.5	18.2
Total		1,119,200	226.6	1,293.1	865.2	182.7	1,949.4	628.0	1,027.0	67.5	301.5



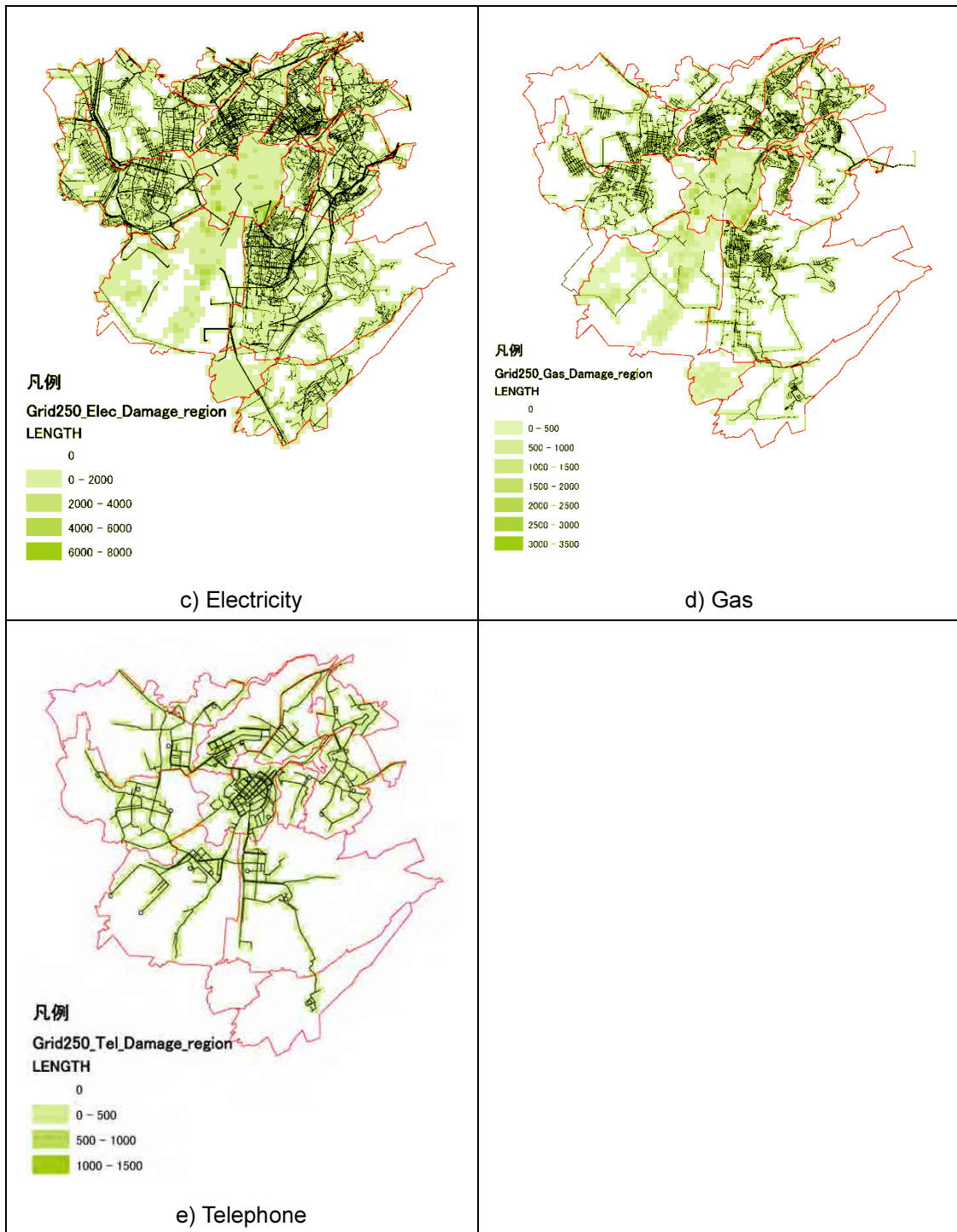


Figure 5.6-1 Distribution of lifeline network, lines show the pipelines or cables by GIS data and color shows the length in 250m grid

5.7 Damage Function of Lifeline Facilities

5.7.1 Concept

It is necessary to set a damage function representing the relationship between the intensity of the seismic ground motion and the extent of damage to predict damage that may occur to lifeline facilities.

Using the damage function established based on earthquakes that have occurred in the past either in Yerevan City or Armenia would enable a more realistic prediction that accurately reflects the actual situation. Therefore, inquiries were made of the relevant agencies about the data on the damage of the lifelines caused by Spitak Earthquake that hit Armenia in 1988 and the lifeline damage function used in Armenia, but such information was not available.

On the other hand, the method to assume the damage on lifelines described in “Seismic Risk (Assessment and Management)”, which is a manual used by the RS and NSSP in assuming the extent of damage, was not derived from the actual earthquake damage. This method applies the damage rate of buildings and ground structures to each type of ground pipelines. With respect to underground pipelines, as it is considered that they are less susceptible to the impact of earthquakes than ground pipelines, the damage rate is set to be one rank lower than that of ground pipelines. Also, an NSSP report entitled “Preliminary Assessment of Seismic Risk of Armenia Lifelines” concludes that a quantitative assessment of earthquake risk is needed in the next stage, while providing a qualitative assessment of the earthquake risk on the lifelines in Armenia.

Integrated digital data on the lifelines in Armenia are currently under preparation. Cadastral has already compiled such data for ten out of the 12 districts in Yerevan City, using GIS, and it is working to prepare the data for the remaining two districts. Some of the lifeline companies have not compiled integrated digital data, either. It will be necessary to prepare digital data and determine the damage function based on the past earthquake disasters that struck Armenia.

In view of the circumstances described above, it was decided that this project will carry out damage prediction in Armenia referring to the existing literatures from the U.S. and Japan that have determined damage function derived from the damage situation of actual earthquakes.

5.7.2 Damage Function

(1) Water supply

The damage function for quantitative prediction of damage rate per km of pipeline based on the analysis of past earthquake damage has been proposed in the U.S. and Japan. (Central Disaster Prevention Council, Cabinet Office, Government of Japan (2005), Japan Water Works Association (1998), Japan Water Research Center (2000), Federal Emergency Management Agency (1999))

The damage functions proposed by these organizations are expressed in terms of standard damage rate and correction coefficient dependent on the type and diameter of the pipelines. In this study, damage is calculated by referring to several damage functions proposed in recent years. The standard damage rate of HAZUS, which is based on the actual record of damage in the U.S. and Mexico, is used to calculate the maximum damage and the standard damage rate proposed by the Central Disaster Prevention Council, Cabinet Office, Government of Japan (2005), which is based on the actual record of damage of the 1995 Kobe Earthquake is used to calculate the average damage.

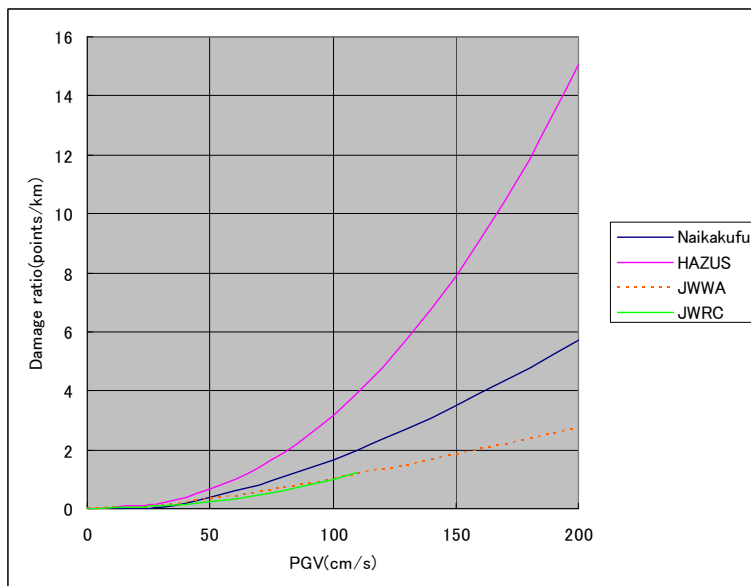


Figure 5.7-1 Standard damage rate of water supply pipes

- *1) Naikakufu: Cabinet Office, Government of Japan (Japan, 2005)
- *2) JWWA: Japan Water Works Association (Japan, 1998)
- *3) JWRC: Japan Water Research Center (Japan, 2000)
- *4) HAZUS: Federal Emergency Management Agency (USA, 1999)

Damage function $R_m = R \cdot C_p \cdot C_d \cdot C_l$

(Maximum damage) $R = 1 \times 10^{-4} \cdot V^{2.25}$

(Average damage) $R = 2.24 \times 10^{-3} \cdot (V-20)^{1.51}$

R_m : Damage function (point/km)

R : Damage rate (point/km)

C_p : Pipe material coefficient (see Table 5.7-1)

C_d : Pipe diameter coefficient (see Table 5.7-1)

C_l : Liquefaction coefficient (Because liquefaction is not assumed, $C_l = 1.0$ is assumed.)

V : Peak ground velocity (cm/sec)

Table 5.7-1 Coefficient of material and diameter of water supply pipes

Material	Diameter (mm)	Cp x Cd					
		correction coefficient				Adopted value	
		Naikakufu	JWWA	JWRC	HAZUS	Max. damage	Average damage
Steel	≤75	0.84	0.48	0.48	0.30	0.84	0.48
	100-150	0.42	0.30	0.30	0.30	0.42	0.30
	200-250	0.42	0.24	0.27	0.30	0.42	0.29
	300-450	0.24	0.24	0.21	0.30	0.30	0.24
	500<	0.24	0.15	0.15	0.30	0.30	0.20
Cast iron	≤75	1.70	1.60	1.60	1.00	1.70	1.60
	100-150	1.20	1.00	1.00	1.00	1.20	1.00
	200-250	1.20	0.80	0.90	1.00	1.20	1.00
	300-450	0.40	0.80	0.90	1.00	1.00	0.90
	500-1000	0.40	0.50	0.50	1.00	1.00	0.50
1000<	0.15	0.50	—	1.00	1.00	0.50	

Asbestos cement	≤75	6.90	1.92	4.00	1.00	6.90	3.00
	100-150	2.70	1.20	2.50	1.00	2.70	1.90
	200-250	2.70	0.96	2.25	1.00	2.70	1.60
	300-450	1.20	0.96	1.75	1.00	1.75	1.10
	500-1000	1.20	0.60	1.25	1.00	1.25	1.10
	1000≤	1.20	0.60	1.25	1.00	1.25	1.10
Polyethylene	≤75	—	—	—	—	0.17	0.16
	100-150	—	—	—	—	0.12	0.10
	200-250	—	—	—	—	0.12	0.10
	300-450	—	—	—	—	0.10	0.09
	500-1000	—	—	—	—	0.10	0.05
	1000≤	—	—	—	—	0.10	0.05
Ceramic	≤75	—	—	—	—	3.40	3.20
	100-150	—	—	—	—	2.40	2.00
	200-250	—	—	—	—	2.40	2.00
	300-450	—	—	—	—	2.00	1.80
	500-1000	—	—	—	—	2.00	1.00
	1000≤	—	—	—	—	2.00	1.00
Concrete	≤75	—	—	—	—	0.85	0.80
	100-150	—	—	—	—	0.60	0.50
	200-250	—	—	—	—	0.60	0.50
	300-450	—	—	—	—	0.50	0.45
	500-1000	—	—	—	—	0.50	0.25
	1000≤	—	—	—	—	0.50	0.25

Note: As the literatures mentioned above do not include the correction coefficient of polyethylene, ceramic and concrete pipes, it was assumed that the correction coefficient of polyethylene pipes is 0.1 times, ceramic pipes is 2.0 times and concrete pipes is 0.5 times that of cast iron pipes.

(2) Sewerage (Waste water, Rain water)

The damage functions of water supply pipes are applicable.

(3) Electricity

1) Aerial cable

The damage functions of HAZUS and Saitama Prefecture (1998) are used to calculate the maximum and average damages, respectively, referring to the existing damage functions (Tokyo Metropolitan Government (1997), Federal Emergency Management Agency (1999) and Saitama Prefecture (1998).

Table 5.7-2 Damage rate of electricity aerial cable (Max damage)

PGA(cm/s ²)	0	49	98	147	196	245	294	343	392	441	490	539	588	637	
Damage ratio(%)	0	1.9E-08	1.2E-03	7.5E-02	0.5	1.5	3.0	5.1	7.5	9.6	11.1	12.9	16.1	21.3	
PGA(cm/s ²)	686	735	784	833	882	931	980	1029	1078	1127	1176	1225	1274	1323	1372
Damage ratio(%)	28.2	35.2	41.3	46.2	50.1	53.7	57.3	61.1	64.9	68.5	71.6	74.1	76.0	77.4	78.4

Table 5.7-3 Damage rate of electricity aerial cable (Average damage)

PGA(cm/s ²)	0	225	350	500	700	1000	1500
Damage ratio(%)	0	1.0E-02	0.3	1.2	8.5	27.0	27.0

2) Underground cable

The damage rate is determined using the damage function of the Tokyo Metropolitan Government (1997).

Table 5.7-4 Damage rate of electricity underground cable (Max. damage)

PGA(cm/s ²)	0	219.8	400	500	738.6	2481.6
Damage ratio(%)	0	0	0	0.8	6.0	16.0

Table 5.7-5 Damage rate of electricity underground line (Average damage)

PGA(cm/s ²)	0	219.8	400	500	738.6	2481.6
Damage ratio(%)	0	0	0	4.0E-02	0.3	4.7

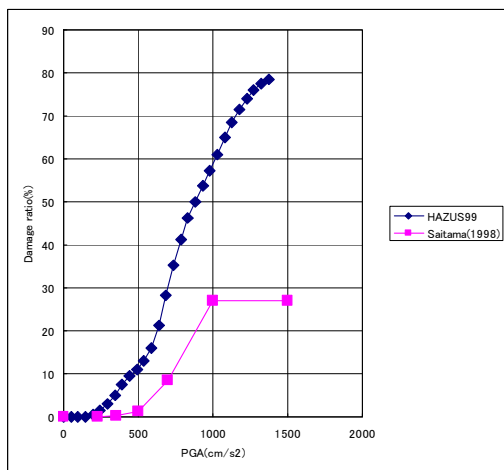


Figure 5.7-2 Damage function of aerial cable

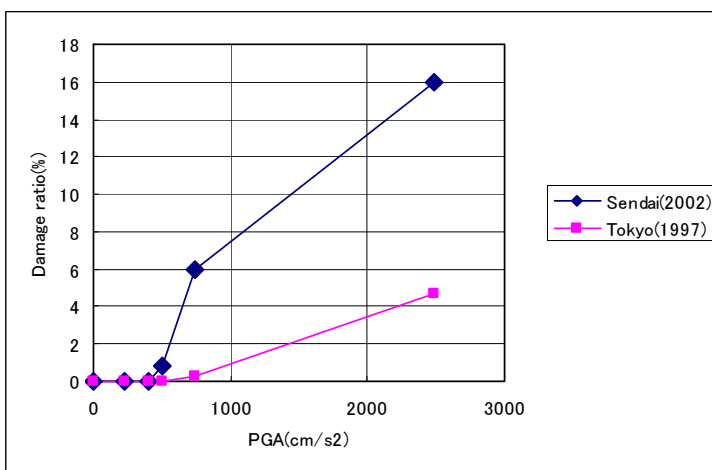


Figure 5.7-3 Damage function of underground cable

- *1) Saitama: Saitama Prefecture (Japan)
- *2) HAZUS: Federal Emergency Management Agency (USA)
- *3) Tokyo: Tokyo Metropolitan (Japan)

(4) Gas

1) Underground pipe

With respect to gas pipes buried underground, the maximum and average damages are calculated by referring to the existing damage functions (Tokyo Metropolitan Government (1997), Federal Emergency Management Agency (1999)), as is the case with water supply pipes.

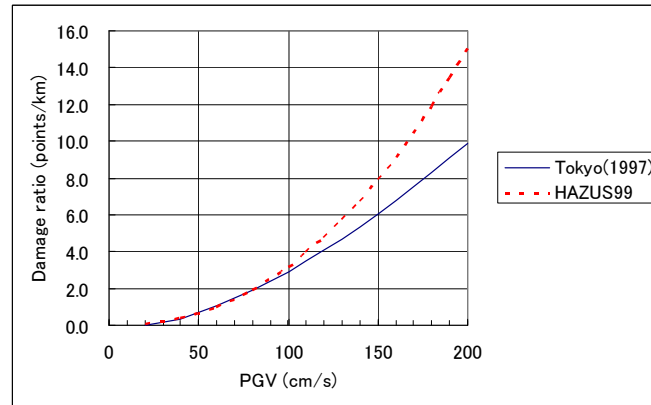


Figure 5.7-4 Standard damage rate of gas underground pipe

*1) Tokyo: Tokyo Metropolitan (Japan)

*2) HAZUS: Federal Emergency Management Agency (USA)

Damage function $R_m = R \cdot C_p \cdot C_d \cdot C_l$ (Maximum damage) $R = 1 \times 10^{-4} \cdot V^{2.25}$ (Average damage) $R = 3.89 \times 10^{-3} \cdot (V-20)^{1.51}$ R_m : Damage function (point/km) R : Damage rate (point/km) C_p : Pipe material coefficient (see Table 5.7-6) C_d : Pipe diameter coefficient (see Table 5.7-6) C_l : Liquefaction coefficient (Because liquefaction is not assumed, $C_l = 1.0$ is assumed.) V : Peak ground velocity (cm/sec)

Table 5.7-6 Coefficient of material and diameter of underground gas pipes

Material	Diameter (mm)	Cp x Cd	
		Max. damage	Average damage
Steel	All	1.0	0.30
Polyethylene	All	0.1	0.03

Note: As the literature mentioned above does not include the correction coefficient of polyethylene pipes, it was assumed to be 0.1 times that of steel pipes.

2) On the ground pipe

Since on the ground pipes are drawn into the buildings through the building walls, it is assumed that they will be damaged as part of the buildings. Therefore, with respect to the pipes on the ground, the length of damage should be calculated by multiplying the pipeline length by the building damage rate.

(5) Telephone line

Similar to the electricity lines, communication lines consist of aerial and underground cables. Therefore, the damage function of the telephone lines should be the same as that of the electricity lines.

5.8 Inventory Database of Structures

The inventory Database for estimating seismic damage consists of buildings, bridges as road infrastructure, lifelines. Additionally grid based population estimated by number of buildings is stored as inventory. Building database consists of private houses, multi-story apartment, school, hospital. Lifeline consists of water supply pipelines, sewage and rain water pipelines, gas pipelines, electricity lines, and telephone lines. The database format is “personal geodatabase” for Arc GIS which is the same format as Microsoft Access. Table 5.8-1 shows the structure of the inventory database and the list of contents.

As damage estimation is executed in the unit of grid cell, the collected data is summed up grid by grid using GIS tools. In the case of buildings, the center points of building polygons in the grid cell are summed up. In the case of lifelines, the length of each line separated by the grid is summed up grid by grid. The summing up process is conducted separately by the type of inventory according to the each damage estimation method, for example, water supply pipeline was summed up by the diameter and material. The procedure to sum up the number of apartment building is shown in Figure 5.8-1 as an example.

The lifeline data in Kentron and Shengavit is not available from Cadastre because they are under construction. Therefore, the length of lifelines is estimated from number of buildings in these two districts. The regression analysis was conducted using the database of other 10 districts and the empirical relations between the lengths of lifeline with number of buildings are derived. The empirical relations are used to make the database in Kentron and Shengavit.

The grid based population living in multi-story apartment or private house is estimated as follows. The newest total statistics of population in each district is available from NSS (2010); however the details concerning the type of living house is not available. The Master Plan (2005) includes the population living in multi-story apartment and private house by district, but the data is not newest. The current population in multi-story building or private house is estimated by multiplying the ratio from Master Plan (2005) to the total number from NSS (2010). The population living in multi-story apartment or private house by 250m grid is estimated assuming the population is proportional to the total floor area. The total floor area of the buildings in 250m grid is calculated from the foot print of the buildings in GIS database and the number of floor.

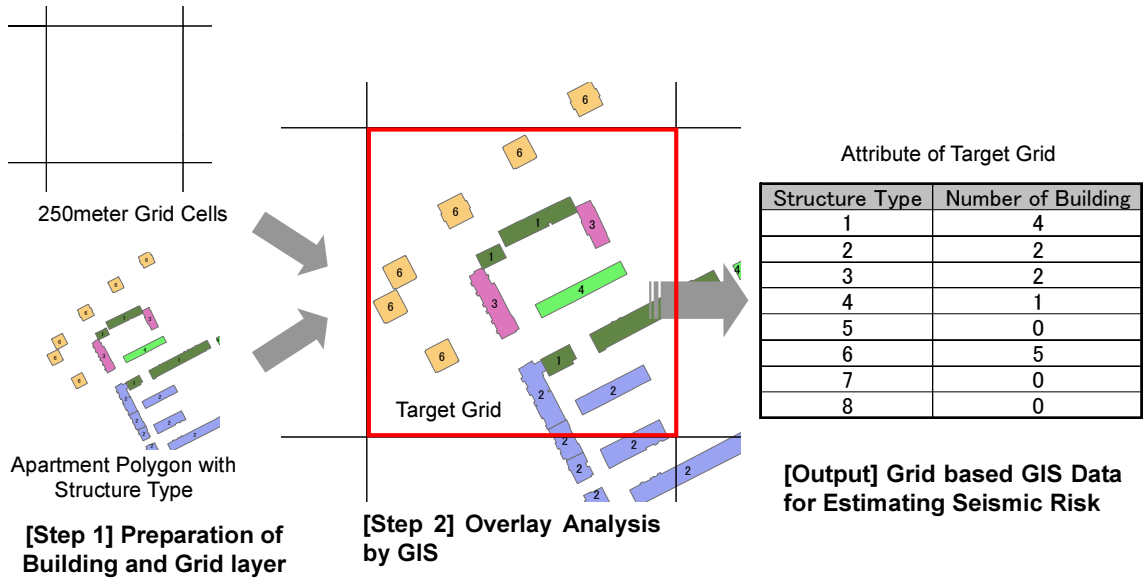


Figure 5.8-1 Steps of creating grid base inventory data, in the case of apartment

Table 5.8-1 List of inventory database

Folder	Geodatabase	Layer	Feature Type	Attribute	
2. Built_Environment	Building.mdb	All_Building	Polygon	residential or not, storey, community name, construction year, footprint area	
		Multi_Apartment_Polygon	Polygon	structure type, construction year, storey, footprint area	
		Grid250_Multi_Apart	Polygon (Grid type)	number of buildings by structure type, total floor area by structure type, grid code	
		Private_House_Polygon	Polygon	storey, construction year, footprint area, community name	
		Grid250_Private_House	Polygon (Grid type)	number of buildings by type (dacha or not), total floor area by type (dacha or not)	
		School_Pt	Point	school name, construction year, storey, number of pupils	
		Hospital_withoutclinic_Pt	Point	construction year, storey, number of beds	
		Bridge.mdb	Bridge_Pt	Point	bridge name, route name, crossing objects, community name
		Lifeline.mdb	Water_Pipelines	Polyline	material, diameter, grid code
	Grid250_Water_Pipeline		Polygon (Grid type)	length of pipeline (actual or estimated) by diameter, grid code	
	Sewage_Pipelines		Polyline	material, diameter, grid code	
	Grid250_Sewage_Pipeline		Polygon (Grid type)	length of pipeline by diameter (actual or estimated), grid code	
	Electricity_Lines		Polyline	type of above or under ground, voltage, grid code	
	Grid250_Electricity_Line		Polygon (Grid type)	length of lines (above or under ground, actual or estimated), grid code	
	Gas_Pipelines		Polyline	type of above or under ground, material, diameter, grid code	
	Grid250_Gas_Pipeline		Polygon (Grid type)	length of pipeline by diameter (actual or estimated), grid code	
	Telephone_Lines		Polyline	length of line, grid code	
	Grid250_Telephone_Line		Polygon (Grid type)	length of line, grid code	
	Population.mdb	Grid250_Population	Polygon (Grid type)	population of apartment, population of private house (dacha or not), grid code	